

1-1-2014

Operation Optimization and Water Quality Simulation of Potable Water Distribution System

Xiongfei Xie

University of South Florida, xxie2@mail.usf.edu

Follow this and additional works at: <http://scholarcommons.usf.edu/etd>

 Part of the [Civil Engineering Commons](#)

Scholar Commons Citation

Xie, Xiongfei, "Operation Optimization and Water Quality Simulation of Potable Water Distribution System" (2014). *Graduate Theses and Dissertations*.

<http://scholarcommons.usf.edu/etd/5406>

This Dissertation is brought to you for free and open access by the Graduate School at Scholar Commons. It has been accepted for inclusion in Graduate Theses and Dissertations by an authorized administrator of Scholar Commons. For more information, please contact scholarcommons@usf.edu.

Operation Optimization and Water Quality Simulation
of Potable Water Distribution System

by

Xiongfei Xie

A dissertation submitted in partial fulfillment
of the requirements for the degree of
Doctor of Philosophy in Civil Engineering
Department of Civil and Environmental Engineering
College of Engineering
University of South Florida

Major Professor: Mahmood Nachabe, Ph.D.

Bo Zeng, Ph.D.

Qiong Zhang, Ph.D.

Maya Trotz, Ph.D.

Ambe Njoh, Ph.D.

Date of Approval:

October 20, 2014

Keywords: Calibration, Sampling Design, Water Saving, Security, Contamination

Copyright © 2014, Xiongfei Xie

Table of Contents

List of Tables.....	iii
List of Figures.....	iv
Abstract.....	vi
Chapter 1: Introduction.....	1
Chapter 2: Sampling Design for Water Distribution Network Chlorine Decay Calibration.....	4
2.1 Introduction.....	4
2.2 Sampling Design Methodology.....	8
2.2.1 Chlorine Decay Modeling.....	9
2.2.2 Description of the Pipe Network.....	10
2.2.3 Chlorine Concentration Relationship of Sampling Pairs.....	11
2.2.4 Sampling Point Matrices.....	15
2.2.5 Mixed Integer Programming Formulation and Solution.....	16
2.2.6 Optimal Sampling Locations.....	19
2.3 Discussions.....	21
2.4 Future Work.....	22
2.5 Conclusions.....	23
2.6 References.....	24
Chapter 3: Optimal Scheduling of Automatic Flushing Devices in Water Network.....	31
3.1 Introduction.....	31
3.2 Methodology.....	34
3.2.1 Model Formulation.....	34
3.2.2 Phase I: Calculating AFD Flow Capacities.....	36
3.2.3 Phase II: Exploring AFD Operation Durations.....	38
3.2.4 Phase III: Exploiting Optimal AFD Discharge Patterns.....	39
3.3 Case Study.....	43
3.3.1 Network Description.....	43
3.3.2 Simulation Parameters Setup	45
3.4 Results and Discussions.....	46
3.5 Conclusions.....	49
3.6 Notations	50
3.7 References.....	51

Chapter 4: Simulation of Chlorine Decay under Contaminant Intrusion in Water Distribution System.....	60
4.1 Introduction.....	60
4.2 Methods.....	63
4.2.1 Simulating Chlorine Decay in Contaminated Water Network.....	63
4.2.2 Reactions between Chlorine and Contaminants.....	64
4.2.3 Measuring Bulk Reaction Coefficient of Contaminated Water.....	67
4.2.4 Determining Contaminated Area.....	69
4.2.5 Assigning Bulk Reaction Coefficients to Contaminated Pipes.....	72
4.3 Case Study.....	79
4.4 Results and Discussions.....	80
4.5 Conclusions.....	82
4.6 Notations.....	83
4.7 References.....	84
Chapter 5: Conclusions.....	96
Appendices.....	99
Appendix A Copyright Permissions.....	100
Appendix B GAMS Code for Chlorine Decay Calibration Sampling Design.....	102

List of Tables

Table 2.1 WDS nodal demands.....	26
Table 2.2 WDS pipe data.....	27
Table 2.3 Chlorine concentration relationship investigations.....	28
Table 2.4 Matrix 30 components.....	28
Table 2.5 List of sampling points.....	29
Table 2.6 Sensitivity matrix.....	29
Table 3.1 Gulf Beach pump station outflow.....	53
Table 3.2 AFD discharge rates.....	54
Table 3.3 AFD open durations.....	54
Table 3.4 AFD optimal open patterns.....	55
Table 4.1 Contaminants identified by USEPA.....	86
Table 4.2 Bulk reaction coefficients.....	86

List of Figures

Figure 2.1 Schematic pipe layout.....	30
Figure 2.2 Objective function values.....	30
Figure 3.1 Chlorine residual of lowest node.....	55
Figure 3.2 Flowchart of methodology.....	56
Figure 3.3 Studied pipe network.....	57
Figure 3.4 Water use patterns of the small city and the County Park.....	58
Figure 3.5 Searching minimal AFD discharge capacities.....	58
Figure 3.6 AFD-50 chlorine die-off curve.....	59
Figure 4.1 Methodology flowchart.....	87
Figure 4.2 Bulk reaction coefficients.....	88
Figure 4.3 Chlorine decay at contaminant attack.....	88
Figure 4.4 Bulk reaction coefficient curves.....	89
Figure 4.5 Regression constants for bulk reaction coefficients.....	89
Figure 4.6 Nonreactive contaminant concentrations.....	90
Figure 4.7(a) Contaminant matrix in single pipe.....	90
Figure 4.7(b) Contaminant matrix in branch pipe network.....	91
Figure 4.8 Step function of bulk reaction coefficient.....	91
Figure 4.9 Step function of chlorine residuals.....	92

Figure 4.10 Studied water network.....	93
Figure 4.11(a) Contaminated junctions for the first contamination sub-event.....	94
Figure 4.11(b) Contaminated junctions for the second contamination sub-event.....	94
Figure 4.12 Concentrations of AFD-39.....	95

Abstract

A potable water distribution system (WDS) consists of pipes, pumps, valves, storage tanks, control and supporting components. Traditionally, it has two basic functions. First, provides end users with potable water at sufficient pressures and good water quality. Second, provides sufficient pressure and flow for fire fighting. Currently, potable water is still the least expensive material for fire fighting. To accomplish these two goals, water utilities have to consider the integrity and security of the water network. As a result, this research selected three research topics that are closely related to the daily operation of water utilities and water quality simulation.

The first study is on optimal sampling design for chlorine decay model calibration. Three questions are investigated: (1) What is the minimum number of chlorine sample locations a water network needs? (2) How many combinations of sampling locations are available? (3) What is the optimal location combination? To answer the first two questions, the mathematical expressions of the chlorine concentrations between any two sampling locations are developed and sampling point relationship matrices are generated, then a mixed integer programming (MIP) algorithm is developed. Once obtained, the solutions to the first two questions are used to calculate the chlorine decay wall reaction coefficients and sensitivity matrix of chlorine concentration wall reaction coefficients; then, sampling location combinations achieved in the second question are sorted using a D-optimality algorithm. The model frame is demonstrated in a case study. The

advantage of this method, compared to the traditional iterative sensitivity matrix method, is that a prior knowledge or estimation of wall reaction coefficients is not necessary.

The second study is on optimizing the operation scheduling of automatic flushing device (AFD) in water distribution system. Discharging stagnant water from the pipeline through AFD is a feasible method to maintain water quality. This study presents a simulation-based optimization method to minimize total AFD discharge volume during a 24-hour horizon. EPANET 2.0 is used as hydraulics and water quality simulator. This is formulated as a single objective optimization problem. The decision variables are the AFD operation patterns. The methodology has three phases. In the first phase, AFD discharge capacities are calculated, whether existing AFDs are able to maintain chlorine residuals in the water network is also evaluated. In the second phase, the decision variables are converted to AFD discharge rates. A reduced gradient algorithm is used to quickly explore and narrow down the solution space. At the end of this phase, decision variables are switched back to the AFD operation patterns. In the third phase, simulated annealing is used to search intensively to exploit the global minimum. The method is demonstrated on the water system located at the south end of Pinellas County, Florida where AFD optimal operation patterns are achieved.

The third study is on simulating contaminant intrusion in water distribution system. When contaminant matrix is introduced into water distribution system, it reacts with chlorine in bulk water rapidly and causes fast disinfectant depletion. Due to the difficulties in identifying contaminant types and chemical and biological properties, it is a challenging task to use EPANET-MSX to simulate chlorine decay under contaminant attack. EPANET 2.0 is used in the study to accomplish this goal. However, EPANET 2.0 cannot directly simulate chlorine depletion in the event of contamination attack because it assigns one time-independent bulk

reaction coefficient to one specific pipe during the simulation. While under contaminant intrusion, chlorine decay bulk coefficient is not a constant. Instead, it is a temporal and spatial variable. This study presents an innovative approach for simulating contaminant intrusion in water distribution systems using EPANET multiple times. The methodology has six general steps. First, test bulk reaction coefficients of contaminant matrix in chemical lab. The uniqueness of this study is that the contaminant matrix is studied as a whole. The investigations of chemical, biological properties of individual aqueous constituents are not needed. Second, assume the contaminants as nonreactive, using EPANET 2.0 to identify where, when and at what concentrations of the inert contaminants will pass by in the water network. Third, determine the number of chlorine residual simulations based on the results in step two. Fourth, use EPANET to simulate the chlorine residual in the water network without the occurrence of contamination. Fifth, assign contaminated bulk coefficients to contaminated pipes; use EPANET to simulate the chlorine residual in the pipe network. Lastly, the chlorine concentrations of the impacted moments of impacted junctions are replaced with the results calculated in step five. This methodology is demonstrated in the south Pinellas County water distribution system.

Chapter 1: Introduction

A potable water distribution system consists of pipes, pumps, valves, storage tanks, control and supporting components. Traditionally, it has two basic functions. First, provides end users with potable water at sufficient pressures and good water quality. Second, provides sufficient pressures and flows for fire fighting.

To accomplish these two goals, water utilities have to consider the integrity of water infrastructures. American Society of Civil Engineers (ASCE) gave US drinking water infrastructures an overall grade D in its 2013 Report Card. The grade was B⁻ and D in 1998 and 2008 respectively. That suggests that the deterioration of US drinking water infrastructures is not stopped in the last five years. Maintaining the integrity of drinking water infrastructures is an urgent task. Maintaining disinfectant residual throughout the water distribution system, termed secondary disinfection, helps to maintain the integrity of the water network by killing harmful microorganisms and restricting biofilm growth on the pipe wall. The most commonly-used secondary disinfectants in the United States are chlorine, chloramines, and chlorine dioxide. In the research, the first topic is on the sampling design for the calibration of chlorine residual simulation in water distribution system. It is closely related to the water network integrity.

US Environment Protection Agency (USEPA) reports show that drinking water and wastewater systems account for approximately 3-4 percent of energy use in the United States, adding over 45 million tons of greenhouse gases annually. Energy as a percent of operating costs

for drinking water systems reaches as high as 40 percent. Water saving measures can result in a saving in energy consumption. EPA estimates that if one out of every 100 US homes is retrofitted with water-efficient fixtures, an energy saving of about 100 million kWh and a reduction of 80,000 tons of greenhouse gas emission will be expected per year. As a result, energy and water savings are beneficial not only to water utilities, and the public, but also to the environment, especially in the context of ever-increasing energy price and water demand. The second topic of this research is on water saving in water distribution system.

Water distribution system is spatially diverse and thus is vulnerable to a variety of threats. One of the most serious ones is a chemical and/or biological contamination intrusion. Contaminants can be intentionally injected into water network by terrorists or unintentionally flow into water network. After September 11 attack in the United States, securities of water infrastructures networks have drawn high attentions in many countries. The third research topic is on the simulations of contaminant attenuation and chlorine decay in the event of contaminant attack.

The first study is on determining optimal sampling locations for chlorine decay model calibration. This procedure is also referred to as sampling design. The purpose is to collect data that, when used for calibration, yield the most optimal results, and to provide the best trade-off between sample design cost and model prediction accuracy. Traditionally, iterative parameter estimation based on a sensitivity matrix was used. This approach cannot provide a definitive guide to practitioners on how to balance the modelling and calibration with the quality of decisions that could be made based on calibrated models. Therefore, most utilities still rely on a set of simple and pragmatic rules based on previous experiences. The objective of this study is to develop one approach to overcome the drawbacks of the existing iterative parameter

estimation method and to find the optimal set of sampling locations for the calibration of the chlorine decay model of water distribution system.

The second study is on saving water in water distribution system. In addition to supplying potable water, the water system is sized for fire flows. Therefore, water network is oversized from a regular water consumption perspective. This is a serious issue for water quality in water network. This study investigates the depletion of unchlorinated water to maintain chlorine residual in water network. This measure requires no modification of existing infrastructure. Therefore, it is widely used by water utilities. However, utilities operators normally perform pipe flushing based on their experiences. It is imperative for the water utilities to investigate whether current flushing practice is optimal, e.g., flushing volume can be reduced. Flushing is accomplished by opening fire hydrant manually or operating automatic flushing device (AFD). Operating AFD needs less labor than manually opening a fire hydrant. So AFDs are gaining popularity in water utilities. This study focuses on studying the operations of timer-controlled AFD to minimize their total daily flushing volume.

The third study is on the simulation of contaminant intrusion in water distribution system. This is the basis for other applications such as sensor placement and contamination source characterization. US EPA identified 33 baseline contaminants in the potable water network. Chlorine can react with most of them. US EPA researches suggest that chlorine residuals, free or total, are the most useful parameters to indicate contamination. As a popular water quality simulation software product, EPANET is not suitable for directly simulating chlorine decay under contamination attack. EPANET-MSX is used by some scholars. However, the complexity of contaminant matrix limits the availability of EPANET-MSX. In this study, an EPANET 2.0-based methodology is developed to simulate contaminant-induced chlorine decay.

Chapter 2: Sampling Design for Water Distribution Network

Chlorine Decay Calibration¹

2.1 Introduction

Drinking water quality is essential to public health; it is usually assessed by various indicators, such as hydraulic residence times, source tracing, and disinfectant concentration. Maintaining disinfectant residual throughout the water distribution system (WDS), termed secondary disinfection, helps to maintain the integrity of the WDS by killing harmful microorganisms and restricting biofilm growth on the pipe wall. Biofilm is a layer of microorganisms bound by a matrix of organic matters that attaches to pipe walls; it hosts pathogenic organisms, accelerates pipe corrosion, and contributes to aesthetic problems such as objectionable odours, disagreeable tastes, and discolouration (Martiny 2005). Therefore, inhibiting biofilm growth is crucial to maintain water quality and water network integrity.

In the United States, the Surface Water Treatment Rule requires utilities that produce drinking water using surface water or ground water under the influence of surface water to monitor and maintain a detectable disinfectant residual throughout the WDS. Under the 1990 USEPA Surface Water Treatment Rule (SWTR), the free or combined disinfectant residual concentration in the WDS must be at least 0.2 mg/L. Secondary disinfection practices vary widely in European countries. The European Union has issued standards for drinking water that

¹ Note: Portion of this chapter was published in *Urban Water Journal* (DOI:10.1080/1573062X.2013.831911). Permission is included in Appendix A.

do not require secondary disinfection. Of the 15 original European Union member states, only Spain and Portugal require secondary disinfection (USEPA 2006).

The most commonly-used secondary disinfectants in the United States are chlorine, chloramines, and chlorine dioxide. Chlorine is a strong oxidant; it reacts with a wide range of chemicals when applied into the WDS. Some of these initial reactions involve organic materials which, when reacting with chlorine, generate compounds that are potentially carcinogenic. These compounds are classified as Disinfection By-Products (DBP). To maintain low concentrations of DBP, the Stage 1 Disinfectant/ Disinfection By-Products Rule, announced in 1998 by USEPA, mandates that residual chlorine in the WDS do not exceed 4.0 mg/L. Chloramines are becoming more widespread in large-scale WDS because they produce lower concentrations of DBP than chlorine and last longer than chlorine in WDS. One of the major drawbacks of chloramines is that ammonia is released when chloramines decompose. Bacteria oxidize ammonia to nitrite and nitrate; this process is known as nitrification. Nitrate can cause a potentially fatal blood disorder in infants who are less than six months old, which is referred to as methemoglobinemia or “blue-baby” syndrome. In addition, nitrification lowers the water pH, which increases corrosion of lead and copper. Nitrification is a serious problem for some utilities, such as the Pinellas County WDS in Florida, which serves half of a million people. Pinellas County WDS switched its secondary disinfectant from chlorine to chloramines in 2002. However, largely due to substantial nitrification episodes that have occurred since 2009, chlorine has to be reintroduced and injected into the WDS periodically to inhibit nitrification. Chlorine dioxide is also a strong disinfectant; it is less frequently used as a secondary disinfectant than chlorine and chloramines because (1) its residual does not last as long as that of other secondary disinfectants, and (2) it can break down into chlorite, which is also a regulated DBP. The USEPA recommends that chlorine dioxide’s

use be limited to smaller WDS. In general, because of its applicability, low cost, and effectiveness, chlorine is still the most widely-used secondary disinfectant in medium distribution systems in the United States.

The behaviour of chlorine dispersion and decay throughout a WDS can be simulated using a chlorine decay model coupled with a hydraulic WDS model. Results from chlorine decay simulation may be used to optimize the chlorine dosing at the water treatment plant or to determine optimum chlorine booster locations (Cozzolino 2005). A chlorine decay model requires calibration before useful results are obtained. Sampling design is essential in calibration as it can significantly affect the accuracy of model calibration. In addition to be used for chlorine decay calibration, sampling design can also be utilized for routine operation and maintenance of WDS (Speight 2004). In essence, the purpose of the optimal sampling design (SD) procedure for WDS residual chlorine model calibration is to determine (1) the most ideal positions within the WDS to observe the chlorine concentrations, (2) the duration and frequency of observations, and (3) the most ideal conditions to observe. The most important is to determine ideal locations within the WDS to observe the chlorine concentrations; therefore, the efforts of this study are focused mainly on location design.

Traditionally, sampling location design has been developed for hydraulic modelling calibration, such as pipe friction loss coefficient and water demand calibrations. The purpose is to collect data that, when used for calibration, yield the most optimal results, and to provide the best trade-off between sample design cost and model prediction accuracy. Several researchers have addressed the complications of sampling design for WDS hydraulic model calibration. Walski (1983) was among the first to suggest where to observe pressure heads and flows to collect data for model calibration. Walski (2000) also discussed the impact of measurement

errors and provided guidelines for collecting good data to achieve meaningful model calibration. Meier (2000) used a genetic algorithm (GA) to find a fixed number of flow test locations that cause water to flow at a noticeable velocity through as much of a pipe network as possible. Bush (1998) developed three simple, yet efficient methods for sampling design: the max-sum, weighted sum, and max-min methods. These methods were based on a Jacobian matrix and inspired by D-optimality criteria. Lansey (2001) developed a three-step sampling design procedure that considers measurement uncertainties and their impacts on model parameter estimates as well as model predictions. These studies show that measurements should be taken at sensitive locations, i.e., locations where the model responses are sensitive to parameters to be estimated. Kapelan (2005) formulated the sampling design problem as a constrained two-objective optimization problem. The objectives are to maximize the calibration accuracy by minimizing relevant uncertainties that are based on sensitivity analysis and to minimize total sampling costs. Most of the current methodologies used for hydraulic model calibration sampling design are based on the sensitivity matrix $\partial y(a)_i / \partial a_k$, where $y(a)$ is the vector of prediction variables, a is the vector of N_a unknown calibration parameters; these derivatives are evaluated at the true value of parameters \hat{a}_k . The paradox of this method is that the true value parameters are not known beforehand. An iterative method is normally used to address this puzzle: first, the parameters are estimated based on a combination of historical information, reconnaissance-level data collection, and the experiences of engineers and operators; second, these pre-assumed parameter values are used to develop the sensitivity matrix and generate a suboptimal sampling design; and third, the suboptimal sampling design is used to collect data and evaluate the initial parameter estimations. This procedure is repeated until differences between the updated parameter estimations and previous estimated values are minimized.

Among the limited research on sampling design for chlorine decay calibration, iterative parameter estimation based on a sensitivity matrix was also used (Bremond 2003, Shang 2005). In the research of Shang (2005), both hydraulic and chlorine measurement errors were taken into consideration. Only first-order wall reaction was considered, and the entire pipe network was assumed to have same wall reaction coefficient.

The literature review shows that existing approaches cannot provide a definitive guide to practitioners on how to balance the modelling and calibration with the quality of decisions that could be made based on calibrated models. Therefore, most utilities still rely on a set of simple and pragmatic rules based on previous experiences.

The objective of this study is to develop one approach to overcome the drawbacks of the existing iterative parameter estimation method and to find the optimal set of sampling locations for the calibration of the WDS chlorine decay model. This study is organized as follows: after this introduction, the WDS sampling design problem is formulated; then, a case study is used to illustrate the optimization methodology; and finally, relevant conclusions are drawn.

2.2 Sampling Design Methodology

This study examines three questions: (1) What is the minimum number of chlorine sample locations needed? (2) How many combinations of sampling locations are available? (3) What is the optimal location combination? The first two questions are closely related; therefore, they were investigated together. To answer the first two questions, the mathematical expressions of the chlorine concentrations between any two sampling locations were developed, and sampling point relationship matrices were generated. Then, a mixed integer programming (MIP) algorithm was developed. Once obtained, the answers to the first two questions were used to solve the third question. The chlorine decay wall reaction coefficients were calculated and

used to generate the sensitivity matrix of chlorine concentration to wall reaction coefficients. Sampling location combinations achieved in the second question were then sorted using a *D*-optimality algorithm. The model frame was demonstrated in a case study.

2.2.1 Chlorine Decay Modelling

The chlorine dispersion and decay behaviour throughout a WDS can be simulated using a chlorine decay model (Jonkergouw 2008). Chlorine decay in WDS pipes involves two mechanisms: (1) reaction with aqueous constituents, such as ammonia and natural organic matter in the bulk water, and (2) reaction with pipe materials and biofilm near the pipe wall. These models are superimposed on a transport model to calculate the chlorine concentration in a given pipe, as follows:

$$\frac{\partial C}{\partial t} = -u \frac{\partial C}{\partial x} - k_b C^m - \frac{k_f k_w}{R_h (k_f + k_w)} C^n \quad (2.1)$$

in which C is chlorine concentration (mg/L); u is flow velocity (m/s); x is distance between the start and end points (m); k_b is bulk reaction rate, which is usually determined by “bottle” or “jar” tests (Savic 2009); m is the bulk reaction order; normally, it takes the value of 1, even though this assumption has several obvious shortcomings and there are other more suitable alternatives (Boccelli 2003); R_h is pipe hydraulic radius (m), which is assumed to be known in this study; k_f is flow-dependent mass transfer coefficient, which increases with flow velocity (Mutoti 2007); it is considered to be given when water distribution hydraulics are known; k_w is pipe wall reaction coefficient, which is an intrinsic pipe property; and n is wall reaction order; EPANET limits it to be either 0 or 1. The first-order wall model best represents the reaction of chlorine to biofilm, a process in which chlorine is the limiting reactant. The zero-order wall model best describes the case in which chlorine immediately oxidizes reductants, such as iron released from pipe wall

encrustation and tuberculation. The reaction rate is dependent on how fast the reductant is produced by the pipe. Biofilm is more significant in consuming chlorine than iron released from pipe corrosion. Therefore, the default setting of pipe wall reaction in EPANET is first order (Rossman 2000). Equation (2.1) demonstrates that chlorine concentration depends on decay reaction rate and water flow velocity; therefore, field measurements of chlorine concentrations can be used to calculate k_w if the hydraulics of the water distribution system are sufficiently understood.

Two methods are generally used for calibrating pipe wall reaction coefficients: direct calibration and correlation calibration. Direct calibration is used to directly calculate the pipe wall reaction coefficients and reaction order for a group of pipes. Correlation calibration is based on the evidence that the same processes that increase a pipe's roughness with age also tend to increase the reactivity of its wall with chlorine (Vasconcelos 1997). For each individual pipe, the multiplication of the wall reaction coefficient k_w and its Hazen Williams Coefficient C is defined as a constant. Direct calibration is more accurate than correlation calibration, but it requires more effort. Therefore, larger-scale WDS (Wu 2006), such as the Pinellas County WDS (Baggett 2008), uses the correlation calibration method for calculating the chlorine wall reaction coefficients. In this study, the direct calibration method was applied.

2.2.2 Description of the Pipe Network

A hypothetical pipe network is presented in Figure 2.1; this WDS was modified from a widely used example "mytown". The WDS depicts the water supply system of a small town; it has 29 demand nodes, 36 pipes, and 1 water treatment plant (WTP). The average water demands of the 29 demand nodes are listed in Table 2.1. WTP is the only chlorine source with a constant outflow chlorine concentration of 4.0 mg/L. The whole WDS is set at elevation zero to save

computational efforts. Chlorine sampling activity is limited to 29 junctions, numbered *SP-1* through *SP-29*. These sample points are located approximately 150 meters apart; this is to simulate a real water distribution network, where water samples can be collected only at fire hydrants or blow-off valves. Junctions *SP-1*, *SP-5*, *SP-6*, *SP-12*, *SP-13*, *SP-15*, *SP-20*, *SP-27*, and *SP-28* are also water users. Pipe characteristics are provided in Table 2.2. Some of the 36 pipes have 2 or more subsections due to the presence of sampling points on these pipes. The 36 pipes fall into four groups, and each group has same wall reaction coefficients k_w . Steady-state hydraulic simulation with the average water demands was conducted using EPANET, and flow directions in the pipes are shown in Figure 2.1.

2.2.3 Chlorine Concentration Relationship of Sampling Pairs

The mathematical expressions of chlorine concentrations of sampling points at steady-state and first-order wall reaction were mainly examined; several typical cases are shown in Table 2.3 and are explained in detail thereafter. Zero-order wall reaction and semi-steady-state chlorine decay were also discussed briefly.

In steady-state, i.e. constant flow condition and first-order wall reaction, Equation (2.1) becomes:

$$0 = -u \frac{\partial C}{\partial x} - k_b C - \frac{k_f k_w}{R_h (k_f + k_w)} C \quad (2.2)$$

In case 1, when chlorine concentrations are measured in *SP-4* and *SP-5*, Equation (2.2) generates:

$$\ln C_4 - \ln C_5 = \left(k_b + \frac{k_{f21.2} k_{w1}}{R_{h21.2} (k_{f21.2} + k_{w1})} \right) \times t_{21.2} \quad (2.3)$$

where $t_{21.2}$ is the water travel time along pipe $P21.2$ from $SP-4$ and $SP-5$. Equation (2.3) is a nonlinear function of wall reaction coefficient k_{w1} ; it can be analytically solved if chlorine concentrations of $SP-4$ and $SP-5$ are measured.

In case 2, Equation (2.4) is generated when Equation (2.2) is integrated from $SP-3$ to $SP-16$:

$$\ln C_3 - \ln C_{16} = \left(k_b + \frac{k_{f25.2} k_{w4}}{R_{h25.2} (k_{f25.2} + k_{w4})} \right) \times t_{25.2} + \left(k_b + \frac{k_{f22.1} k_{w4}}{R_{h22.1} (k_{f22.1} + k_{w4})} \right) \times t_{22.1} \quad (2.4)$$

This is a second-order polynomial equation of k_{w4} ; it can be solved analytically when chlorine concentrations of $SP-3$ and $SP-16$ are available.

In case 3, when integrated between $SP-2$ and $SP-3$, Equation (2.2) generates a third-order polynomial equation of k_{w4} (which is not shown here because of its excessive length). Since third- or higher-order polynomial equations have no theoretical solutions, k_{w4} cannot be solved analytically, even if chlorine concentrations at $SP-2$ and $SP-3$ are available.

In case 4, when integrated between $SP-11$ and $SP-12$, Equation (2.2) becomes:

$$\ln C_{11} - \ln C_{12} = \left(k_b + \frac{k_{f4.3} k_{w1}}{R_{h4.3} (k_{f4.3} + k_{w1})} \right) \times t_{4.3} + \left(k_b + \frac{k_{f6} k_{w3}}{R_{h6} (k_{f6} + k_{w3})} \right) \times t_6 \quad (2.5)$$

This equation is essentially a second-order polynomial equation with two variables, k_{w1} and k_{w3} . It can be solved analytically when a second first- or second-order polynomial equation is available.

In case 5, water flows received by $SP-1$ and $SP-2$ are both from Node I ; the chlorine concentrations at $SP-1$ and Node I have the relationship shown in Equation (2.6a); and chlorine concentrations of Node I and $SP-2$ have the relationship shown in Equation (2.6b).

$$\ln C_1 = \ln C_{n1} - \frac{k_{f2} k_{w2}}{R_{h2} (k_{f2} + k_{w2})} \times t_2 \quad (2.6a)$$

$$\ln C_2 = \ln C_{n1} - \frac{k_{f3.1} k_{w4}}{R_{h3.1} (k_{f3.1} + k_{w4})} \times t_{3.1} \quad (2.6b)$$

where C_{n1} is the chlorine concentration at Node 1, which is not measurable since the sampling activity is limited to 29 junctions. However, it can be eliminated by subtracting Equation (2.6b) from (2.6a); the result is shown in Equation (2.6c), which is the equation of the chlorine concentrations of *SP-1* and *SP-2*.

$$\ln C_2 - \ln C_1 = -\frac{k_{f3.1} k_{w4}}{R_{h3.1} (k_{f3.1} + k_{w4})} \times t_{3.1} + \frac{k_{f2} k_{w2}}{R_{h2} (k_{f2} + k_{w2})} t_2 \quad (2.6c)$$

It can be seen that Equation (2.6c) has the same format as Equation (2.5).

In case 6, due to the mixing of water flow Q_{18} and Q_{19} at *SP-6*, the chlorine concentration at *SP-6* is expressed as:

$$C_6 = \frac{C_{6l} \times Q_{18} + C_{6r} \times Q_{19}}{Q_{18} + Q_{19}} \quad (2.7)$$

where C_{6l} is the chlorine concentration at Q_{18} close to *SP-6* from left side; C_{6r} is the chlorine concentration at Q_{19} close to *SP-6* from right side; it is normally assumed that mixing at junctions is instantaneous and complete. C_{6r} and C_5 have a similar expression as Equation (2.4), and C_{6l} and C_7 have a similar expression as Equation (2.5). However, chlorine concentrations C_{6l} and C_{6r} are not measurable because the sampling activities are limited to 29 junctions. The relationship between C_5 and C_6 is an extremely complicated exponential expression that also involves C_7 . As a result, measuring chlorine concentration at *SP-5* and *SP-6* cannot solve k_{w3} analytically. In general, junction with inflow mixing is the end point of the chlorine

concentration expression for upstream nodes; however, it is the starting point for downstream sampling points. *SP-15* is an example for this case; the chlorine concentrations of *SP-15* and *SP-18* can be written as the same format as Equation (2.5). Consequently, measuring chlorine concentrations at the junctions with more than one inflow and without outflow, like *SP-6*, are avoided.

When the wall reaction is zero-order, Equation (2.1) becomes:

$$0 = -u \frac{\partial C}{\partial x} - k_b C - \frac{k_f k_w}{R_h (k_f + k_w)} \quad (2.8)$$

Using the pipe sections between *SP-11* and *SP-12* as example, when integrated between these two points, Equation (8) becomes:

$$k_b C_{11} + \frac{k_{f43} k_{w1}}{R_{h43} (k_{f43} + k_{w1})} = \left(\left(k_b C_{12} + \frac{k_{f6} k_{w3}}{R_{h6} (k_{f6} + k_{w3})} \right) e^{k_b x_6} - \frac{k_{f6} k_{w3}}{R_{h6} (k_{f6} + k_{w3})} + \frac{k_{f43} k_{w1}}{R_{h43} (k_{f43} + k_{w1})} \right) e^{k_b x_43} \quad (2.9)$$

As in Equation (2.5), Equation (2.9) is also a second-order polynomial equation with two variables, k_{w1} and k_{w3} . The difference between these two equations is also obvious: Equation (2.5) is the expression of the logarithm of chlorine concentration, and Equation (2.9) is the expression of concentration itself. This suggests that the junction mixing at *SP-6* can be calculated analytically when the chlorine wall reaction is zero order. As explained previously, first-order wall reaction is more common than zero-order wall reaction; therefore, it is discussed in the subsequent study.

In a semi-steady state, i.e., an extended period simulation (EPS), the equation of chlorine concentrations of the sampling pair, such as *SP-4* and *SP-5*, is still the function of k_{w1} , just in a more complicated format (Shang 2005, Fabrie 2010). As a result, measuring chlorine concentrations at these two points at semi-steady state can also be used to analytically

solve k_{wI} if the EPS is sufficiently accurate. Actually, when the sampling activity is undertaken within a relatively short time period, the water distribution system can be assumed to be in a steady state.

2.2.4 Sampling Point Matrices

In this research, the WTP discharge point is a permanent sampling point, which is numbered *SP-30*. Based on the pipe network and the flow directions shown in Figure 2.1, Matrix 1 through Matrix 30 were established, which correspond to 29 potential sample points and *SP-30*. Matrix 30 is presented in Table 4 as an example to explain how these matrices were generated. The matrix has the size of 30 rows and four columns, and row k represents the information of four wall reaction coefficients captured by the sampling pair made by point k and *SP-30*. Take the second and third rows as examples. The second row shows the information captured by sampling pair of *SP-2* and *SP-30*; it indicates that 1) k_{w1} and k_{w2} are both zero, which suggests that information of k_{w1} and k_{w2} is not available if sampling occurs at these two points; and, 2) both k_{w3} and k_{w4} are one, which reveals there is one section of pipe, *P1*, that contains the information of k_{w3} , and one section of pipe, *P3.1*, that has the information of k_{w4} . There are four zeros at the third row of Matrix 30; this suggests that sampling at *SP-3* and *SP-30* will not provide any useful information to solve the four wall reaction coefficients. Note that such information captured in the pair of sampling points i and j will be duplicated in the pair of j and i . So we can employ this symmetric property to populate those matrices.

For a large scale WDS, constructing these sampling point matrices is a time-consuming task. A few strategies can be used to improve the efficiency: 1) highlighting the junctions where flow mixing occurs, such as *SP-6*, *SP-15*, and Junction 11 if the wall reaction is first-order. Any sampling points downstream of Junction 11 have no mathematical relationships with those

upstream of this junction. Similarly, *SP-19* only has mathematical relationships to *SP-18* and *SP-15*. Therefore, all the rows in Matrix *19* are zeros except 15th and 18th rows. And, 2) decomposing the large WDS into several independent sub-networks. Sampling relationship matrices can be developed for each individual sub-network. For example, the pipe network shown in Figure 2.1 can be divided into two sub-networks at Junction *11*. The sub-network west of Junction *11* has 10 sampling points, while the east has 20 sampling points. In fact, given the network topology and the water flow, we anticipate that an algorithm or automatic procedure can be developed to construct those matrices.

2.2.5 Mixed Integer Programming Formulation and Solution

So far, genetic algorithm (GA) is the most widely used mathematical tool in sampling design. It is fast for obtaining a solution, but it has no guarantee on whether the solution is optimal or even how good it is. As a result, in this study, a mixed integer programming (MIP) optimization algorithm was developed to solve questions 1 and 2. MIP is gaining popularity in the water industry and has been used in optimal sensor placement in water distribution system for contamination identification study (Berry 2005, 2006) and disinfectant booster pump location optimization (Propato 2004). In this study, the objective function of the MIP algorithm is to minimize sampling points selected from the 29 allowable sampling locations plus *SP-30*, as follows:

$$\text{Minimize } \sum_{i=1}^{30} C_i \quad (2.10)$$

where C_i is a binary variable used to represent whether sampling activity occurs at point i ; it takes 1 when sampling activity is performed at this point, and zero otherwise. As explained previously, C_{30} takes 1.

To compute four wall reaction coefficients, four independent equations are needed, which constitute the constraints for the MIP algorithm. A sampling collection with six sampling points, e.g., *SP-1*, *SP-2*, *SP-3*, *SP-4*, *SP-5*, and *SP-30*, is used to explain how the constraints were formulated mathematically. Sampling at these six points means selecting Matrices 1, 2, 3, 4, 5, and 30 and rows 1, 2, 3, 4, 5, and 30 from each matrix; this constitutes a set of $6 \times 6 / 2 = 18$ equations. If by linear combination, i.e., multiplying with certain coefficients, these 18 sampling equations generate an equation that contains only k_{w1} , written as a unit row vector [1 0 0 0]. This sampling combination is said to be able to solve k_{w1} . Similarly, if this selection of sampling points can generate four equations, each is the function of k_{w1} through k_{w4} , respectively; this selection of sampling points is said to be able to solve the four wall reaction coefficients. Mathematically, these constraints of MIP algorithm are expressed as:

$$\sum_{i=1}^{30} \sum_{j=1}^{30} C_i \times C_j \times \lambda_{i,j} \times Matrix_i(j, k_{w1}, k_{w2}, k_{w3}, k_{w4}) = [1000] \quad (2.11a)$$

$$\sum_{i=1}^{30} \sum_{j=1}^{30} C_i \times C_j \times \lambda_{i,j} \times Matrix_i(j, k_{w1}, k_{w2}, k_{w3}, k_{w4}) = [0100] \quad (2.11b)$$

$$\sum_{i=1}^{30} \sum_{j=1}^{30} C_i \times C_j \times \lambda_{i,j} \times Matrix_i(j, k_{w1}, k_{w2}, k_{w3}, k_{w4}) = [0010] \quad (2.11c)$$

$$\sum_{i=1}^{30} \sum_{j=1}^{30} C_i \times C_j \times \lambda_{i,j} \times Matrix_i(j, k_{w1}, k_{w2}, k_{w3}, k_{w4}) = [0001] \quad (2.11d)$$

where $\lambda_{i,j}$ are linear combination coefficients, which are variables, for the linear combination; C_i and C_j are binary variables as explained in Equation (2.10); and $Matrix_i(j, k_{w1}, k_{w2}, k_{w3}, k_{w4})$ is the j^{th} row of Matrix i . From Equations (2.11a)–(2.11d), we note that there are quadratic terms that make the formulation nonlinear and hard to compute. To address this problem, we applied the

big- M linearization technique to obtain a linear formulation (Nemhauser 1988). This task was fulfilled in two steps: 1) linearization of $C_i \times C_j$ (result denoted as $W_{i,j}$), and 2) linearization of $W_{i,j} \times \lambda_{i,j}$, denoted as $Z_{i,j}$. The first step was accomplished by including the following inequalities into our initial model:

$$W_{i,j} \leq C_i \quad (2.12a)$$

$$W_{i,j} \leq C_j \quad (2.12b)$$

$$W_{i,j} \geq C_i + C_j - 1 \quad (2.12c)$$

The above three equations ensure that when $C_i = C_j = 1$, we have $W_{i,j} = C_i \times C_j = 1$ and $W_{i,j} = 0$ whenever one of them equals to zero. Note that $W_{i,j}$ takes binary values. The second step was performed by implementing the following four equations:

$$Z_{i,j} \leq M \times W_{i,j} \quad (2.13a)$$

$$Z_{i,j} \leq \lambda_{i,j} \quad (2.13b)$$

$$Z_{i,j} \geq M \times (W_{i,j} - 1) + \lambda_{i,j} \quad (2.13c)$$

$$Z_{i,j} \geq -(M \times W_{i,j}) \quad (2.13d)$$

where M is a large positive constant. The above four equations ensure that when $W_{i,j}=0$, then $Z_{i,j}=0$ and that $Z_{i,j}=\lambda_{i,j}$ when $W_{i,j}=1$.

The nonlinear formulation was converted into a mixed integer linear programming question (MILP). Linear programming is classified as exact algorithm because it is guaranteed to find an optimal solution and to prove its optimality. The MILP was implemented by GAMS

(General Algebraic Modeling System), a high-level mathematical programming and optimization modeling system (Brooke 2003). GAMS consists of a language compiler and a stable of integrated high-performance solvers. The linear programming solver CPLEX 12.1 was employed to solve the model. The calculation results reveal that the answer to the first question is 5. Additionally, the solver can also find where the five points are located in the WDS in each calculation. By restricting the solution different from existing ones, a new solution, i.e., a new combination of sampling points can be derived. Finally, 98 sets of solutions were obtained, as shown in Table 2.5.

2.2.6 Optimal Sampling Locations

For the 98 sampling sets shown in Table 2.5, sampling at each combination will generate one set of solutions of wall reaction coefficients. These solutions will be equivalent if the hydraulic simulation and field measurement of chlorine are accurate. In practice, however, errors exist in chlorine measurements and hydraulic analysis. For example, if the chlorine concentration difference between the upstream and downstream nodes is small compared to the chlorine measurement error, the wall reaction coefficient calculation will contain uncertainty. In this study, hydraulic analysis is assumed to be error-free; the only uncertainty is from chlorine measurement. Therefore, these 98 sets of sampling points are not equivalent in calculating chlorine wall reaction coefficients; there exists one set of sampling locations that can best estimate wall reaction coefficients. An exhaustive method, i.e., calculating wall reaction coefficients by sampling all these 98 sets, can be used to find the best sampling location set; however, this method is costly and labor-intensive.

A sensitivity-matrix-based method was used to identify the optimal sampling set. Variance was used to represent uncertainty. The chlorine measurement variance σ_c^2 will

propagate to the estimation of wall reaction coefficient variance σ_w^2 . Sensitivities of chlorine concentrations of 29 potential sampling points to four wall reaction coefficients; $\partial C_i / \partial k_{wj}$ were calculated using a perturbation method and evaluated at the “true” values of the four wall reaction coefficients. However, in a real water distribution system, the “true” values are not known beforehand; they can only be estimated from limited sampling activities from the 98 sampling sets. The parameter estimation uncertainty σ_w^2 will decrease with the increase of efforts of sampling activities. By assuming that the wall reaction coefficients follow normal distribution and using a central limit theorem, it was determined that the randomly-selected 10 sampling sets can accurately estimate the true values of wall reaction coefficients. The average values of the 10 sets of solutions are the “true” values of the wall reaction coefficients. Using these wall reaction coefficients, the sensitivities of chlorine concentrations to wall reaction coefficients $\partial C_i / \partial k_{wj}$ were calculated, and the results are presented in Table 2.6.

Sampling on four points (since WTP is a permanent sampling point) is mathematically equivalent to picking up four rows from the 29×4 matrix; this generates a 4×4 sub matrix, which is written as J in this study. The calibration accuracy objective can be based on either prediction uncertainties or parameter uncertainties (Kapelan 2003). A-optimality and D-optimality criteria are based on parameter uncertainties, while V-optimality is based on prediction uncertainties. In this study, a D-optimality design algorithm (Savic 2009) was applied to evaluate the sampling point sets. The objective function is $F = \det((J^T J))^{1/(2 \times N_a)}$, where N_a is the number of parameters, which is four in this study. The sampling point set with the maximum F are the optimal sampling locations. The analysis results show that sampling point set {3, 5, 8, 16,

30} has the highest F value. Therefore, sampling at these five points will generate the most accurate calculation of four wall reaction coefficients, while sampling point set {2, 8, 9, 10, 30} has the lowest accuracy in calculating the four wall reaction coefficients. The best selection set is approximately four times more accurate than the worst set. The accuracy values of the 98 sets are presented in Figure 2.2.

2.3 Discussions

This study presents a novel approach to sampling location design for calibrating chlorine decay simulation. The advantage of this method, compared to the traditional iterative sensitivity matrix method, is that a prior knowledge or estimation of wall reaction coefficients is not necessary.

The study mainly investigates a sampling location design algorithm for the calibration of WDS chlorine decay simulation with first-order wall reaction in a steady-state flow condition. Its application can be extended to two directions: (1) zero order wall reaction and (2) semi-steady state, with a diurnal water demand pattern and/or chlorine injection pattern. Equation (2.9) demonstrates that this method also works at zero-order wall reaction. The only difference between the first-order and zero-order reactions is the flow mixing at the junction. As shown in Equation (2.7), in first-order wall reaction, sampling at a junction with more than one inflow and without outflows cannot be used to calculate wall reaction coefficients; in zero-order wall reaction, this limitation does not exist. By changing the sampling point matrices, the algorithm developed for first-order wall reaction can be used for zero-order wall reaction. When applied in the event of a semi-steady state, pipe flow directions must be reviewed, and the pipes whose flow directions change during the simulation period must be marked. Allowable sampling points located on or connected to these marked pipes shall be eliminated from the 29 candidate

sampling points. Therefore, by modifying only the matrices shown in Table 2.4, this methodology can be readily applied for sampling location design in a semi-steady state.

2.4 Future Work

Calibrating hydraulic parameters such as pipe friction coefficients and demands are very important. The methodology developed in this study can be used in the sampling design for calibrating hydraulic parameters. Equation (2.14) describes the friction loss inside a pipe with $J-1$ and $J-2$ at each end when the flow through the pipe is constant.

$$P_1 - P_2 = \frac{10.67 \times L \times Q^{1.852}}{C^{1.852} \times D^{4.87}} = K \times \left(\frac{Q}{C}\right)^{1.852} \quad (2.14)$$

where P_1 and P_2 are the pressures at $J-1$ and $J-2$ (m of pressure head); L is the pipe length (m); Q is the flow in this pipe (l/s); C is the friction loss coefficient; and D is the pipe diameter (cm). In this study, pipe length, diameters will both be assumed as known a priori. They are consolidated into constant K . As shown in Equation (2.14), C can be calculated after P_1 , P_2 and Q are given. However, placing pressure sensor is easier than installing flow meters. That is because most of the pipes are buried underground and only a few components such as fire hydrants are above ground. Pressure gauges can be installed on fire hydrants while flow meter can only be installed on pipes. Therefore, in our future study, calibrating pipe friction coefficients only using pressure gauges will be investigated. With the absence of flow meter, a third pressure gauge is required to calculate the flow in the pipe. This is termed three-point principle. In this future study, this principle will be fully investigated.

The major difference between calibrating chlorine decay wall reaction coefficients and friction loss coefficients is that the flow inside a pipe is known in calibrating wall reaction coefficient and it is unknown in calibrating pipe friction loss coefficients. As a result, the

sampling pair matrices used for pipe friction loss coefficient calibration will be different from those used in wall reaction coefficient calibration. For a pipe network with n pipe friction coefficients to be calibrated, each sampling pair matrix will have $n+1$ columns. This is one more than those used calibrating wall reaction coefficients. That is because flow inside a pipe is calculated as a byproduct of calibrating pipe friction coefficients.

Another modification in calibrating pipe friction coefficient is the method to sort the sampling combinations using the sensitivity matrix shown in Table 6. An alternate, sensitivity matrix based method will be used. In the modified method, true values of pipe roughness are not needed to be calculated or even estimated. Utilities engineers shall estimate the range of pipe roughness based on theirs' experiences. Each element in the matrix shows the sensitivity of pressure gauge locations to pipe friction coefficients. Instead of using regular $\partial p/\partial c$, σ_p/σ_c will be calculated to populate the matrix. Regular partial difference $\partial p/\partial c$ is based on Taylor series expansion around the mean value of the parameter and dropping the higher order terms (Tung 2005). The paradox of this approach is that the true values of the pipe friction coefficients are not known beforehand. Monte Carlo simulation (MCS) will be used to evaluate the propagation of pipe roughness σ_c to uncertainty of pressure gauge readings σ_p . The higher ratio of pressure gauges uncertainty to pipe roughness indicates this is good place to put pressure gauge for the calibration of pipe friction coefficients. MCS is a random enumeration technique in which large sets of samples is developed and evaluated. It is assumed to be correct if a sufficient large sample size is used (Kang 2009).

2.5 Conclusions

This technique was applied in a pilot water distribution system; it can be used in large-scale WDS without any changes in the algorithm since a large distribution system can

be divided into several small systems, and each small system can be calibrated individually. Future efforts will be focused on developing an efficient procedure to construct the sampling point matrices and investigating the best method to decompose big pipe network. Meanwhile, after minor modifications, this methodology can be used for the sampling design of calibrating hydraulic parameters such as pipe friction loss coefficients and demands.

2.6 References

- Baggett, C., et al. (2008). “From start to finish: Calibrating Pinellas County’s 2000-mile hydraulic water distribution system model.” *Florida Water Resour. J.*, 60(12), 44–54.
- Berry, J., Fleischer, L., Hart, W., Phillips, C., and Watson, J. (2005). “Sensor placement in municipal water networks.” *J. Water Resour. Plann. Manage.*, 131(3), 237–243.
- Berry, J., William E. Hart, W., and Phillips, C., (2006). “Sensor placement in municipal water networks with temporal integer programming models.” *J. Water Resour. Plann. Manage.*, 132(4), 218–224.
- Boccelli, D., Tryby M, Uber J, and Summers R. (2003). “A reactive species model for chlorine decay and THM formation under rechlorination conditions.” *Water Research*, 37(11), 2654–2666.
- Bremond, B., Chesneau, O., and Piller, O., (2003). “Calibration methodology for a residual chlorine-decreasing model in drinking water networks.” In: P. Bizier and P. DeBarry, eds. *World Water Congress*, Vol. 118. Philadelphia: ASCE, 270.
- Brooke A., Kendrick, D., Meeraus, A. and Raman, R. (2003). *General Algebraic Modelling System: a User’s Guide*. Washington DC: Commun.
- Bush, C., and Uber, J. (1998). “Sampling design methods for water distribution model calibration.” *J. Water Resour. Plann. Manage.*, 124 (6), 334–344.
- Cozzolino, L., Pianese, D., and Pirozzi, F. (2005). “Control of DBPs in water distribution systems through optimal chlorine dosage and disinfection station allocation.” *Desalination*, 176(1-3), 113–125.
- Fabrie, P., Gancel, G., Mortazavi, I., and Piller, O. (2010). “Quality modelling of water distribution systems using sensitivity equations.” *J. Water Resour. Plann. Manage.*, 136(1), 34–44.
- Jonkergouw, P., Khu, S., Kapelan, Z., and Savić, D. (2008). “Water quality model calibration under unknown demands.” *J. Water Resour. Plann. Manage.*, 134(4), 326–336.

- Kang, D., (2009). "Approximate methods for uncertainty analysis of water distribution systems." *Urban Water Journal*, 6(3), 233–249.
- Kapelan, Z., Savic, D., and Walters, G. (2005). "Optimal sampling design methodologies for water distribution model calibration." *J. Water Resour. Plann. Manage.*, 131(3), 190–200.
- Kapelan, Z., Savic, D., and Walters, G. (2003). "Multiobjective sampling design for water distribution model calibration." *J. Water Resour. Plann. Manage.*, 129 (6), 466–479.
- Lansey, K., El-Shorbagy, W., Ahmed, I., Araujo, J., and Haan, C. (2001). "Calibration assessment and data collection for water distribution networks." *J. Hydraulic Eng.*, 127(4), 270–279.
- Martiny, A., Albrechtsen H, Arvin E, and Molin S. (2005). "Identification of bacteria in biofilm and bulk water samples from a nonchlorinated model drinking water distribution system: Detection of a large nitrite-oxidizing population associated with nitrospira spp." *Applied and Environmental Microbiology*, 71(12), 8611–8617.
- Meier, R., and Barkdoll, B. (2000). "Sampling design methods for network model calibration using genetic algorithm." *J. Water Resour. Plann. Manage.*, 126(4), 245–250.
- Mutoti, G., Dietz, J, Arevalo, J, and Taylor, J. (2007). "Combined chlorine dissipation: Pipe material, water quality, and hydraulic effects." *J. AWWA*, 99(10), 96–106.
- Nemhauser, G., Laurence A., and Wolsey, L. (1988). *Integer and Combinatorial Optimization*. New York: John Wiley and Sons.
- Propato, M., and Uber, J. (2004). "Booster system design using mixed-integer quadratic programming." *J. Water Resour. Plann. Manage*, 130(4), 348–352.
- Rossman, L., (2000). *EPANET2 User's Manual*. USEPA.
- Savic, D., Kapelan Z. and Jonkergouw, P. (2009). "Quo vadis water distribution model calibration?" *Urban Water J.*, 6(1), 3–32.
- Shang, F., (2005). *Path-dependent approach to estimate chlorine wall demand coefficient in water distribution system*. Thesis (PhD). University of Cincinnati.
- Speight, V., Kalsbeek, W, and DiGiano, F. (2004). "Randomized stratified sampling methodology for water quality in distribution systems." *J. Water Resour. Plann. Manage*, 130(4), 330–338.
- Tung, Y., (2005). *Hydrosystems engineering uncertainty analysis*. New York, McGraw-Hill.

USEPA, (2006). The effectiveness of disinfectant residuals in the distribution system. Office of Ground Water and Drinking Water, Washington DC

Vasconcelos, J., Rossman, L., Grayman, W., Boulos, P., and Clark R. (1997). “Kinetics of chlorine decay.” *J. AWWA*, 89(7), 54-65.

Walski, T., (2000). “Model calibration data: The good, the bad, and the useless.” *J. AWWA*, 92(1), 94–99.

Walski, T., (1983). “Technique for calibrating network models.” *J. Water Resour. Plann. Manage.*, 109(4), 360–372.

Wu, Z., (2006). “Optimal calibration method for water distribution water quality model.” *J. Environ. Sci. and Health, Part A*, 41, 1–16.

Table 2.1 WDS nodal demands

Node ID	Demand (l/m)	Node ID	Demand (l/m)	Node ID	Demand (l/m)
SP-1	37.8	3	37.8	23	75.6
SP-5	68.04	4	37.8	24	37.8
SP-6	75.6	7	37.8	25	226.8
SP-12	37.8	9	56.7	28	75.6
SP-13	37.8	10	151.2	30	75.6
SP-15	68.04	11	37.8	32	45.36
SP-20	75.6	12	75.6	33	37.8
SP-27	37.8	14	37.8	34	83.16
SP-28	75.6	15	75.6	36	37.8
		19	75.6	40	75.6

Table 2.2 WDS pipe data

ID	Length (m)	Diameter (cm)	Roughness	Type
P1	61	40.64	115	3
P2	111	25.4	105	2
P3.1	40	25.4	105	4
P3.2	43	25.4	105	4
P4.1	42	25.4	115	1
P4.2	152	25.4	120	1
P4.3	61	25.4	115	1
P5	140	25.4	105	2
P6	79	20.32	115	3
P7	126	20.32	115	1
P8	82	20.32	115	3
P9	81	20.32	115	2
P10	79	20.32	115	3
P11.1	61	20.32	115	1
P11.2	152	20.32	115	1
P11.3	73	20.32	115	1
P12	109	20.32	115	1
P13	78	20.32	115	2
P14.1	73	20.32	115	1
P14.2	136	20.32	115	1
P15.1	110	20.32	115	2
P15.2	67	20.32	115	2
P16.1	61	20.32	115	2
P16.2	129	20.32	115	2
P17.1	67	20.32	115	2
P17.2	12	20.32	115	2
P18	85	20.32	115	3
P19	61	20.32	115	3
P20	91	20.32	115	3
P21.1	122	20.32	115	1
P21.2	122	20.32	115	1
P22.1	122	20.32	115	4
P22.2	84	20.32	115	4
P23.1	67	20.32	115	4
P23.2	61	20.32	115	4
P24	57	20.32	115	4
P25.1	55	20.32	115	4
P25.2	21	20.32	115	4
P26	82	20.32	115	4
P27	85	20.32	105	4
P28.1	90	20.32	115	4

Table 2.2 (Continued)

ID	Length (m)	Diameter (cm)	Roughness	Type
P28.2	21	20.32	115	4
P29	79	20.32	115	4
P30	81	20.32	125	3
P31.1	61	20.32	125	1
P31.2	152	20.32	125	1
P31.3	52	20.32	115	1
P32.1	92	20.32	125	1
P32.2	152	20.32	125	1
P32.3	69	20.32	125	1
P33.1	76	20.32	125	2
P33.2	40	20.32	125	2
P34.1	152	20.32	125	1
P34.2	113	20.32	125	1
P35	70	20.32	125	3
P36	81	20.32	125	3

Table 2.3 Chlorine concentration relationship investigations

Case	Number of pipe sections	Flow directions	Number of k_w involved	Example
1	1	1	1	<i>P21.2</i> between <i>SP-4</i> and <i>SP-5</i>
2	2	1	1	<i>P25.2, P22.1</i> between <i>SP-3</i> and <i>SP-16</i>
3	>2	1	1	<i>P3.2, P24, P25.1</i> between <i>SP-2</i> and <i>SP-3</i>
4	2	1	2	<i>P4.3, P6</i> between <i>SP-11</i> and <i>SP-12</i>
5	2	1	2	<i>P2, P3.1</i> between <i>SP-1</i> and <i>SP-2</i>
6	2	2	1	<i>P19, P20</i> between <i>SP-5</i> and <i>SP-6</i>

Table 2.4 Matrix 30 components

Sampling points	k_{w1}	k_{w2}	k_{w3}	k_{w4}
1	0.00	1.00	1.00	0.00
2	0.00	0.00	1.00	1.00
3	0.00	0.00	0.00	0.00
...
29	0.00	0.00	0.00	0.00
30	0.00	0.00	0.00	0.00

Table 2.5 List of sampling points

Sampling points				
1	2	4	9	30
1	3	5	16	30
---	---	---	---	---
9	10	11	17	30

Table 2.6 Sensitivity matrix

Sampling points	$\partial C_i / \partial k_{w1}$	$\partial C_i / \partial k_{w2}$	$\partial C_i / \partial k_{w3}$	$\partial C_i / \partial k_{w4}$
1	0.00	0.09	0.03	0.00
2	0.00	0.00	0.03	0.04
3	0.00	0.00	0.03	0.22
4	0.37	0.00	0.03	0.23
5	0.70	0.00	0.03	0.22
6	0.00	0.66	0.36	0.05
7	0.00	0.72	0.03	0.07
8	0.00	0.44	0.03	0.07
9	0.00	0.20	0.03	0.07
10	0.07	0.00	0.04	0.00
11	0.29	0.00	0.04	0.00
12	0.36	0.00	0.13	0.00
13	0.57	0.06	0.05	0.00
14	0.73	0.24	0.05	0.00
15	0.70	0.23	0.14	0.00
16	0.00	0.00	0.02	0.52
17	0.28	0.00	0.21	0.27
18	0.98	0.21	0.25	0.00
19	1.50	0.18	0.22	0.00
20	0.18	0.22	0.05	0.06
21	0.17	0.21	0.05	0.21
22	0.31	0.19	0.05	0.28
23	0.69	0.17	0.03	0.25
24	1.10	0.15	0.03	0.23
25	1.45	0.13	0.03	0.20
26	0.40	0.73	0.01	0.05
27	0.14	0.18	0.18	0.27
28	0.11	0.14	0.46	0.21
29	1.12	0.10	0.33	0.15

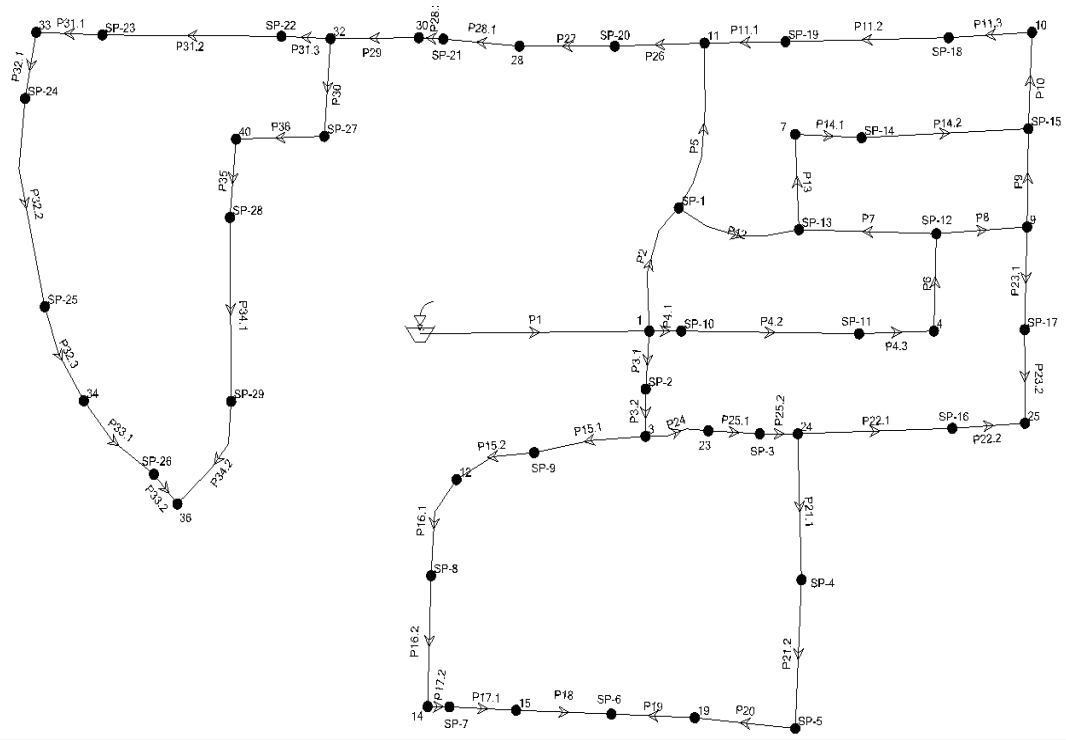


Figure 2.1 Schematic pipe layout

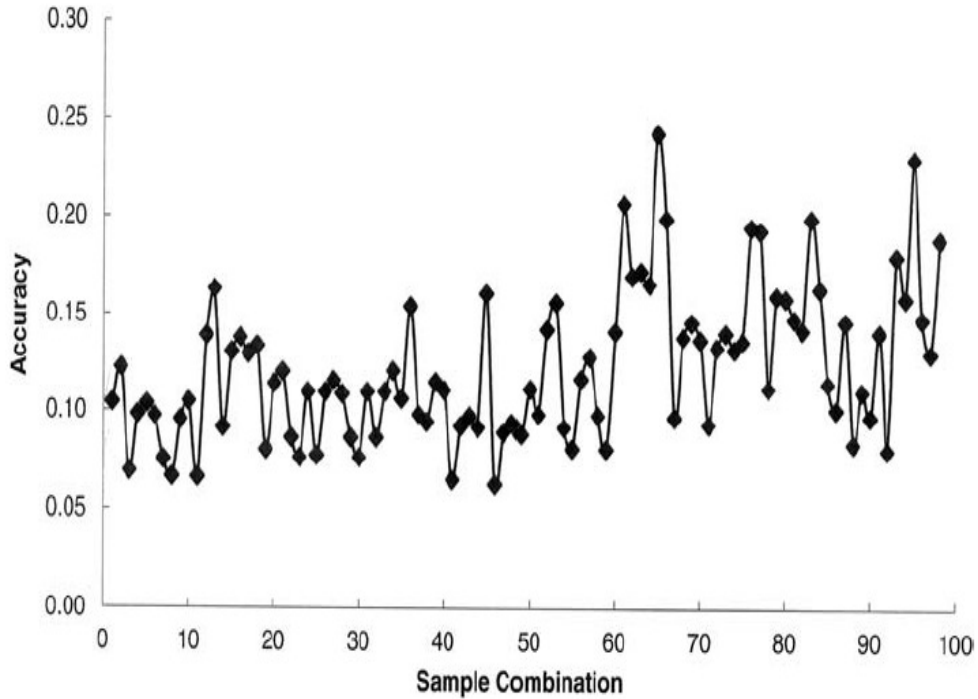


Figure 2.2 Objective function values

Chapter 3: Optimal Scheduling of Automatic Flushing Devices in Water Network²

3.1 Introduction

Drinking water is produced at water treatment facilities and delivered to end users through a water distribution system. In addition to supplying potable water, the water system is sized for fire flows. Florida Administrative Code (FAC) (2003) requires the minimum size of the water main serving fire hydrants shall be 15 cm (6 inches), which is significantly oversized from a regular water consumption perspective. This leads to extended retention of water in a pipe network and degraded water quality. Maintaining sufficient disinfectant residual, termed secondary disinfection, helps to maintain water quality and the integrity of the water system. The most commonly used secondary disinfectants in the United States are chlorine and chloramines (U.S. Environment Protection Agency 2006). The Pinellas County water distribution system in Florida uses chloramines as secondary disinfectant. Operation experiences show keeping total chlorine residual above 2.0 mg/l is crucial for controlling nitrification in this utility (Hua 2011).

Typical methods for maintaining chlorine residual include: (1) injecting chlorine into water network through booster stations (Munavalli 2003, Boccelli 1998); (2) replacing aged metal pipes such as galvanized steel and ductile iron pipes with new PVC pipes (Al-Jasser 2007, Hua 2011); and, (3) flushing distribution pipes to deplete un-chlorinated water (Friedman 2002).

² Note: Part of this chapter was published in Journal of Water Resource Planning and Management (10.1061/(ASCE)WR.1943-5452.0000477). Permission is included in Appendix A.

Options 1 and 2 both require high capital investment. Therefore, they remain beyond the routine means of many water utilities. Option 3 requires no modification of existing infrastructure, it only involves operation optimization. Therefore, it is widely used by water utilities. However, utilities operators normally perform pipe flushing based on their experiences. It is imperative for the water utilities to investigate whether current flushing practice is optimal, e.g., flushing volume can be reduced. Minimizing flushing water volume can save water production and distribution costs, alleviate low pressure complaints and negative public perception, and conserve water resources. As a result, it is beneficial not only to water utilities, and the public, but also to the environment, especially in the context of ever-increasing energy price and water demand.

Water utilities normally perform two types of flushing operations: conventional flushing and unidirectional flushing (UDF). Conventional flushing is accomplished by opening fire hydrant manually or operating automatic flushing device (AFD). Conventional flushing is normally used to replace poor quality water and raise disinfectant residuals, not intended to remove scales and tuberculation attached to pipe wall (Friedman 2002). FAC (2010) regulates a water supplier shall flush potable water main dead-ends quarterly or develop a written flushing program and implement accordingly. UDF removes deposits and debris attached to pipe walls using a single-direction, high velocity flow (≥ 1.5 m/s) created by isolating a particular pipe section of loop (Barbeau 2005, Carriere 2005). UDF needs careful planning, and heavy labour (Friedman 2002, Lehtola 2004, Husband 2010). Consequently, it is not suitable for routine maintenance of water distribution system. This research therefore studied optimization of conventional flushing. An AFD typically comprises flush piping, solenoid valve, and a programmable controller. The flushing pipe is connected to the dead end of potable water line.

The solenoid valve is mounted to the flushing pipe. The programmable controller opens and closes the solenoid valve. Operating AFD needs less labour than manually opening a fire hydrant. Therefore, AFDs are gaining popularity in water utilities. For example, Pinellas County installed 55 AFDs at strategic locations in its water system (Hua 2012). Records in 2009 showed 70% of flushed water in this system was discharged via AFDs. The potable water network in City of Saint Petersburg, Florida has eight AFDs (Riera 2012). AFDs are reported to be installed in water utilities in Birmingham Alabama, Clayton County Georgia, Naples and North Miami Beach Florida (Benson, 2010).

This study focuses on studying AFD operations to minimize their total daily flushing volume. AFD can be operated either by timer or chemical sensor, e.g. chlorine sensor (Benson 2010). However, two reasons limit the wide use of chlorine sensor. First, manufacturing, installation, operation, and maintenance costs of chlorine sensor are high. Chlorine sensor controlled AFD is approximately three times more costly than timer controlled AFD. Second, chlorine sensor is not capable of temporally and spatially capturing the lowest chlorine residual in the pipe network. Chlorine residual in any demand node in a water network is time-dependent due to diurnal variations of the water consumptions and system operations. The prerequisite for maintaining certain level of chlorine residual is to identify the lowest chlorine concentration, referred to as Lowest Chlorine, and its location in the pipe network, termed Lowest Node in this study. Figure 4.1 shows a chlorine concentration curve of Lowest Node in a 24-hour duration. In addition to Lowest Chlorine, three concepts associated with Lowest Node are created: Highest Chlorine, Lowest Moment and Highest Moment. Highest Chlorine is the highest chlorine residual of the Lowest Node in the 24-hour duration. Lowest Moment is the moment when Lowest Chlorine occurs. Highest Moment is the moment when Highest Chlorine occurs.

Chlorine sensors can not locate Lowest Node and quantify the four associated parameters because it is financially infeasible to install chlorine sensors everywhere in the water network. The least expensive method of locating Lowest Node is using a full scale, well calibrated water quality model. Therefore, using timer controlled AFD working in tandem with a water model is a feasible method to minimize AFD discharge. Currently, most AFDs in water utilities are controlled by timers. For example, all the 55 AFDs in the Pinellas County water system are timer controlled.

Literature review shows that no studies have been directly aimed at minimizing AFD discharge. Similar researches such as pump scheduling optimization to minimize energy costs were reviewed. A variety of optimization algorithms on pump scheduling have been developed. Examples include Boolean integer nonlinear programming (BINLP) (El Mouatasimm 2012), evolutionary algorithm (Lopez-Ibanez 2009), ant colony algorithm (Lopez-Ibanez 2007) and linear programming greedy (LPG) algorithm (Giacomello 2013), to name a few. This study presents a simulation-optimization method to minimize the flushing volume through AFDs. This is formulated as a single objective operation optimization problem.

3.2 Methodology

3.2.1 Model Formulation

Consider a water distribution system with J junctions, M demand nodes, N AFDs, which are operated for T time intervals for a 24-hour time horizon. The objective function is the minimization of the total AFD discharge volume of these AFDs within one day:

$$\text{Minimize } E = \sum_{t=1}^T \sum_{n=1}^N Q_{n,t} \times L \quad (3.1)$$

where $Q_{n,t}$ = the discharge rate of AFD n at time t (L/min); and L = chlorine simulation time step (min). This optimization problem is subject to three constraints: hydraulics, water quality, and operation. They are given as

$$P_{j,t} \geq P_{\min} \quad 1 \leq j \leq J, \quad 1 \leq t \leq T \quad (3.2)$$

$$C_{m,t} \geq C_{\min} \quad 1 \leq m \leq M, \quad 1 \leq t \leq T \quad (3.3)$$

$$S_n \leq S_o \quad 1 \leq n \leq N \quad (3.4)$$

where $P_{j,t}$ = pressure at Junction j at time t (m of head); P_{\min} = minimum allowable pressure in the water system (m of head); $C_{m,t}$ = chlorine residual of Node m at time t (mg/l); C_{\min} = specified minimum chlorine concentration (mg/l); S_n = number of starts for AFD n ; and, S_o = maximum allowable AFD starts per day.

This study performs hydraulic and water quality simulations using EPANET 2.0 (Rossman 2000) and take pipe network topology, base demands and diurnal patterns of regular water nodes as given. Chlorine concentrations of all the nodes are functions of the AFD discharge rates. They are given as

$$C_{m,t} = H_m(Q_{1,t} \quad \dots \quad Q_{n,t} \quad \dots \quad Q_{N,t}) \quad (3.5)$$

In theory, $C_{m,t}$ rises with the increase of the discharge rate $Q_{n,t}$ because high AFD discharge rates result in reduced water age, which raises chlorine residual. Equation (3.5) implies laws of mass balance and energy conservation, which are highly nonlinear for a water network. So this optimization problem is highly nonlinear, and has no theoretical solutions.

Two parameters can describe the AFD working status: flow rate and open/close state. Accordingly, the instantaneous discharge rate $Q_{n,t}$ for each AFD is decomposed as a base discharge rate multiplying the open/close status of the AFD. It is given as

$$Q_{n,t} = Q_n \times I_{n,t} \quad (3.6)$$

where Q_n = base discharge rate for AFD n (L/min); and, $I_{n,t}$ = the open/close status of AFD n at time t . It is a binary constant, 1 to show AFD is open, and 0 to indicate that AFD is closed. Therefore, a vector with T binary elements represents the open/close status of AFD n within a 24-hour horizon.

The flowchart for calculating globally minimal AFD discharge volume is shown in Figure 3.2. To more efficiently search optimal minimum, the problem is solved in three phases. Phase one includes steps 1 to 6. It calculates AFD flow capacities, and evaluates whether a water network is capable of maintaining sufficient chlorine residual at existing AFD layout. Phase two includes steps 7 to 14; it uses a gradient-based method to quickly explore and narrow down the solution space. Phase three includes steps 15 to 41; it intensively exploits the AFD operation patterns using simulated annealing (SA). These phases have to be performed sequentially; results of phases one and two are the inputs to phases two and three respectively. Optimization methodology is programmed using Matlab 7.0 (Hanselman 2005).

3.2.2 Phase I: Calculating AFD Flow Capacities

The discharge rate of one specific AFD is dependent on system pressure, which is determined by the water demands of all regular nodes and other AFDs in a water network. Ideally, all AFDs shall be simulated as flow emitters, using the available functionality in EPANET 2.0. In this study, however, AFDs are turned on and off to minimize the total discharge volume. The best way in EPANET is to simulate AFDs as demand-driven nodes with their individual operation patterns. In step 1 of the flowchart, all AFDs are simulated as flow emitters with constant discharge coefficients, and model all regular nodes as demand-driven nodes with their diurnal water use patterns. The assumption on regular nodes is valid when

water system pressure is adequate for delivering the required nodal demands (Wu 2006). Q_n falls into a range due to system pressure fluctuations. The mean of the range \overline{Q}_n is used as the discharge capacity for AFD n , as shown in step 2 of the flowchart. In the following steps of the flowchart, all the nodes including AFDs, are modeled as demand-driven nodes.

In step 3, all the AFDs are open all the time; then use EPANET 2.0 to simulate chlorine residuals (step 4 of the flowchart). Step 5 determines if Lowest Chlorine is lower than C_{min} . An answer of “yes” indicates existing AFDs are not able to maintain chlorine residuals, water utilities have to install more AFDs or modify the AFD layout (step 6). This triggers capital investment or AFD location optimization; which is not discussed herein. If Lowest Chlorine is higher than C_{min} , the AFD discharge volume can be reduced until Lowest Chlorine is lower than C_{min} . This is accomplished by decreasing AFD open durations. In this study, open duration D is defined as the total open minutes of one AFD in a 24-hour horizon. It is given as:

$$D_n = L \times \sum_{t=1}^T I_{n,t} \quad (3.7)$$

Therefore, the research is a discrete-control optimization problem and the decision variables are AFD operation patterns.

To solve this highly nonlinear problem, multiple calculation cycles, or trials, are needed (Phase II hereafter). In each calculation cycle, EPANET 2.0 identifies the Lowest Node and calculates the Lowest and Highest Chlorines, and Lowest and Highest Moments. Meanwhile, the open duration of each AFD is reduced from that in the previous cycle at a pace based on the Lowest Chlorine simulated in the previous calculation cycle. Too slow reduction will require excessive computational efforts. Too fast reduction will result in calculation oscillation and the generation of invalid results.

3.2.3 Phase II: Exploring AFD Operation Durations

From the viewpoint of calculating water discharge volume, turning on AFD n with reduced open durations is equivalent to turning on a smaller AFD (denoted as AFD ns) all the time in the 24-hour duration (1,440 minutes). This is given as:

$$D_n = \frac{1,440 \times Q_{ns}}{Q_n} \quad (3.8)$$

where Q_{ns} is the flow capacity of AFD ns (L/min). Note that AFD ns is imaginary. Replacing existing AFD with a smaller AFD is a computational technique that will not occur in the field (step 7). Using this technique, this study converts the problem from solving AFD n operation patterns to sizing the flow capacity of AFD ns . This conversion reduces the number of decision variables from $N \times T$ to N . For a network having one AFD ($N=1$) and one hour time step in a 24-hour horizon ($T=24$), the number of decision variables reduces from 24 to 1. Therefore, the conversion will accelerate the computation.

Parameter k in step 7 of the flowchart counts the number of calculation cycles needed to obtain the global minimum of AFD flow capacities. At this step, the flow capacity of the imaginary AFD ns equals \overline{Q}_n . In step 8 of the flowchart, flow capacity Q_{ns} decreases at a pace proportional to the difference between the chlorine residual at AFD ns calculated at the previous cycle and the C_{min} . It is termed reduced gradient algorithm in this study, which is shown below

$$Q_{ns,k+1} = Q_{n,k} \times \left(1 - \frac{(C_{ns,k} - C_{min})}{10} \right) \quad (3.9)$$

where $Q_{ns,k}$ = flow capacity of the AFD ns at k^{th} calculation cycle (L/min); and, $C_{ns,k}$ = minimum instantaneous chlorine concentration of the AFD ns at the k^{th} cycle (mg/l). Constant 10 is used in Equation (3.9) for two reasons. First, it guarantees that term on the right side of the

equation is positive since chlorine concentration in water network is normally no more than 10 mg/l. Second, it ensures the flow capacity Q_{ns} decreases at an appropriate pace. Step 9 arbitrarily increases the AFD discharge rates for the purpose of searching the global minimum of AFD flow capacities. At the end of each calculation cycle, flow capacities of these imaginary AFD are saved. Steps 8 to 12 are repeated until C_{min} is violated. As shown in step 13, the flow capacities of AFDs in $(k-1)^{th}$ cycle are the optimal flow capacities for these imaginary AFDs.

Equation (3.8) calculates AFD operation duration D_n based on the flow capacity of AFD ns . By doing this, the decision variables change back to the AFD n operation patterns (step 14). The outputs of this phase of study are the open durations for all AFDs. The detailed operation pattern for each AFD will be solved in phase three.

3.2.4 Phase III: Exploiting Optimal AFD Discharge Patterns

Prior to searching for optimal AFD operation patterns, two concepts are created: sensitive and non-sensitive AFD. Sensitive AFD is an AFD whose operation pattern substantially affects the chlorine residual of Lowest Node. Non-sensitive AFD is an AFD whose operation pattern insignificantly affects the chlorine residual of Lowest Node. Since every node in a pipe network can potentially be the Lowest Node, it is necessary to determine sensitive and non-sensitive AFDs for each node. A sensitivity matrix with M rows and N columns is created after performing $N+1$ water quality simulations in the 24-hour horizon. In the n^{th} simulation, AFD n is turned on and all other AFDs are turned off. In the $(N+1)^{th}$ simulation, all the AFDs are closed. Due to demand fluctuations, chlorine concentration of Node m is time-dependent in the 24-hour horizon.

The element of m^{th} row and n^{th} column of the sensitivity matrix is $\frac{\overline{C}_{m,n} - \overline{C}_{m,0}}{Q_n}$, where

$\overline{C}_{m,n}$ is the average chlorine residual of Node m when AFD n is turned on; and $\overline{C}_{m,0}$ is

the average chlorine residual of Node m when all the AFDs are turned off. In each row of the

sensitivity matrix, the mean, $\frac{\sum_{n=1}^N \frac{\overline{C}_{m,n} - \overline{C}_{m,0}}{\overline{Q}_n}}{N}$, is used to differentiate sensitive and non-

sensitive AFDs for Node m . Those AFDs whose sensitivities are higher than the mean are defined as sensitive AFDs to Node m , and the remaining AFDs are non-sensitive to Node m .

Decision variables in this phase of study are N vectors, each has T binary variables. The whole search space has $2^{N \times T}$ combinations. For a simple system having one AFD ($N=1$) and an hourly AFD operation pattern ($T=24$), the search space has $2^{24}=16,777,214$ combinations. The solution space for the Pinellas County water system with 55 AFDs is like a mountainous region with multiple valleys. The bottom of each valley is a local minimum, and the bottom of the deepest valley is the global minimum. The feasible region to this question is discrete. A widely used gradient method alone cannot guarantee finding the global minimum. A heuristic method, such as simulated annealing (SA), is a desirable tool in solving this problem.

The open duration D_n calculated using Equation (3.8) is used to create an initial operation pattern of AFD n (see step 15 in Figure 3.2). For example, D_n is 100 minutes in the 24-hour horizon. Assume the water quality simulation time step to be 5 minutes; the 24-hour horizon is divided into 288 consecutive time intervals. 20 elements will be “1” and they are randomly distributed into 288 time intervals by conforming to Equation (3.4). The remaining 268 elements will be populated with 0.

Steps 16 and 17 of the flowchart simulate and determine if the Lowest Chlorine under the current AFD operation patterns is above C_{min} . When the Lowest Chlorine is lower than C_{min} , AFD open durations shall be increased until Lowest Chlorine is higher than C_{min} . Steps 18 and 19 in Figure 3.2 show the effort. Three questions are investigated: 1) which AFDs to

choose; 2) for the selected AFDs, increase the open durations at which moments; and, 3) for the selected AFDs, how to increase the operation durations in each calculation cycle. The answers to the first and second questions are sensitive AFDs of the Lowest Node and Lowest Moment. When some sensitive AFDs have been turned on at Lowest Moment, the first following closed moment for these AFDs shall be turned on. The answer to the third question is determined by the difference between the C_{min} and Lowest Chlorine, ΔC . Big ΔC means substantial increases in the AFD open durations. This question has no absolute answer.

Steps 20 to 26 show how to achieve a local minimum of objective function by gradually reducing AFD open durations. This is similar to rolling a ball downhill to a valley bottom. Parameter k shown in Step 20 is the same as that in step 7. Three questions are investigated to improve the efficiency of searching for the local minimum: 1) which AFDs to choose; 2) for the selected AFDs, reduce the discharge durations at which moments; and, 3) for the selected AFDs, how to reduce the operation durations in each calculation cycle. The answers to the first and second questions are non-sensitive AFDs of the Lowest Node and Highest Moment. When some non-sensitive AFDs have been turned off in the Highest Moment, first following open moment for these AFDs shall be turned off. The answer to the third question is determined by the difference between the Lowest Chlorine and C_{min} . Big difference means substantial reductions in AFD open durations. This question has no absolute answer. Step 26 of the flowchart shows one local minimum of objective function is achieved (at $(k-1)^{th}$ cycle). After obtaining one local minimum, the search goes to a new valley. This is accomplished by randomly reorganizing the AFD operation patterns (step 27 of the flowchart). The new operation pattern for each AFD has to meet the constraint shown in Equation (3.4). Steps 28 to 31 show the computational efforts to ensure the Lowest Chlorine is higher than C_{min} .

This study chooses SA to search global minimum for two reasons. First, SA is simple. It is a heuristic stochastic optimization approach, and does not require derivatives. This makes it a desirable tool when the search space is discrete or the problem structure is insufficiently understood (Bertsimas 1993). Second, SA is accurate. It converges to global optimal solution with probability of one. In other words, if computational time allows being forever, SA can find global optimal solution (Ingber 1993). Other popular heuristic methods, such as Genetic Algorithm, do not offer any statistical guarantee of global convergence to an optimal solution (Savic 2009). SA has been reported in water distribution system pump scheduling optimization (Sousa 2006, Goldman 1998, 2005), and water network design (Tospornsampan 2007, Cunha 1999). In addition, it has been applied in water resource engineering (Teegavarapu 2002, Wang 2009) and irrigation water system design (Martinez 2008, Monem 2005), to name a few. In this study, “temperature” TE is also used as an analogy with the original application in metal heat treatment. System energy E is the objective function shown in Equation (3.1). System energy difference ΔE is the discharge volume difference in the previous valley bottom and first point in the new valley. Before implementing SA, the following parameters are determined: beginning temperature TE_b , ending temperature TE_e , and temperature decay constant α . TE_b is given by

$$TE_b = -\Delta E / \ln(0.8) \quad (3.10)$$

where 0.8 shows that a change which increases the objective function will be accepted with 80% probability. TE_e is given by

$$TE_e = -\Delta E / \ln(0.001) \quad (3.11)$$

where 0.001 shows that a change which increases the objective function will be accepted with 0.1% probability. Temperature decreases according to an exponential cooling scheme.

The SA determines whether a jumping to a new valley (step 32 in Figure 3.2) is acceptable. Steps 27 to 32 will be repeated until SA accepts the jumping to a new valley. Searching a new local minimum is performed thereafter (steps 33 to 39). In step 40 of the flowchart, SA system temperature reduces according to the cooling scheme. The searching of multiple local minima terminates when the following conditions occur: (1) no improvements occur in an entire Markov chain at one SA system temperature; i.e., the ball fails to bounce out of a valley bottom after multiple trials; (2) SA system energy reaches the ending temperature TE_e ; and, 3) no substantial improvements are accomplished before the SA system energy reaches the ending temperature (step 41).

Parameter F in steps 26 and 39 of the flowchart counts how many local minima have been obtained. These local minima form a set, the lowest value of the set is the global minimum for this optimization problem (step 42).

3.3 Case Study

3.3.1 Network Description

The Pinellas County water distribution system serves approximately half a million people. Chloramines are used as secondary disinfectant. Nitrification is a serious issue for this utility. Survey indicated that 30% of chloraminated water systems in the United States had experienced nitrification episodes. Of these utilities having nitrification issues, 54% flush the networks to control nitrification (Seidel 2005).

The studied pipe network is at the south end of the Pinellas County water system (Figure 3.3). It is referred to as the Gulf Beach system because all end users receive potable water from the Gulf Beach pump station. The distance from the pump station to the south end is approximately 8 kilometres. The full scale water network has been digitized and has 1,116

junctions, 855 demand nodes, 1,200 links and 14 AFDs. They are numbered from AFD-37 to 50 by County operators. The same labels are used in this study for consistency. This study investigated this pipe network for two reasons. First, the Gulf Beach pump station only serves the water users in this pipe network. So this network is an isolated system. Second, the selected pipe network is located in a coastal area with numerous small islands and marinas. The distribution pipes serving these small islands have many dead ends that have low water consumptions and are costly to be looped. Pinellas County has to flush large volumes of stagnant water every day to maintain minimum chlorine residual of 2.0 mg/l for the water users located along the dead end pipes. Water use records in recent years indicated that County water treatment plant provided approximately 220,000 m³/d of drinking water. 2.6%, i.e., 5,800 m³/d were flushed out via AFDs and fire hydrants. In the same duration, the Gulf Beach pump station supplied 5,300 m³/d of drinking water. 48.1%, i.e., 2,550 m³/d were flushed via the 14 AFDs. So it is compelling for Pinellas County to investigate the feasibility of reducing total AFD discharge volume in the Gulf Beach system. The studied water system has one chlorine source, which is located at the pump station. The chlorine concentration at the discharge point maintains at 4.0 mg/l. Historical data showed that discharge pressures in this pump station ranged from 38.7 to 54.8 m of head (55-78 psi). Low pressure is not an operation issue during low AFD discharges. Therefore, it is suitable to simulate regular nodes in this pipe network as demand-driven nodes in hydraulic and water quality simulations. Low pressure complaints have been recorded in the south end during high AFD discharges. This proves the necessity of minimizing the AFD discharge.

The Gulf Beach system serves a small city located at the upper part of Figure 3.3, and Fort Desoto County Park located at south end of the pipe network. The major economy in the

small city is tourism and retail business. So the water use of the small city follows domestic water use pattern. The small city has a population of approximately 6,000 to 7,000. The park has no permanent residents. Records in 2012 showed that on average 4,000 tourists visited this park every day. The park opens from 7AM to 7 PM every day, and no regular water consumption occurs between 7 PM and 7 AM of the next day. Annual average daily water uses from March 2012 to February 2013 of the Gulf Beach system are provided in Table 3.1. The second and third rows list the regular water consumptions of the park and small city. The fourth row is the summary of the average daily discharge rates through the 14 AFDs. This is the quantity Pinellas County wants to reduce.

3.3.2 Simulation Parameters Setup

This study assumes that the network hydraulics is periodic over simulation duration. Once repeatable behaviour is established, the last period of the simulation period is saved for analysis. After multiple trials, that EPANET simulation duration was determined as 10 days. The simulation results of last 24 hours were saved for analysis. The hydraulic and water quality time steps were both set at five minutes. All the water users in the small city were assigned with identical hourly diurnal pattern (Figure 3.4), which was calculated using the County's water use records. With regard to the park, it was assumed that regular water use is held constant during the 12 open hours (Figure 3.4).

Excessive turnings on/off may result in premature failure of AFDs. As a result, the Pinellas County water system operators recommend that AFD to be turned on no more than four times per day. This limitation was incorporated into the research. All the 14 AFDs are identical and have 5 cm (2-inch) PVC discharge pipe. Using the AFD performance curve, the discharge coefficient was calculated to be $68 \text{ lpm/m}^{0.5}$ ($15 \text{ gpm/psi}^{0.5}$). The pipe network shall

maintain a minimum pressure of 14 m of head (20 psi). In the chlorine decay simulation, bulk and wall reactions are both first order. The bulk chlorine decay coefficient is 0.07/day. It was achieved by collecting water samples in the water network and testing in the County's chemical lab (Baggett 2008). The wall reaction coefficients range from 0.012-0.016 m/day (0.041-0.054 ft/day); they were calibrated using field data.

With regard to the SA parameters, the investigation suggested that the average objective function increase ΔE was 60 m³/d. As a result, the beginning "temperature" TE_b was 270 m³/d; the ending "temperature" TE_e was 9 m³/d. The temperature decay constant α was set at 0.95.

3.4 Results and Discussions

The discharge rates of the AFDs are shown in Table 3.2. It reveals that the AFD discharge rates vary within $\pm 10\%$ of their average flows. This suggests that AFD discharge rates are weakly affected by system pressure fluctuations. In the subsequent study, the values shown in the fourth column of Table 3.2 were used as flow capacities of these AFDs (step 2 in the flowchart). Therefore, all the nodes, including AFDs, were simulated as demand-driven nodes thereafter. The simulation results also show that when all the AFDs are opened all the time in the 24-hour horizon, the Lowest Chlorine is 3.1 mg/l, minimum system pressure is 5.2 m of head (7.4 psi) and total AFD discharge volume is 7,817 m³/d. That suggests: 1) existing AFDs are capable of maintaining water quality, the water utility does not need to install new AFDs; and, 2) opening all the AFDs all the time will cause pressure deficiency in the water network (step 5 in the flowchart).

As illustrated in step 9 in Figure 3.2, flow capacities of the imaginary AFDs are randomly increased to avoid being trapped into a local minimum. In this study, a sensitivity analysis was performed to obtain a suitable increase ratio. Three ratios were chosen: 0, 5 and 10%. In each

calculation cycle, two AFDs were randomly selected to increase their flow capacities from previous calculation cycle at the specified ratio. The evolutions of total discharge volume of the 14 AFDs are presented in Figure 3.5. It shows that when employing 10% increase of AFD flow capacities, the total discharge volume of the 14 AFDs is 684 m³/d. The minimal pressure in the pipe network is 35 m of head (50 psi). In comparison, without AFD flow capacity perturbation, the total discharge volume is 890 m³/day. This represents 23% water saving when using 10% perturbation of AFD flow capacities. With regard to calculation efforts, it took 23 iterations to finish the solution searching when using 10% perturbation. In comparison, it took 18 iterations when no perturbation was implemented. Therefore, it took 28% more computational time to find a 23% better solution. To approach global minimum more closely, more AFDs can be selected and their flow capacities can be perturbed at higher ratios. However, that requires greater computational efforts.

The minimum flow capacities of the 14 imaginary AFDs are listed in the second column in Table 3.3 (step 13 in the flowchart). The flows shown in the second and third columns in Table 3.3 were used to calculate the initial AFD open durations using Equation (3.8). The results were then rounded up to the closest multiplier of five, and are listed in the fourth column in Table 3.3 (step 14 in the flowchart). The initial AFD durations were then used as a starting point for the third phase of optimization. Following the flowchart shown in Figure 3.2, open duration and optimal operation pattern were calculated for each AFD. The results are presented the third and fourth columns in Table 3.4. It reveals that each AFD starts less than four times in the 24-hour horizon. The total discharge volume of the 14 AFDs is 139 m³/d; 80% less than the calculated 684 m³/d in phase two. In addition, minimum system pressures were examined when AFDs were operated at the optimal operation patterns shown in Table 3.4. The results suggest

that the minimum pressure of the water distribution system is 36 m of head (51 psi), higher than the P_{min} of 14 m of head (20 psi).

In addition, chlorine residual die-off was examined for all the AFDs in the water system. Chlorine die-off simulations show chlorine residual developments at all the AFDs in the water network when these AFDs are turned off and on according to the patterns shown in Table 3.4. The results demonstrate that lowest instantaneous chlorine residuals of ten AFDs are higher than 2.0 mg/l; and for the remaining four AFDs, AFD-47, 48, 49, and 50, their lowest instantaneous chlorine residuals are lower than 2.0 mg/l. Nevertheless, the average daily chlorine residuals of AFD-48 and 49 are higher than 2.0 mg/l. The average daily chlorine concentrations at AFD-47 and 50 are 1.96 and 1.86 mg/l respectively. AFD-50 has the lowest instantaneous chlorine concentration among all the AFDs. This is because AFD-50 is located at the furthest dead end pipe at Gulf Beach system. Field chlorine tests at this AFD also show that low chlorine residuals (<2.0 mg/l) are more frequently observed than at other locations. AFD-50 chlorine die-off curve is shown in Figure 3.6. It reveals that chlorine concentration is 2.11 mg/ at 00:00 AM when this AFD is turned off. It reaches the highest value of 2.16 mg/l at 00:10 AM; then drops to the lowest value at 1.58 mg/l at 11:05 PM when this AFD is turned on. Note that all the 14 AFDs are not assigned with regular water demands in the digitized water network. So, they do not need to meet the minimum requirement of 2.0 mg/l chlorine residual. The laptop computer used in this study has Core i5 CPU, 4-GB memory and 32-bit Windows 7 operation system. It took approximately 4 minutes to complete one calculation cycle. This includes the data reading, computing, and result saving. The procedure for searching the global minimum took 4 hours.

AFD field operation data from March 2012 and March 2013 indicate that on average, 14 AFDs totally discharged 2,554 m³ of potable water per day (Table 3.1), significantly higher

than the calculated optimal flushing volume. That suggests the necessities of reviewing existing AFD operation practice of the studied network and field testing of the obtained optimal AFD operation patterns.

3.5 Conclusions

This study provides an insightful approach on AFD operation optimization in a water distribution system. This problem is formulated as a single objective discrete optimization problem and is solved in three phases. In the first phase, AFD flow capacities are calculated and whether existing AFDs are able to maintain chlorine residual in the water network is evaluated. All the nodes, including the AFDs are simulated as demand-driven nodes in the hydraulic and water quality simulations. In the second phase, decision variables are converted to the AFD flow capacities. This conversion substantially reduces the number of decision variables. A gradient-based method is then used to quickly explore and narrow down the solution space. At the end of this phase, the decision variables are changed back to AFD operation patterns. In the third phase, SA is used to intensively exploit the optimal solution. This method was applied to a chloraminated water distribution system in Pinellas County, Florida. The results suggest that water flushing volume calculated by optimal AFD operation configuration is significantly less than current field practice. Since this approach was developed based on EPANET, it is readily applicable to chlorinated or any other water distribution systems that EPANET can simulate.

Optimizing AFD operations in a large water network using EPANET 2.0 is a challenging task. This can be improved by implementing two methods. The first method comprises studying the network, identifying the areas with high AFD density, isolating and studying the key areas of the water network. This is the method used in this study. The second method includes speeding up water system simulation using techniques such as parallel computation, or domain

decomposition. As long as the hydraulic and water quality simulator works at fast speed, methodology presented herein will be applicable in solving big water networks.

3.6 Notations

The following symbols are used in this study:

$C_{m,t}$ = chlorine concentration at Node m at time t (mg/l);

C_{min} = specified minimum chlorine concentration (mg/l);

D_n = open duration for AFD n (min);

E = objective function;

$I_{n,t}$ = open/close status of AFD n (binary);

J = number of junctions in water distribution system;

L = duration of time interval (min);

M = number of demand nodes in water distribution system;

N = number of AFD installed in water distribution system;

$P_{m,t}$ = pressure at Node m at time t (m of head);

P_{min} = specified minimum pressure (m of head);

Q_n = discharge rate of AFD n (L/min);

\overline{Q}_n = flow capacity of AFD n (L/min);

S_n = number of AFD turn on/off switch per day;

S_o = maximally allowed number of AFD turn on/off switch per day;

T = number of time intervals within one day;

TE =pseudotemperature in SA;

TE_b =beginning temperature in SA calculation;

TE_e = ending temperature in SA calculation;

3.7 References

- Al-Jasser, A. (2007). "Chlorine decay in drinking-water transmission and distribution systems: Pipe service age effect." *Water Research*, 41(2), 387-396.
- Baggett, C. (2008). "From start to finish: calibrating Pinellas County's 2,000-mile hydraulic water distribution system model." *Florida Water Resour. J.*, 60(12), 44-54.
- Barbeau, B. (2005). "Dead-end flushing of a distribution system: short and long-term effects on water quality." *J. Water Supply: Res. and Technol.-AQUA*, 54(6), 371-383.
- Benson, R. (2010). "Advanced maintenance flushing for improving water quality within water distribution systems." *Florida Section of AWWA 2010 Fall Conference*, Orlando, Florida.
- Bertsimas, D. (1993). "Simulated Annealing." *Statistical Science*, 8(1), 10-16.
- Boccelli, D. (1998). "Optimal scheduling of booster disinfection in water distribution network." *J. Water Resour. Plann. Manage.*, 124(2), 99-111.
- Carriere, A. (2005). "Evaluation of loose deposits in distribution systems through unidirectional flushing." *J. AWWA*, (97)9, 82-92.
- Cunha, M. (1999). "Water distribution network design optimization: simulated annealing approach." *J. Water Resour. Plann. Manage.*, 125(4), 215-221.
- El Mouatasim, A. (2012). "Boolean integer nonlinear programming for water multireservoir operation." *J. Water Resour. Plann. Manage.*, 138(2), 176-181.
- Florida Administrative Code. 2003. 62-555.320(21). Tallahassee.
- Florida Administrative Code. 2010. 62-555.350(2). Tallahassee.
- Friedman, M. (2002). "Developing and implementing a distribution system flushing program." *J. AWWA*, (94)7, 48-56.
- Giacomello, C. (2013). "Fast hybrid optimization method for effective pump scheduling." *J. Water Resour. Plann. Manage.*, 139(2), 175-183.
- Goldman, F. (1998). "The application of simulated annealing for optimal operation of water distribution systems." PhD. thesis, Arizona State University, Tempe, Arizona.
- Goldman, F. (2005). *Water resources systems management tools. Chapter 5: Water distribution system operation: application of simulated annealing*, McGraw-Hill, New York.
- Hanselman, D. (2005). *Mastering Matlab 7*, Pearson/Prentice Hall, Upper Saddle River, NJ.

- Hua, G. (2011). "Controlling nitrification in a distribution system receiving blended multiple source waters: the experience of Pinellas County Utilities." *Florida Water Resour. J.*, 63(12), 42-48.
- Hua, G. (2012). "Using water quality modeling as a decision making tool to plan distribution system improvements for Pinellas County Utilities." *Florida Water Resour. J.*, 64(12), 52-58.
- Husband, S. (2010). "Field studies of discoloration in water distribution systems: model verification and practical implication." *J. Environ. Eng.*, 136(1), 86-94.
- Ingber, L. (1993). "Simulated annealing: practice versus theory." *Mathematical and Computer Modeling*, (18)11, 29-57.
- Lehtola, M. (2004). "Removal of soft deposits from the distribution system improves the drinking water quality." *Water Research*, 38(3), 601-610.
- Lopez-Ibanez, M. (2007). "Ant colony optimization for optimal control of pumps in water distribution networks." *J. Water Resour. Plann. Manage.*, 134(4), 337-346.
- Lopez-Ibanez, M. (2009). "Operation optimization of water distribution networks." Ph.D. thesis, Edinburgh Napier University, U.K.
- Martinez, R. (2008). "Application of several meta-heuristic techniques to the optimization of real looped water distribution networks." *Water Resour. Manage.*, 22(10), 1367-1379.
- Monem, M. (2005). "Application of simulated annealing (SA) techniques for optimal water distribution in irrigation canals." *Irrigation and Drainage*, (54)4, 365-373.
- Munavalli, G. (2003). "Optimal scheduling of multiple chlorine sources in water distribution systems." *J. Water Resour. Plann. Manage.*, 129(6), 493-503.
- Riera, J. (2012). "Water quality modeling targets and innovative nitrification strategies for City of St. Petersburg." *Florida Water Resour. J.*, 64(12), 38-45.
- Rossman, L. (2002). EPANET 2.0: User's manual, National Risk Management Research Laboratory, U.S. EPA, Cincinnati.
- Savic D. (2009). "Quo vadis water distribution model calibration?" *Urban Water J.*, 6(1), 401-428.
- Seidel C. (2005). "Have utilities switched to chloramines?" *J. AWWA*, 97(10), 87-97.
- Sousa, J. (2006). "A simulated annealing algorithm for the optimal operation of water distribution networks." *Joint International Conference on Computing and Decision Making in Civil and Building Engineering*, Montréal, Canada, 3060-3069.

- Teegavarapu, R. (2002). "Optimal operation of reservoir systems using simulated annealing." *Water Resour. Manage.*, 16(5), 401-428.
- Tospornsampan, J. (2007). "Split-pipe design of water distribution network using simulated annealing." *International J. Computer Information Eng.*, (1)3, 154-164.
- U.S. Environment Protection Agency. (2006). "The effects of disinfectant residuals in the distribution system." *EPA-68-C-00-113*, Office of Ground Water and Drinking Water, U.S. EPA, Washington, D.C.
- Wang, X. (2009). "An eco-environmental water demand based model for optimising water resource using hybrid genetic simulated annealing algorithms. Part I. Model development." *J. Environ. Manage.*, (90)8, 2628-2635.
- Wu, Z. (2006). "Efficient Pressure Dependent Demand Model for Large Water Distribution System Analysis." *8th annual international symposium on Water Distribution Systems Analysis*, Cincinnati, Ohio, 1-15.

Table 3.1 Gulf Beach pump station outflow

User	Water Flow (m ³ /d)
County Park	322
Small city	2,415
Flushing	2,554
Total	5,292

Table 3.2 AFD discharge rates

AFD #	Flow (L/min)		
	Minimum	Maximum	Average
AFD-37	432	481	458
AFD-38	416	466	443
AFD-39	420	473	447
AFD-40	409	458	435
AFD-41	401	450	428
AFD-42	405	454	432
AFD-43	397	443	420
AFD-44	356	397	379
AFD-45	375	416	397
AFD-46	352	394	375
AFD-47	333	375	356
AFD-48	280	337	310
AFD-49	280	337	310
AFD-50	216	261	238

Table 3.3 AFD open durations

AFD #	Flow (L/min)		Open Duration (min)
	Q_{ns}	\overline{Q}_n	
AFD-37	36	458	115
AFD-38	40	443	130
AFD-39	24	447	80
AFD-40	35	435	115
AFD-41	29	428	100
AFD-42	32	432	110
AFD-43	27	420	95
AFD-44	45	379	175
AFD-45	28	397	105
AFD-46	33	375	130
AFD-47	49	356	200
AFD-48	32	310	150
AFD-49	31	310	145
AFD-50	35	238	210

Table 3.4 AFD optimal open patterns

AFD #	Open (min)		Optimal Open Patterns
	Initial Duration	Optimal Duration	
AFD-37	115	0	
AFD-38	130	0	
AFD-39	80	25	(00:00-00:25)
AFD-40	115	30	(00:00-00:15) (10:00-10:15)
AFD-41	100	20	(00:00-00:20)
AFD-42	110	30	(23:45-00:15)
AFD-43	95	15	(01:45-02:00)
AFD-44	175	35	(0:00-0:20) (02:00-02:15)
AFD-45	105	20	(00:00-00:20)
AFD-46	130	35	(08:00-08:15) (23:40-24:00)
AFD-47	200	60	(23:00-24:00)
AFD-48	150	60	(22:45-23:45)
AFD-49	145	0	
AFD-50	210	55	(23:05-24:00)

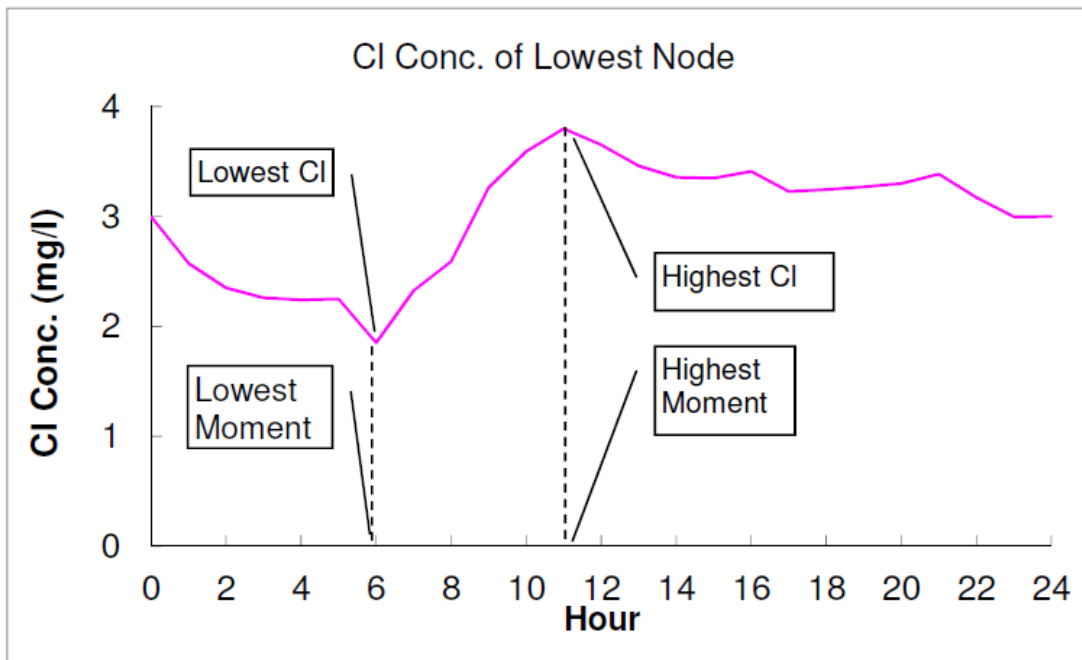


Figure 3.1 Chlorine residual of lowest node

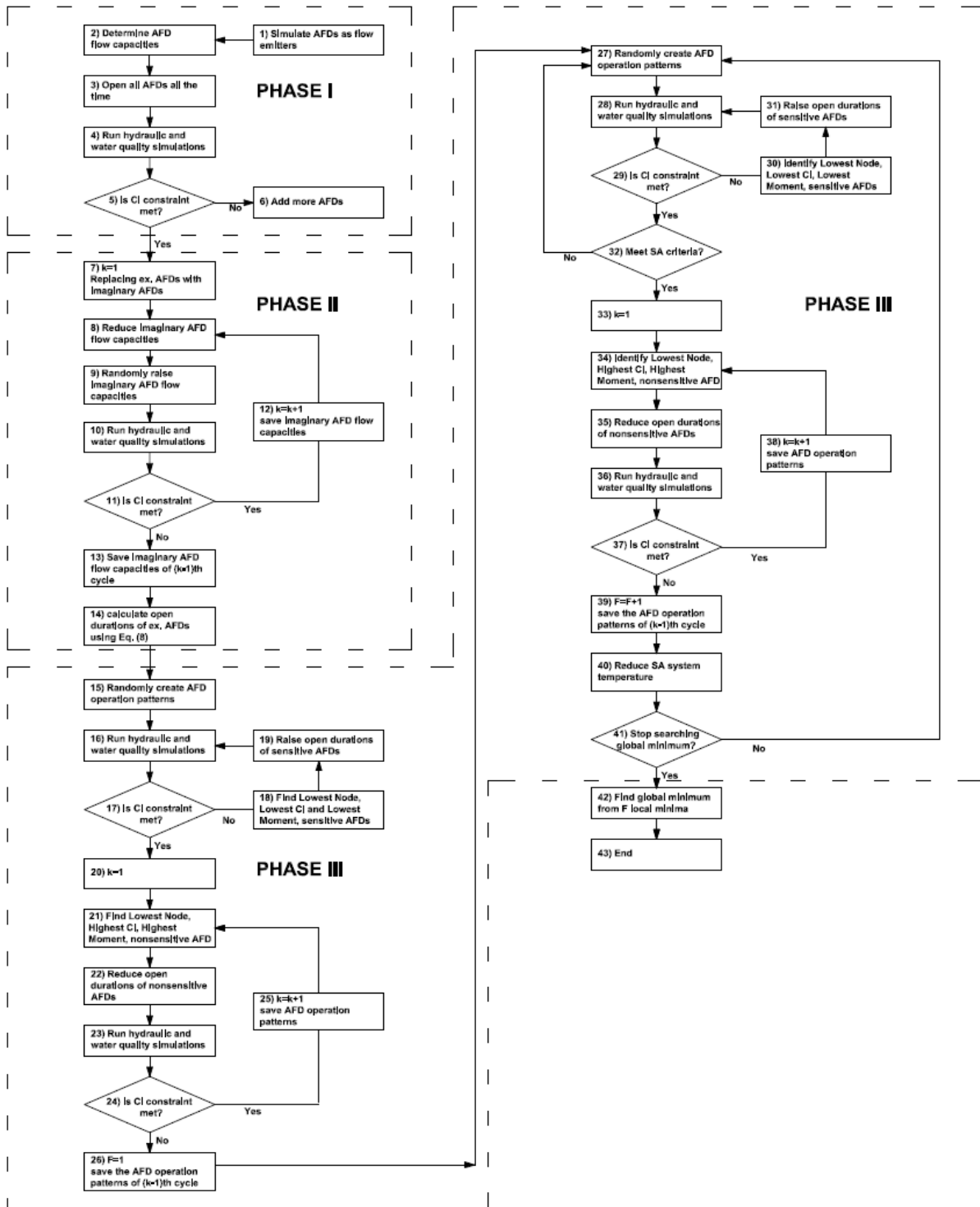


Figure 3.2 Flowchart of methodology

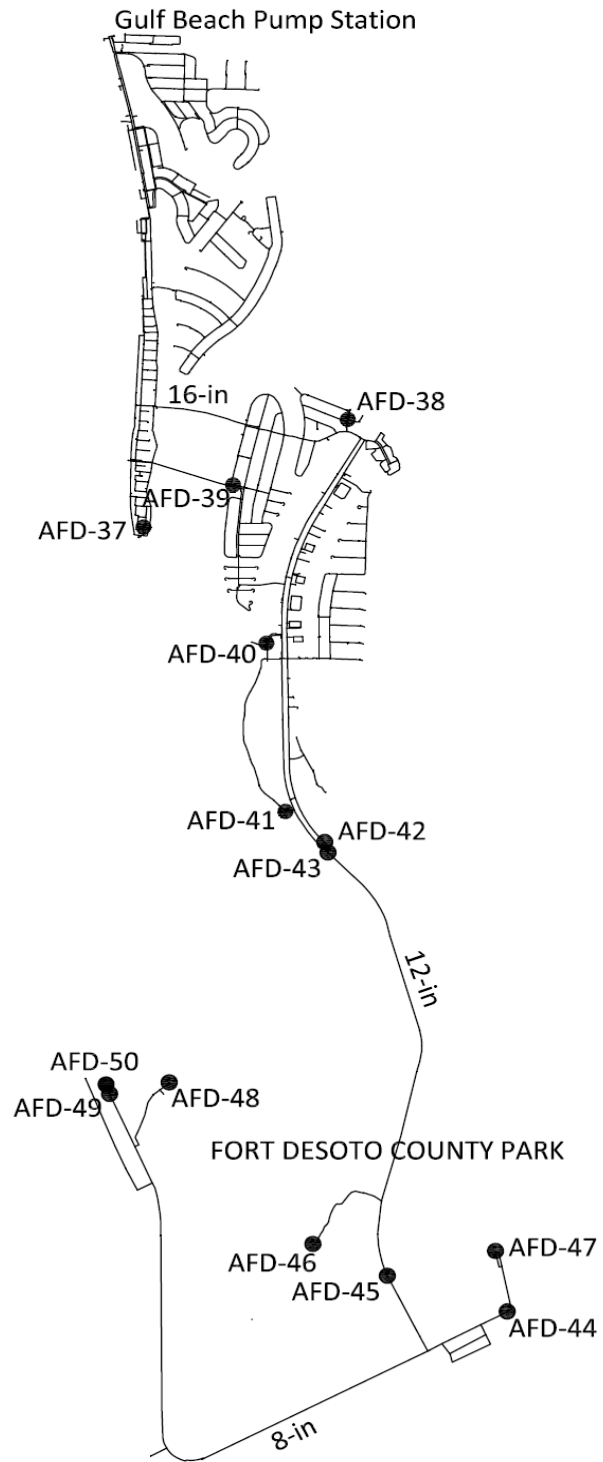


Figure 3.3 Studied pipe network

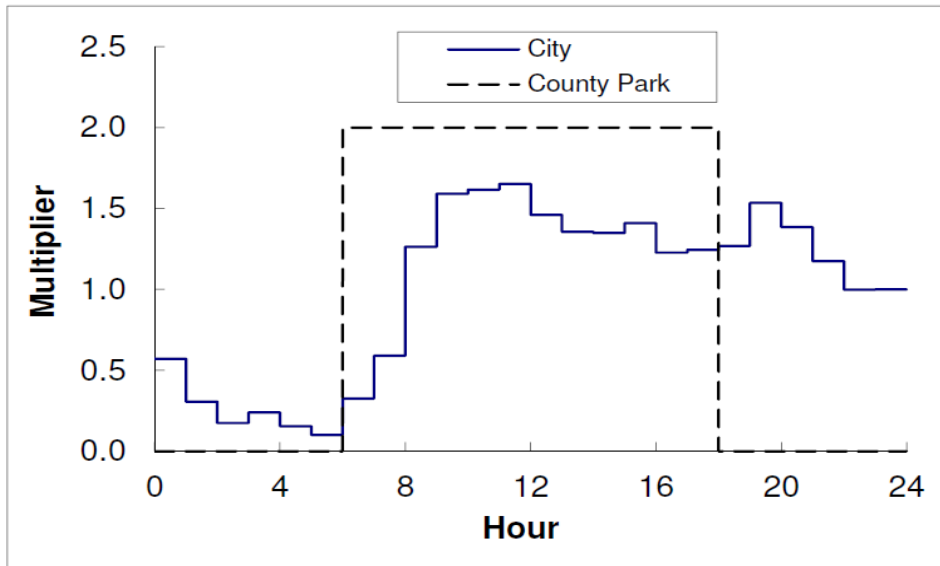


Figure 3.4 Water use patterns of the small city and the County Park

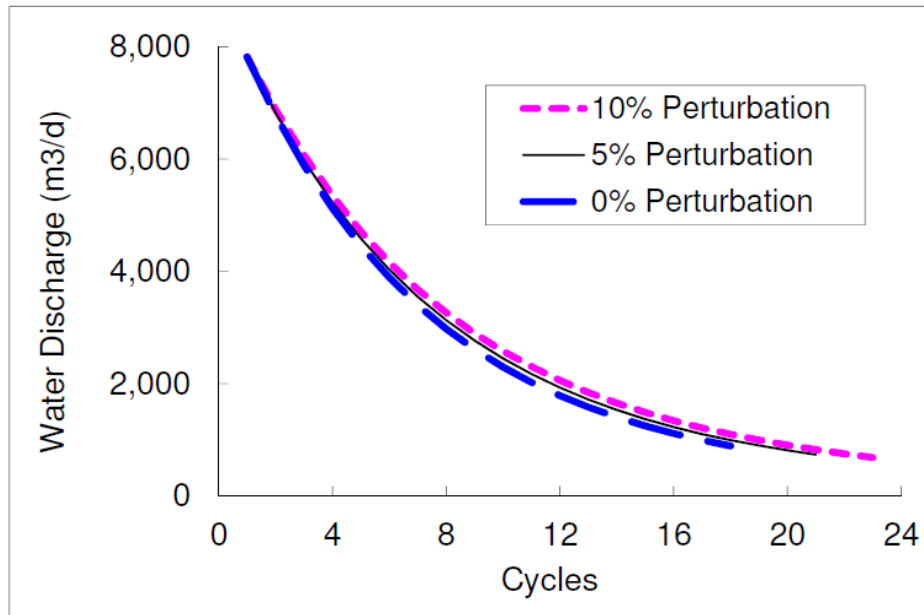


Figure 3.5 Searching minimal AFD discharge capacities

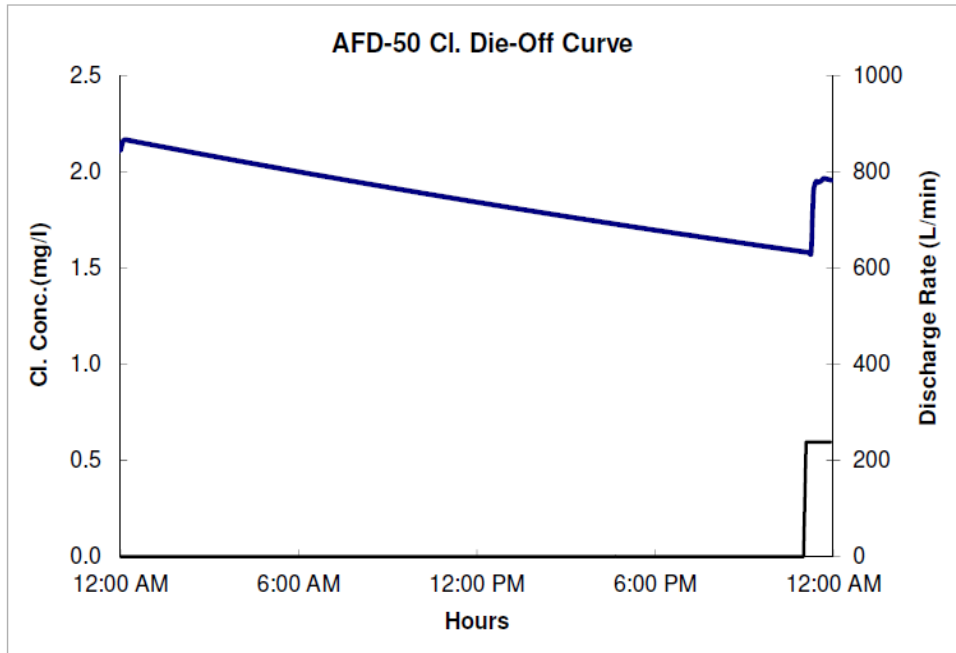


Figure 3.6 AFD-50 chlorine die-off curve

Chapter 4: Simulation of Chlorine Decay under Contaminant Intrusion in Water Distribution System³

4.1 Introduction

Potable water distribution system is an infrastructure which delivers potable water from water treatment plants to end users. It is spatially diverse and thus is vulnerable to a variety of threats. One of the most serious ones is a chemical and/or biological contaminant intrusion. September 11, 2001 event in the United States raised concerns over the safety of water distribution systems. To reduce potential exposure of contamination agents to public, US Environment Protection Agency (USEPA) recommended implementing early warning system (2009). Contaminants can be intentionally injected into water network by terrorists or unintentionally flow into water network. A normally operated potable water network maintains sufficient internal pressure (normally in the range of 30-50 m of pressure head) to prevent external contaminants from entering the water network. However, pipe fractures, joint dislocations or surge event can cause localized, instantaneous low pressures where alien materials enter the water network (Karim 2003, Gullick 2004). After September 11 attack in the United States, water networks in many countries have gained high levels of protections. Intentional injecting of contaminants into water network is less possible. On the other hand, most

³ Note: Portions of this chapter are being prepared for submission to the Journal of “Water Research”. The co-author of the manuscript is Mahmoud Nachabe. Research questions, methodology, computations and comments were provided by both authors.

of the United States' drinking water infrastructure is nearing the end of its useful life. The American Society of Civil Engineers (ASCE) gave the US water infrastructure a grade of D-minus in its 2009 Report Card for America's Infrastructure (Qureshi 2014). Therefore, unintentional contamination is gaining more attentions, especially in the locations where potable water network is close to wastewater collection system, or the locations with high groundwater tables.

US EPA (2005a) identified 33 baseline contaminants in the potable water network; they are shown in Table 4.1. According to detection techniques, these contaminants were grouped into 12 classes. As a strong oxidant, chlorine, either in the forms of chlorine gas, hypochlorite or chlorine dioxide, is widely used as secondary disinfectant in the water distribution system. Chlorine can react with most of the contaminants listed in Table 4.1. Therefore, an abnormal, substantial reduction of chlorine residual in water distribution system might be an indication of contaminant intrusion. In this study, the contaminant that can react with chlorine is referred to as reactive contaminant. US EPA research results (2005b) suggest that chlorine and total organic carbon (TOC) are two most important parameters to indicate the presence of contamination. High production and maintenance costs of TOC instruments limit their wide application in water distribution systems. As a result, chlorine residuals, free or total, are the most useful parameters to indicate contamination. Chlorine sensors are used in Cities of Ann Arbor, Cincinnati of the United States as important components of early warning system (USEPA 2010). Before implementing early warning system, the behaviors of contaminants inside water network shall be investigated using hydraulic and water quality simulation software.

EPANET 2.0 (Rossman 2000) is a free hydraulic and water quality simulation software product that is widely used in academia and industry. All the commercial software products

use the similar principles as those in EPANET 2.0 on simulating chlorine residual in water network. EPANET 2.0 has the capability to model water age and predict flow of non-reactive and, under simplified conditions, reactive materials. This capability is frequently used to predict chlorine residuals. In EPANET 2.0, all the chlorine-demanding constituents are grouped as single-species and are in excess. Therefore, the water quality simulation capabilities of EPANET 2.0 only evaluate decay or growth of a single constituent. This restricts the application of EPANET 2.0 on simulating contamination attack. Some of the scholars (Schwartz 2014, Helbling 2010, Munavalli 2004) used EPANET-MSX (Shang 2008) to model the interactions between constituents. EPANET-MSX is an extension of EPANET which can simulate complex chemical and biological reactions within the water network. Prior to employing EPANET-MSX, four tasks shall be accomplished: 1) identify all the aqueous constituents; 2) list all the chemical reactions related to these aqueous constituents; 3) understand all the principles of these reactions and list all the reaction kinetics equations; and, 4) obtain the reaction coefficients of all the reactions. This is a difficult, if not impossible, mission for the simulation of contamination attack. As a result, most of the researches normally selected a few of aqueous constituents and investigated their kinetic behavior before using EPANET-MSX (Helbling 2007, 2009).

In this study, an EPANET 2.0-based methodology is developed for simulating the chlorine decay in the event of contamination intrusion. In EPANET 2.0, chlorine decay simulation is performed by adjusting three input parameters: bulk reaction coefficient b_k , wall reaction coefficient k_w , and chlorine concentration at source junction(s). Chlorine concentrations at source junction(s) are not affected by contamination intrusion. After contaminant matrix is intentionally injected or unintentionally flows into water network, it reacts with chlorine. Both chlorine and contaminant concentrations drop. k_b or k_w shall vary. However, in EPANET 2.0,

both these two parameters are constant during the chlorine decay simulation. Therefore, EPANET 2.0 cannot simulate the reaction between chlorine and reactive contaminants directly. The methodology utilizes EPANET 2.0 multiply times to accomplish the goal of simulating chlorine decay under contamination attack.

4.2. Methods

4.2.1 Simulating Chlorine Decay in Contaminated Water Network

In a well maintained water distribution system, chlorine decay involves two principles: (1) reaction with aqueous constituents, such as ammonia and natural organic matters (NOM) in the bulk water, and (2) reaction with pipe materials and biofilm near the pipe wall (Jonker *et al.* 2008). Water migration inside the pipe network is modelled as plug flow and longitudinal dispersion is not considered. These models are superimposed on a transport model to calculate the chlorine concentration in a given pipe

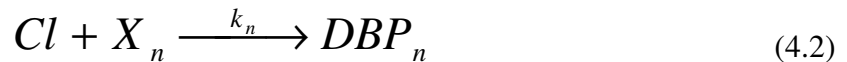
$$\frac{\partial[Cl(x,t)]}{\partial t} = -u \frac{\partial[Cl(x,t)]}{\partial x} - k_b [Cl(x,t)]^g - \frac{k_f k_w}{R_h (k_f + k_w)} [C(x,t)]^h \quad (4.1)$$

in which x is the distance to the starting junction (m); $Cl(x,t)$ is chlorine concentration (mg/L) at a distance x at time t ; u is flow velocity (m/s); g is the bulk reaction order; normally, it takes the value of one; R_h is pipe hydraulic radius (m); k_f is flow-dependent mass transfer coefficient; and h is wall reaction order; EPANET limits it to be either 0 or 1. Both k_b and k_w are properties of pipes, not to junctions. k_b is considered to be time-independent for a well maintained water production and distribution system. This is the basis for chlorine decay simulation for EPANET 2.0. When one water network has only one water source, all the pipes can be assigned with one uniform k_b . In this research, the impact of contaminants on chlorine decay wall reaction is not considered. Contaminants are considered as a group of materials that react with chlorine

instantaneously in bulk water. From the perspective of chlorine depletion, contaminants are not different from NOM that exists in bulk water. Equation (4.1) is still applicable in describing chlorine decay with the presence of contaminants. However, k_b is not a constant for each pipe in this case. This is incorporated in the methodology. A flowchart is created and shown in Figure 4.1 to represent the methodology. It basically answers four questions: 1) what occurs when contaminant matrix is added to potable water; 2) how to calculate k_b with the presence of contamination attack; 3) where is the impacted area of the intrusion; and, 4) how to calculate pipe k_b to simulate the chlorine decay behavior in a water network. Each of the four questions is discussed in Sections 2.2-2.5 respectively. Software tools needed for this research include Matlab 7.0 (Hanselman 2005), EPANET 2.0, and Microsoft Excel VBA (Bovey 2009).

4.2.2 Reactions between Chlorine and Contaminants

Potable water is not pure water; it contains small amounts of impurities such as humus, pathogens, and sulfide. After potable water leaves water treatment plant and enters water distribution system, disinfectant, mainly chlorine, is injected into water network to maintain water quality and the integrity of water network. As a strong oxidant, chlorine reacts with most of these impurities. For a chlorine-demanding matrix that has N constituents, the reaction between chlorine and n^{th} aqueous species is



where X_n is the n^{th} constituent in the chlorine demanding matrix; k_n is the reaction rate coefficient for X_n , it is a constituent specific parameter; DBP_n is the n^{th} disinfection byproduct. The reaction is a second-order reaction. Mutual chemical reactions among these aqueous constituents are not shown here. Overall chlorine decay rate is

$$\frac{d[Cl_t]}{dt} = -\left(\sum_{n=1}^N k_n \times [X_{n,t}]\right) \times [Cl_t] \quad (4.3)$$

where $[Cl_t]$ is the chlorine concentration (mg/l) at time t after chlorine is introduced; $[X_{n,t}]$ is chlorine-demand constituent X_n concentration (mg/l) at time t . Reaction rate constant k_n is positive, the minus sign on the right hand of Equation (4.3) shows that chlorine residual drops as a result of these reactions. Similarly, the decay rate of X_n is

$$\frac{d[X_{n,t}]}{dt} = -k_n \times [Cl_t] \times [X_{n,t}] \quad (4.4)$$

Fisher et al (2011) divided these chlorine demanding constituents into two general categories: fast and slow chlorine-demanding. *E. coli* is one example of fast chlorine demanding constituent. *M. aurum* is very resistant to chlorine in the water, so it is slow-demanding constituent (Helbling 2007). As a result, the overall chlorine decay rate in potable water is

$$\frac{d[Cl_t]}{dt} = -\left(\sum_{nf=1}^{NF} k_{nf} \times [X_{nf,t}] + \sum_{ns=1}^{NS} k_{ns} \times [X_{ns,t}]\right) \times [Cl_t] \quad (4.5)$$

where NF and NS are the numbers of fast and slow chlorine demand constituents. For a water sample collected from a well maintained drinking water production and distribution system, the concentrations of rapid chlorine-demanding chemicals are low because a large portion of these materials are removed or destroyed inside water treatment plant. That

is $\left(\sum_{nf=1}^{NF} k_{nf} \times [X_{nf,t}]\right) \approx 0$ and $\left(\sum_{n=1}^N k_n \times [X_{n,t}]\right) \approx \left(\sum_{ns=1}^{NS} k_{ns} \times [X_{ns,t}]\right)$. Since the reaction

between X_{ns} and chlorine is slow, $[X_{ns,t}]$ is considered as a time-independent. Therefore, overall chlorine decay rate coefficient inside a normally operated distribution system is considered as constant. It is written as k_{bn} in this study, where n in the subscript stands for normal condition.

$$k_{bn} = \left(\sum_{ns=1}^{NS} k_{ns} \times [X_{ns,t}] \right) \quad (4.6)$$

So, in a normally operated water network, chlorine decay in the bulk water is a first order reaction, which is by far the most commonly used bulk decay model in water industry (Jonkergouw 2009). In this research, k_{bn} is a positive value since k_{ns} is higher than zero.

Bulk water and contaminant matrix are assumed to be completely mixed when a contaminant matrix is released into water network. The overall chlorine decay rate of the contaminated potable water is

$$\frac{d[Cl_t]}{dt} = - \left(\sum_{ns=1}^{NS} k_{ns} \times [X_{ns,t}] + \sum_{mf=1}^{MF} k_{mf} \times [X_{mf,t}] + \sum_{ms=1}^{MS} k_{ms} \times [X_{ms,t}] \right) \times [Cl_t] \quad (4.7)$$

where MF and MS are the numbers of fast and slow chlorine-demanding constituents that are introduced into potable water by contaminant matrix; $[X_{mf,t}]$ is the concentration of fast chlorine-demanding constituent X_{mf} in potable water at time t . The three terms inside the bracket of Equation (4.7) are collectively referred to as contaminated bulk reaction coefficient k_{bc} , where c stands for contamination.

$$k_{bc} = \left(\sum_{ns=1}^{NS} k_{ns} \times [X_{ns,t}] + \sum_{mf=1}^{MF} k_{mf} \times [X_{mf,t}] + \sum_{ms=1}^{MS} k_{ms} \times [X_{ms,t}] \right) \quad (4.8)$$

When contaminant matrix is diluted to some extent so that its effect on water quality is ignorable, the water is considered as normal potable water. This dilution ratio is termed threshold dilution ratio R_t . The fast chlorine-demanding constituents in the contaminant matrix react with chlorine rapidly when contaminant matrix contacts potable water. Therefore, k_{bc} is time-dependent; it is initially high and drops with time. After fast chlorine-demanding constituents are fully oxidized, k_{bc} gradually reaches a constant. Figure 4.2 shows the temporal

developments of k_{bc} and k_{bn} . With the depletion of fast chlorine demanding components introduced by contamination intrusion, eventually k_{bc} becomes

$$k_{bc} = \left(\sum_{ns=1}^{NS} k_{ns} \times [X_{ns,t}] + \sum_{ms=1}^{MS} k_{ms} \times [X_{ms,t}] \right) \quad (4.9)$$

Differentiate k_{bc} over time

$$\frac{dk_{bc}}{dt} = \left(\sum_{ns=1}^{NS} k_{ns} \times \frac{d[X_{ns,t}]}{dt} + \sum_{mf=1}^{MF} k_{mf} \times \frac{d[X_{mf,t}]}{dt} + \sum_{ms=1}^{MS} k_{ms} \times \frac{d[X_{ms,t}]}{dt} \right) \quad (4.10)$$

Replace the derivative terms on the right side of Equation (4.10) with Equation (4.4), Equation (4.10) becomes

$$\frac{dk_{bc}}{dt} = - \left(\sum_{ns=1}^{NS} k_{ns}^2 \times [X_{ns,t}] + \sum_{mf=1}^{MF} k_{mf}^2 \times [X_{mf,t}] + \sum_{s=1}^{MS} k_{ms}^2 \times [X_{ms,t}] \right) \times [Cl_t] \quad (4.11)$$

Equation (4.11) shows that dk_{bc}/dt is not a constant either; it drops with the reductions of chlorine and contaminant concentrations. Equations (4.6) and (4.9) suggest that k_{bc} is higher than k_{bn} all the time, even after fast-chlorine demanding constituents introduced by contamination intrusion are depleted.

4.2.3 Measuring Bulk Reaction Coefficient of Contaminated Water

This study studied the intrusion of municipal wastewater into potable water network. This is one of the most possible ways of unintentional intrusion into drinking water distribution system, especially for those communities that have old water distribution and wastewater collection systems. Wastewater sample was collected from a Pinellas County wastewater pump station on August 3, 2014, 10:30 AM. Test results indicated that the wastewater sample has 250 mg/l BOD₅ and 180 mg/l TOC. Pinellas County is a major tourist destination in Florida. Historical records show that manufacturing sector contributes to approximately 3% of total

wastewater. Thus, the collected wastewater is dominantly municipal wastewater. Jar test was performed to: 1) investigate the relationship between k_{bc} and wastewater dilution; 2) determine the threshold dilution ratio R_t of residential wastewater; and, 3) study temporal variation of k_{bc} .

Four water samples were prepared at same time and ambient environment. The first sample was prepared by adding 1 ml of the wastewater into 999 ml of potable water. This sample is recorded as 0.1% contamination dilution. To better understand the methodology, municipal wastewater is considered as a 100% contaminant matrix in this study. The second and third samples have 0.5% and 1.0% contamination dilutions respectively. The fourth sample is potable water used as blank. 4,000 ml of potable water were collected in one bucket at Gulf Beach Pump Station, which is owned and operated by Pinellas County Utilities Department. The upper limit of contamination dilution is set at 1% in the lab tests because the effect of contaminant flow to pipe network hydraulics is ignorable at or below this limit. The 4,000 ml potable water was mixed before used to prepare the four samples. This ensured the potable water used in the four samples has same physical and chemical properties. Total chlorine residuals were tested using Hach DR890 Chlorimeter. During all the tests, temperature was maintained at 27°C. The tests were repeated in three batches with the separation of one week. In each batch of test, the chlorine concentrations of the potable water were adjusted to 3.0 mg/l to ensure the repeatability of the test results. The averages of the three batches at each dilution level were used to determine k_{bc} .

Chlorine decay at different contamination concentrations are shown in Figure 4.3. As expected, 1% contamination has the lowest chlorine residuals. The temporal variation of k_{bc} at different contamination levels and their fit functions are shown in Figure 5.4. k_{bc} are shown in natural logarithm scale to make the figure clearer. All the fit equations have the format of

$$\ln(k_{bc}) = -a \times \ln(t) + b \quad (5.12)$$

In all the fit equations, k_{bc} has the unit of 1/day and t has the unit of minute. Figure 4.4 shows that: 1) k_{bc} turn into horizontal after $t=720$ minutes for all contamination levels; 2) k_{bc} for all the contaminated water samples are higher than k_{bn} . This proves the correctness of Equations (4.6) and (4.9). For contamination concentration not shown in Figure 4.3, its k_{bc} curve can be interpolated from the parameters show in Figure 5.4. Linear regression equations can be used to achieve the parameters. The results are shown in Figure 4.5. For a 0.25% contamination, parameters a and b are 0.5157 and 2.2526 respectively. So k_{bc} of this concentration is $\ln(k_b) = -0.5157 \times \ln(t) + 2.2526$. Using the parameters shown on Figure 4.5, threshold dilution ratio was calculated and it is 1:2,000 or 0.05%. k_{bn} was calculated to be 0.20 /day for the potable water collected in Gulf Beach Pump Station (Step 1 in Figure 4.1). If the chemical test duration goes forever, k_{bc} will go below 0.20/day. This suggests that at this time, contaminates inside the potable water are completely decomposed. In this case, the bulk reaction coefficient is k_{bn} . In the lab tests, contaminant matrix is considered as a whole, detailed analysis of wastewater constituents and reaction rate constant for each individual species are not needed in this method. This facilitates the application of EPANET 2.0 to simulate chlorine residual in the event of contaminant intrusion.

4.2.4 Determining Contaminated Area

k_{bc} is a temporal variable and drops rapidly when contaminant matrix contacts drinking water. It is crucial to accurately determine the travel time of contaminant matrix from source junction to one specific junction in the water network, especially for a contamination event with long release duration. Therefore, it is desirable to implement two measures. First, set water quality simulation time step short so that EPANET can capture the rapid change of k_{bc} .

The weakness of this measure is that short water quality simulation time step will lead to excessive computational efforts. As a result, it is the utilities engineers' responsibility to decide optimal water quality simulation time step. Second, break the contamination event into E independent sub-events. Each sub-event shall have the same duration as the water quality simulation time step in EPANET (step 2 in Figure 4.1). Chlorine residuals for each junction obtained in each sub-event are finally recombined to create the chlorine residual of that junction in the whole release event. This measure is compulsory when contaminant matrix is released at varying intensities.

As contaminant matrix enter water network, it is immediately and completely diluted by water flow at the injection point. This dilution at the injection point is named as primary dilution in this study. The dilution ratio of contamination matrix flow Q_x to the flow of water at the source junction Q_w at the moment of injection is referred to as primary dilution ratio R_p . Primary dilution creates a mixture of contaminant matrix and potable water, which is denoted as contamination parcel. As contamination parcel moves inside the water network, contaminant concentrations drop due to two reasons: dilution and chlorine reaction. The dilution inside water network is referred to as secondary dilution. It happens at those junctions with more than one inflow pipe; contaminants at one inflow pipe are diluted by the water streams from other inflow pipe(s). One related concept is threshold secondary dilution ratio R_s . It is the dilution ratio that causes the contamination parcel to be diluted as regular potable water. R_s is calculated as

$$R_s = \frac{R_t}{R_p} \quad (5.13)$$

Contamination parcel may not pass all components of a network. The area that is not affected by the intrusion is referred to as uncontaminated area. There are two types of

uncontaminated areas: 1) the area where contaminant parcel does not pass; and, 2) the area where contaminant parcel passes at a concentration lower than the threshold concentration. Chlorine residuals of the uncontaminated area are not affected by the contamination event. For any specific pipe inside uncontaminated area, its bulk reaction coefficient is k_{bn} . The portion of water network where contaminant parcel(s) passing by at a concentration higher than the threshold concentration is referred to as contaminated area of this intrusion event. The size of contaminated area is positively correlated to the primary dilution ratio. In other words, low contamination concentration at the injection point creates a small contaminated area. The pipes inside contaminated area are named as contaminated pipes; or c-pipes. Similarly, uncontaminated pipes or u-pipes referred to as these pipes that are not affected by one contamination event. Same naming rule applies to other network components such as junctions or storage tanks. For a specific c-junction, not the all the moments are contaminated, the moment when contaminant parcel passes by is referred to as contaminated moment, or c-moment. The key of this research is how to calculate bulk reaction coefficients of c-pipes. Locating c-pipes is a prerequisite for calculating bulk reaction coefficients of these pipes.

EPANET 2.0 is not capable of identifying c-pipes directly. This research developed an indirect method: identify c-junctions; then determine c-pipes using the information of c-junctions. Contaminant is assumed to be nonreactive in searching c-junctions. This is because the concentrations of nonreactive contaminant in water network are linear to secondary dilution ratio R_s . C-junctions are identified by three steps. First, calculate threshold secondary dilution ratio R_s based on the primary dilution ratio using Equation (4.12). Second, perform water quality simulation of nonreactive contaminants by assigning zero to k_b of all the pipes in the water network. At the source junction, assign a big mass load of nonreactive contaminant to create

a significant contaminant concentration, say, 500 mg/l. This arrangement eliminates computational noises caused by EPANET 2.0. The simulation of the nonreactive contamination shall use the same parameters such as simulation duration, water quality time step, and contamination release duration as those will be used to simulate reactive contaminants. Third, determine c-junctions using R_s and the contaminant concentration at source junction. For a municipal wastewater intrusion event that has R_t of 1:2,000 and R_p of 1:100, the threshold secondary dilution ratio R_s is calculated to be 1:20 or 5%. Therefore, any junction whose maximum concentration of nonreactive contaminant is higher than 25 mg/l (5% of 500 mg/l) is a c-junction for this contamination event (Figure 4.6). The moment when the nonreactive contaminant concentration is higher than 25 mg/l is a c-moment for this c-junction. Continuous c-moments cluster into a c-interval for this c-junction (step 3 in Figure 4.1). For each c-junction j_c , the number of c-intervals is counted and recorded as I_j ; this information will be used in Section 2.5 (step 4 in Figure 4.1). For each c-interval, the moment that has highest contaminant concentration is recorded as t_p (Figure 4.6). For a c-junction that has more than one c-interval, there exists one t_p for each c-interval. They are named as t_{p1} , t_{p2} and etc. After identifying all c-junctions, water network topology is used to determine if a pipe is c-pipe. For a specific pipe, if and only if both end junctions are c-junctions, this pipe is a c-pipe (steps 5 in Figure 4.1).

4.2.5 Assigning Bulk Reaction Coefficients to Contaminated Pipes

Two examples with ascending complexity are used to explain how to calculate bulk reaction coefficients of c-pipes. Easy or “good” parameters are used to make these examples more understandable. Figure 4.7(a) shows a single pipe P_I where junction B is a single user and has a constant water demand. For simplicity and without losing generality, chlorine decay by wall reaction is not considered. Water quality simulation time step is set at 10 min. Based on

the pipe geometry data and the water demand at junction B , travel time from junctions A to B is calculated to be 120 min. Chlorine concentration at junction A is maintained at C_A mg/l. Without contamination, junction B 's chlorine residual C_B is calculated using the following equation

$$\ln C_B = \ln C_A - k_{bn} \times 120 \quad (4.14)$$

Wastewater flows into junction A from 00:00 to 00:10 at a primary dilution ratio R_p of 1:400, or 0.25%. The impact of contamination matrix on system hydraulics is ignorable because wastewater inflow Q_x is only 0.25% of the water demand at junction B . Since the contamination release duration is the same as water quality simulation step, no division of contamination event is needed, i.e, $E=1$ in this case (step 2 in Figure 4.1). Since the wastewater concentration is higher than the threshold concentration, junction A is the source for this contamination event. For this one-pipe example, secondary dilution ratio R_s is 1:1. Therefore, the contaminant concentration at junction B is higher than the 0.05% threshold. Junction B is also contaminated at this contamination event. For junction B , there is only one c-interval, which is 02:00-02:10 (steps 3 & 4 in Figure 4.1). Since both junctions A and B are c-junctions, pipe P_1 is a c-pipe (step 5 in Figure 4.1). Junction B only has one c-interval; step 6 in the methodology flowchart (Figure 4.1) is not applicable. It is explained in next example.

The contamination matrix is constantly released within ten minutes, contaminants at the head of the contamination parcel have reacted with chlorine for ten minutes when the last drop of contaminant matrix enters junction A . Therefore, the water quality inside the contamination parcel is not uniform. It is reasonable to divide the contamination parcel into infinite sub-parcels, each has a small length of Δx . Contaminants are completely mixed with potable water inside the sub-parcel. Longitudinal dispersion does not occur between sub-parcels. Thus, each sub-parcel is considered to be located inside an imaginary mini beaker where contaminants react with

chlorine. This is shown in Figure 4.7(a). At 00:05, the sub-parcel at the midpoint of the contamination parcel is formed by injecting Δv of wastewater in to $399\Delta v$ of potable water. The imaginary mini beaker moves forward and reaches junction B at 02:05. Initial contaminant concentration of the sub-parcel is 0.25% at junction A . In Figure 4.7(a), the contamination concentration at junction B is also shown as 0.25%. This just indicates that no secondary dilution occurs between these two junctions. Since water flow pushes the sub-parcels forward at constant velocity, for any sub-parcel, the travel time from junctions A to B is 120 min. So, for junction B , chlorine residual observed within its c-interval is a time-independent value less than C_B calculated by Equation (4.14). k_{bc} is calculated using the method shown Section 2.2. It is a natural logarithm curve and is shown in Figure 4.8. According to the water quality time step, 120 min travel time from junctions A to B is divided into 12 discrete intervals, each lasts 10 min. k_{bc} within the 10-min interval is set at a uniform value. k_{bc} at $t=5$ min is used to represent the average k_{bc} for this contamination parcel between $t=00:00$ and 00:10 min, it is written as $k_{bc(5)}$. Same rule is used for the following 11 k_{bc} . Note that $k_{bc(5)}$ and other 11 k_{bc} are constants. The step function is also shown in Figure 4.8. The chlorine residual at the front of contamination parcel at $t=10$ min is shown in first row in Equation (4.15)

$$\begin{aligned}
 \ln C_{10} &= \ln C_0 - k_{bc,5} \times 10 & t = 10 \text{ min} \\
 \ln C_{20} &= \ln C_{10} - k_{bc,15} \times 10 & t = 20 \text{ min} \\
 &\dots & \dots \\
 \ln C_{120} &= \ln C_{110} - k_{bc,115} \times 10 & t = 120 \text{ min}
 \end{aligned} \tag{4.15}$$

where C_0 is the chlorine concentration at the head of the contamination parcel at $t=0$ min, it is also the chlorine residual at junction A . As the contamination parcel moves forward for another 10 min, the head and the tail of the contamination parcel have reacted with chlorine for 20 and

10 min respectively. The chlorine residual of the head of the contamination parcel is shown in the second row of Equation (4.15). At $t=120$ min, the head of the contamination parcel reaches junction B . The chlorine residual at the head of the contamination parcel is calculated and is shown in the last row in Equation (4.15). Chlorine residuals of junction B in the event of contaminant attack are calculated by summarizing all the rows of Equation (4.15). C_{120} is replaced with C_{BC} to emphasize this is the concentration of junction B in the event of contaminant attack. Similarly, C_0 is replaced with C_A .

$$\begin{aligned}\ln C_{BC} &= \ln C_A - (k_{bc,(5)} + k_{bc,(15)} + \dots + k_{bc,(115)}) \times 10 \\ &= \ln C_A - \frac{(k_{bc,(5)} + k_{bc,(15)} + \dots + k_{bc,(115)})}{12} \times 120\end{aligned}\quad (4.16)$$

In Equation (4.16), 120 is the travel time in minute from junctions A to B . k_b for pipe P_1 is achieved by comparing Equation (4.14) and (4.16). It is a step function.

$$(P_1) k_b = \begin{cases} \frac{k_{bc,(5)} + k_{bc,(15)} + \dots + k_{bc,(115)}}{12} & t \in [120, 130] \\ k_{bn} & \text{else} \end{cases}\quad (4.17)$$

The second row is considered as a special case of the first row of Equation (4.17), where $k_{bc,(5)}=k_{bc,(15)}=\dots=k_{bc,(115)}=k_{bn}$ (step 7 in Figure 4.1). In general, bulk reaction coefficient for a c-pipe is a step function. It equals k_{bn} when t is outside the c-intervals of downstream junction. When t is within c-intervals, k_b is the average of the k_{bc} between the t_p of the upstream and downstream junctions as shown in Equation (4.17). In a real water network, flow direction inside a pipe may vary with time. For such a c-pipe, it is important to determine its upstream and downstream junctions. This is determined by the t_p of these two junctions. The junction

whose t_p comes earlier is the upstream junction for a c-pipe. In the example shown in Figure 4.7(a), t_p of junction A is 00:05, while t_p for junction B is 02:05. Therefore, junction A is upstream of pipe P_1 , and junction B is downstream of pipe P_1 .

To achieve the chlorine residuals of junction B in the 10-min contamination event, two water quality simulations are needed. In the first simulation, bulk reaction coefficient of pipe P_1 equals the first row in Equation (4.17) (steps 7 through 9 in Figure 4.1). The chlorine residual is shown at the lower horizon line at Figure 4.9. In this example, step 10 in the methodology flowchart (Figure 4.1) is not applicable. It is explained in next example. In the second simulation, bulk reaction coefficient of pipe P_1 equals the second row in Equation (4.17) (steps 11 & 12 in Figure 4.1). The results are presented as the top horizon line in Figure 4.9. The c-interval is also shown in Figure 4.9. Chlorine residuals inside the c-interval of junction B take value in the lower horizon line. Outside the c-interval, chlorine residuals of junction B take the value of the higher horizontal line as the solid line sections shown in Figure 4.9 (step 13 in Figure 4.1). Note that in EPANET 2.0, bulk reaction coefficient takes a negative value to indicate chlorine decay. All the k_b calculated by this research shall multiply with -1 to match the functionality of EPANET 2.0. Since $E=1$ in the example, steps 14 and 15 of the methodology flowchart are not applicable. They are explained in the next example.

Figure 4.7(b) shows a more complicated network than Figure 4.7(a). It has two parallel pipes, P_2 and P_3 between Junctions B and C . Both junctions B and C have no demands, and junction D has a constant demand. Flows in the four pipes are recorded as Q_{w1} through Q_{w4} respectively. Q_{w2} is three times of Q_{w3} . Travel time at these four pipes are 120, 120, 240 and 240 min respectively. Water quality simulation time step is 10 min. Municipal wastewater is released at junction A with a primary dilution ratio of 1:100 between 00:00 and 01:00. The

contaminant release duration is six times that of water quality time step. As a result, the 60-min release event is divided into 6 independent events (step 2 in Figure 4.1). Only the first sub-event is discussed below. The c-interval for junction B is 02:00-02:10 for the first sub-event. After leaving junction B , the contamination parcel breaks into two parts; the one in pipe P_2 is denoted as CP_2 and the one in P_3 is referred to as CP_3 . Accordingly, junction C has two c-intervals. The first is 04:00-04:10; the second is 06:00-06:10. Similarly, junction D has two c-intervals: 08:00-08:20 and 10:00-10:20. For any of the four junctions in this network, at most two c-intervals are observed. CP_2 reaches junction C 04:00-04:10. At this time interval, CP_3 is still in the midpoint of pipe P_3 . When CP_2 reaches junction C , it mixes with the potable water (which has no contaminants) flow from pipe P_3 . Therefore CP_2 dilution ratio at junction B is

$$\frac{X_2 Q_{w2} + X_3 Q_{w3}}{Q_{w2} + Q_{w3}} = \frac{0.01 \times 3 \times Q_{w3} + 0 \times Q_{w3}}{3Q_{s3} + Q_{w3}} = 0.75\% = 1:133 \quad (4.18)$$

Similarly, when CP_3 reaches junction C , CP_2 is in the midpoint of pipe P_4 . So CP_3 dilution ratio at junction C is 0.25% or 1:400 after mixing with potable water from pipe P_2 . These two contamination parcels move inside pipe P_4 at different time. One k_{bc} is needed to represent the movement of one contamination parcel in this pipe.

For any the four pipes in this water network, at most two contaminant parcels pass through. This equals to the maximum number of c-intervals for any of the four junctions. The maximum number of c-intervals for all the c-junctions is

$$I_{\max} = \max(I_j) \quad 1 \leq j \leq J_c \quad (4.19)$$

where J_c is the set of c-junctions. I_{\max} determines the number of chlorine residual simulations in the event of contamination attack. In this first 10-min sub-event, $I_{\max}=2$ (step 6 in Figure 4.1). Therefore, bulk reaction coefficient for pipe P_4 is a step function with three sections. In

EPANET 2.0, one pipe can only be assigned with one single bulk reaction coefficient in each chlorine residual simulation. Consequently, the chlorine residuals of junctions C and D need three simulations. One k_{bc} shall be assigned to represent each contamination parcel. They are denoted as $(P_4)k_{bc}$ and $(P_4)k_{bc}'$ respectively. For pipes P_1 , P_2 and P_3 , they each have one contamination parcel passing by. Therefore, they all have one k_{bc} , which are denoted as $(P_1)k_{bc}$, $(P_2)k_{bc}$ and $(P_3)k_{bc}$ respectively. These k_{bc} are calculated using the method presented in Section 2.3 and the logic described in Equations (4.15)-(4.17).

The bulk reaction coefficient assignments for the three simulations are shown in Table 4.2. The first simulation is to determine the chlorine residual with regard to CP_1 . The second is to calculate the chlorine residual with regard to CP_2 . The third simulation calculates the chlorine residual with the absence of contaminant intrusion. Since both CP_1 and CP_2 originally come from pipe P_1 , $(P_1)k_{bc}$ is used in both the first and second simulations. Three simulations create three sets of chlorine residual data. For each junction and at any specific moment, the chlorine residual is achieved by organizing the three sets of data using the logic shown in Figure 4.9. This chlorine residual of first sub-event is completed.

Chlorine residual analysis is performed for each sub-event (steps 13-14 in Figure 4.1). For each sub-event, the contaminated area, c-junctions, c-pipes are determined. For a pipe network with J junctions, each sub-event creates one chlorine residual for junction j at time t , which are written as $C_{j,t,1}$ through $C_{j,t,E}$. The chlorine residual of junction j at time t with the absence of contaminant attack is written as $C_{j,t,0}$. Each contamination sub-event causes a non-negative chlorine residual change $\Delta C_{j,t}$ at this junction.

$$\Delta C_{j,t,e} = C_{j,t,0} - C_{j,t,e} \quad e \in [1, E] \quad (4.20)$$

Summarization of these chlorine residual changes $\sum_{e=1}^E C_{j,t,0} - C_{j,t,e}$ is the chlorine residual drop caused by these E sub-events; or the whole single event (step 15 in Figure 4.1). The chlorine residual at junction j at time t is

$$C_{j,t} = C_{j,t,0} - \sum_{e=1}^E C_{j,t,0} - C_{j,t,e} = \sum_{e=1}^E C_{j,t,e} - (E - 1) \times C_{j,t,0} \quad 4.21)$$

4.3 Case Study

The studied pipe network is at the south end of the Pinellas County water system (Figure 4.10). Pinellas County is located at southwest Florida. It is a peninsula sandwiched between Gulf of Mexico and Tampa Bay. This county has a humid subtropical climate, resulting in warm, humid summers with frequent thunderstorms, and drier winters. The studied water network is located at south end of Pinellas County, tip of the peninsula. It is referred to as the Gulf Beach system because all end users receive potable water from the Gulf Beach pump station. The distance from the pump station to the south end is approximately 8 kilometers. The full scale water network has been digitized; it has 739 junctions and 851 links. This pipe network is investigated for two reasons: 1) the Gulf Beach pump station only serves the water users in this pipe network. So this network is an isolated system. And, 2) the network is in coastal area with average elevation of 1.5 m above sea level, salt water intrusion and high groundwater table make the water network vulnerable to contaminant attack. Gulf Beach water system has one chlorine source, which is located at the pump station. The chlorine concentration at the discharge point maintains at 3.0 mg/l. Historical data showed that discharge pressures in this pump station ranged from 39 to 55 m of head (55-78 psi). The Gulf Beach system serves a small city located at the upper part of Figure 4.10, and Fort Desoto County Park located at south end of the pipe

network. The major economy in the small city is tourism and retail business. So the water use of the small city follows domestic water use pattern. The small city has a population of approximately 6,000 to 7,000. The park has no permanent residents. Records in 2012 showed that on average 4,000 tourists visited this park every day. The park opens from 7AM to 7 PM every day, and no regular water consumption occurs between 7 PM and 7 AM of the next day. Pipe wall reaction coefficients of this network range from 0.012-0.016 m/day (0.041-0.054 ft/day); they were calibrated using field data (Baggett 2008).

Water quality analysis indicates that the chlorine residuals for all the junctions become cyclical after three days of simulation. Consequently, contamination event occurs at the 4th day of the simulation. Water quality analysis shows that the maximum water age of the network is within two days. Therefore, the simulation duration is set at 6 days. A wastewater leakage event is assumed to occur at junction *J-50111782* 00:00-00:20 at the fourth day. The wastewater has the same chemical and physical properties as that used in the chemical lab tests. Contaminant inflow is 1.84 L/min between 00:00 and 00:10, 3.67 L/min between 00:10 and 00:20. No water consumption occurs at this junction. The flow through this junction is 367 L/min (97 gpm) in the contamination release interval. Therefore, at the source junction, the contamination primary dilution ratio is 0.5% for the first 10 min and 1.0% for the second 10 min. As a result, the contamination event was divided into two 10-min sub-events (step 2 in Figure 4.1).

4.4 Results and Discussions

Before performing water quality simulation on municipal wastewater intrusion, the simulation of nonreactive contaminants is carried out. Same as the release duration of municipal wastewater, nonreactive contaminate is also released at two separate events: 00:00-00:10 and 00:10-00:20. The nonreactive contaminant enters the water system at 200 g/min in both

events. This causes a concentration of 545 mg/l at the source junction in both events. These two events are analysed individually.

For the first sub-event, primary dilution ratio R_p is 1:200. Based on the R_t of 1:2,000 and Equation (4.13), the threshold secondary dilution ratio R_s was calculated to be 1:10. Therefore, any junction whose peak concentration of nonreactive contaminant is higher than 54.5 mg/l (10% of 545 mg/l in the source junction) is a c-junction for the first sub-event. Using this standard, 74 of the 739 junctions are categorized as c-junctions. They are highlighted in Figure 4.11(a). Among these c-junctions, the moments when contaminant concentrations are less than 54.5 mg/l are excluded from c-intervals. Using the information of c-junctions, 84 pipes are determined to be c-pipes. Hydraulics analysis shows that 82 pipes has one flow direction during the six-day simulation, two pipes have varying flow directions. For those c-junctions, the maximum number of c-intervals, I_{max} , is one. Therefore, one simulation was performed to model chlorine decay due to the 10-min contaminant event. Junction *AFD-39* is selected to show the chlorine residuals as a result of the 10-min contamination event. Hydraulic and water quality simulations show that the contamination event only affects this junction on the fourth day. Therefore, chlorine residual curve of the fourth day of this junction is presented in Figure 4.12. It shows that minimum chlorine residual is 1.55 mg/l at 09:50-10:00.

For the second sub-event, primary dilution ratio R_p is 1:100. Therefore, the threshold secondary dilution ratio R_s is 1:20. Therefore, any junction whose peak concentration of nonreactive contaminant is higher than 27.3 mg/l (5% of 545 mg/l in the source junction) is a c-junction at this sub-event. Using this standard, 164 junctions are determined to be c-junctions; they are highlighted in Figure 4.11(b). Using the information of the c-junction, 185 pipes are determined to be c-pipes. For those c- junctions, the maximum numbers of c-interval,

D_{max} is two. Therefore, two simulations were performed to model chlorine decay due to the 10-min contaminant event. Hydraulic and water quality simulations show that the contamination event only affects junction *AFD-39* on the fourth day. Therefore, chlorine residual curve of the fourth day of this junction is presented in Figure 4.12. The results suggest that the minimum chlorine residual is 1.10 mg/l between 09:40-10:20.

Since these two 10-min sub-events are intentionally created from a single 20-min event, the chlorine residual simulations of each junction at these two sub-events shall be consolidated to represent a single contamination event as explained in step 15 of the methodology flowchart. The chlorine residual curve of *AFD-39* at the fourth day at the 20-min single event was created using Equation (4.21) and is shown in Figure 4.12. The results indicate that the minimum chlorine residual is 0.40 mg/l between 09:40-10:00.

The union of the c-junction sets of these two 10-min sub-events is the set of c-junctions for this 20-min contamination event. Figures 4.11(a) and (b) reveal that the c-junctions of the second sub-event cover all c-junctions of the first c-junctions. Therefore, the 20-min contamination event totally pollutes 164 junctions. This study discusses contamination intrusion at single source junction. With regard to multiple source intrusions, each single source can be separately analysed using the methodology shown in Figure 4.1. The cumulative effect of multiple sources on chlorine decay can be calculated using Equation (4.21).

4.5 Conclusions

This study developed an EPANET-based methodology to simulate the chlorine residual of water distribution system in the event of contaminant intrusion. Contaminants are considered as a group of materials that react with chlorine in bulk water. Regular chlorine decay and transport model is used to describe the chlorine decay in the event of contaminant

attack. Unlike simulating normally operated potable water network, where pipe bulk reaction coefficients are constants. In this study, pipe bulk reaction coefficients are temporal variables whose values depend on instantaneous contaminant concentrations. Municipal wastewater is chosen as a contaminant matrix. This methodology is applicable for water utilities due to its two advantages: 1) simplicity in chemical analyses. The contaminant matrix is studied as a whole; no detailed chemical analyses of contaminant matrix are needed. Chemical tests are performed to study the chlorine decay kinetics and temporal development of bulk reaction coefficient for contaminated potable water samples. Water utilities can use the same method shown in Section 4.2.3 to investigate other types of contaminants, such as regular groundwater, food processing wastewater, petrochemicals, and storm water runoff and establish standard databases for reference. 2) Simplicity in water quality simulation. The contaminant matrix is studied as a whole, it is not necessary to investigate the principles of reactions between contaminants and chlorine and achieve the reaction kinetics coefficient of each of the reaction. Therefore, Only EPANET is needed in this methodology. The two advantages improve the work efficiencies of lab chemists and hydraulic engineers in water utilities.

4.6 Notations

The following symbols are used in this study:

$C_{j,t}$ = chlorine residual of junction j at time t (mg/l);

D_j = number of contamination intervals for a contaminated junction;

I_j = number of contaminated intervals for contaminated junction j ;

J = number of junctions of a water network;

J_c = number of contaminated junctions of a water network;

k_b = bulk reaction coefficient for one specific pipe;

k_{bn} = bulk reaction coefficient for one pipe with the absence of a contamination event;

k_{bc} = bulk reaction coefficient for one pipe in the event of contaminant attack;

M = number of chlorine demanding constituents in contaminant matrix;

MF = number of fast chlorine demanding constituents in contaminant matrix;

MS = number of slow chlorine demanding constituents in contaminant matrix;

N = number of chlorine demanding constituents in normal potable water;

NF = number of fast chlorine demanding constituents in normal potable water;

NS = number of slow chlorine demanding constituents in normal potable water;

R = dilution ratio of contaminant matrix to water;

Q_x = inflow of contaminant matrix at source junction (L/min);

Q_w = water flow in pipes (L/min);

t_p = moment with highest contaminant concentration within a c-interval of a c-pipe;

$[X]$ = contaminant concentration (mg/l);

4.7 References

Baggett, C., et al. (2008). "From start to finish: calibrating Pinellas County's 2,000-mile hydraulic water distribution system model." *Florida Water Resour. J.*, 60(12), 44-54.

Bovey, B., Wallentin, D., and Bullen, S. (2009). *Professional Excel Development: The Definitive Guide to Developing Applications Using Microsoft Excel, VBA, and .NET.* Addison-Wesley Professional, New York

Fisher, I., and Kastl, G., (2011). "Evaluation of suitable chlorine bulk decay models for water distribution systems." *Water Research*, 45(16), 4896-4908.

Gullick, R., LeChevallier, M., Svindland, R., and Friedman, M. (2004). "Occurrence of transient low and negative pressures in distribution systems." *J. AWWA*, 96(11), 52-66.

Hanselman, D., and Littlefield, B. (2005). *Mastering Matlab 7*, Pearson/Prentice Hall, Upper Saddle River, NJ.

Helbling, D., and Vanbriesen, J. (2007). "Free chlorine demand and cell survival of microbial suspensions." *Water Research*, 41(10), 4424-4434.

- Helbling, D., and VanBriesen, J., (2009). “Modelling residual chlorine response to a microbial contamination event in drinking water distribution systems.” *J. Environ. Eng.*, 135(10), 918-927.
- Jonkergouw, P., Khu, S., Kapelan, Z., and Savić, D. (2008). “Water quality model calibration under unknown demands.” *J. Water Resour. Plann. Manage.*, 134(4), 326–336.
- Jonkergouw, P., Khu S, Savic D, Zhong D., Hou X., and Zhao H. (2009). “A variable rate coefficient chlorine decay model.” *Environ. Sci. Technol.*, 43(2), 408–414.
- Karim, M., Abbaszadegan, M, and LeChevallier, M. (2003). “Potential for pathogen intrusion during pressure transients.” *J. AWWA.*, 95(5), 134–146.
- Munavalli, G., and Kumar, M. (2004). “Dynamic simulation of multicomponent reaction transport in water distribution systems.” *J. AWWA.* 95(5), 134–146.
- Qureshi N., and Shah, J., (2014). “Aging infrastructure and decreasing demand: A dilemma for water utilities.” *J. AWWA.*, 106(1), 51-61.
- Rossman, L., (2000). EPANE2 user’s manual, Risk Reduction Engineering Laboratory, US Environmental Protection Agency, Cincinnati.
- Schwartz, R., Lahav, O., and Ostfeld, A., (2014). “Integrated hydraulic and organophosphate pesticide injection simulations for enhancing event detection in water distribution systems.” *Water Research*, 63, 271-284
- Shang, F., and Ulber, J., (2008). “Modelling Reaction and Transport of multiple species in water distribution systems.” *Environ. Sci. Technol.*, 42(2), 808-814
- USEPA. (2005a). WaterSentinel Online water quality monitoring as an indicator of drinking water contamination. Water Security Division. Washington DC.
- USEPA. (2005b). WaterSentinel System Architecture. Water Security Division. Washington DC.
- USEPA. (2009). Distribution System Water Quality Monitoring: Sensor Technology Evaluation Methodology and Results. National Homeland Security Research Centre. Cincinnati, Ohio.
- USEPA. (2010). Sensor network design for drinking water contamination warning systems. National Homeland Security Research Centre
- Zechman, E., and Ranjithan, R. (2009). “Evolutionary computation-based methods for characterizing contaminant sources in a water distribution system.” *J. Water Resour. Plann. Manage.*, 131(2), 263-273

Table 4.1 Contaminants identified by USEPA

Contaminant Detection Class	Description
1	Petroleum products
2	Pesticides (chlorine reactive)
3	Inorganic compounds
4	Metals
5	Pesticides (chlorine resistant)
6	Chemical warfare agents
7	Radionuclides
8	Bacterial toxins
9	Plant toxins
10	Pathogens causing diseases with unique symptoms
11	Pathogens causing diseases with common symptoms
12	Persistent chlorinated organic compounds

Table 4.2 Bulk reaction coefficients

Simulation	Bulk Reaction Coefficients			
	P_1	P_2	P_3	P_4
1	$(P_1)k_{bc}$	$(P_2)k_{bc}$	k_{bn}	$(P_4)k_{bc}$
2	$(P_1)k_{bc}$	k_{bn}	$(P_3)k_{bc}$	$(P_4)k_{bc}'$
3	k_{bn}	k_{bn}	k_{bn}	k_{bn}

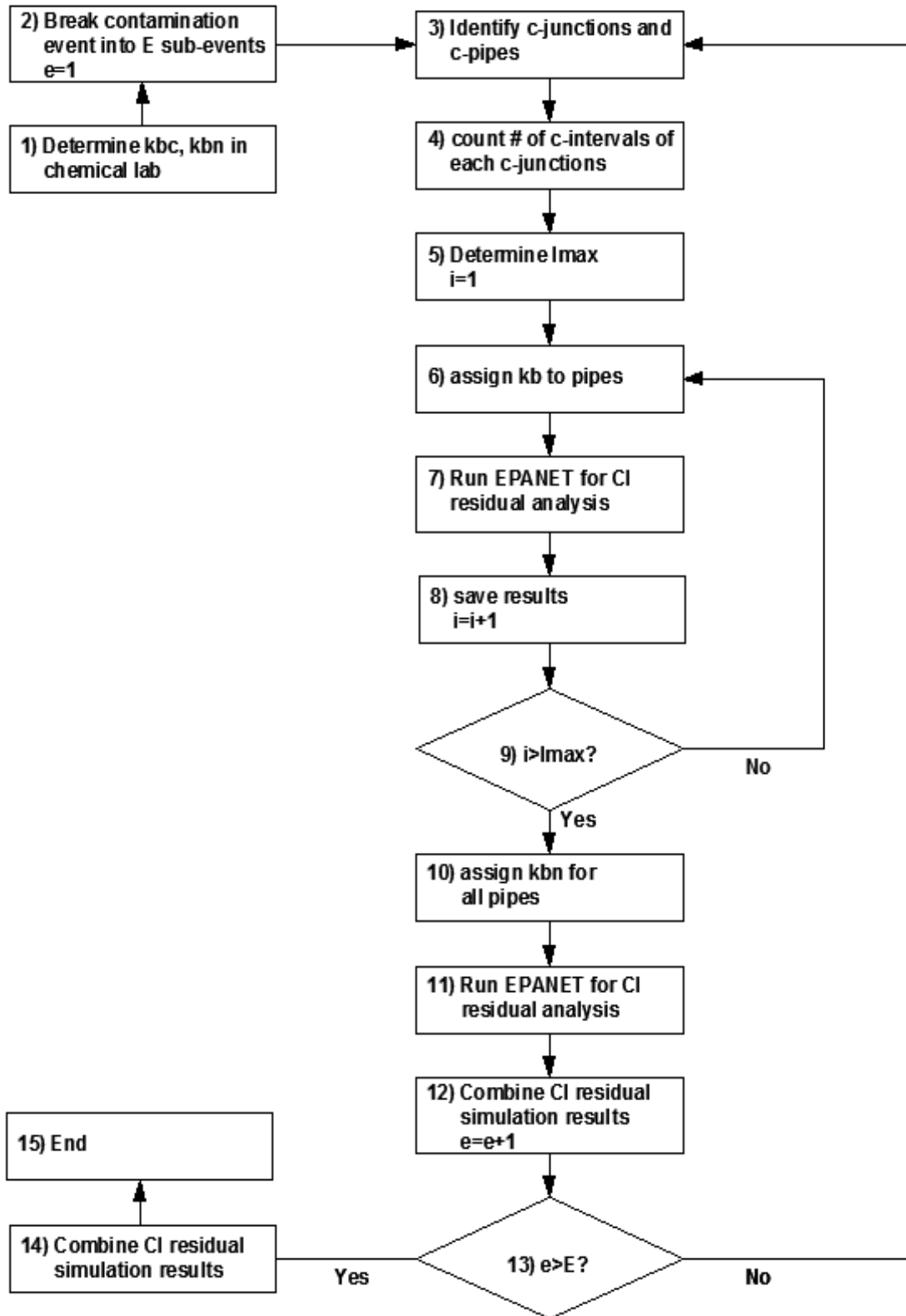


Figure 4.1 Methodology flowchart

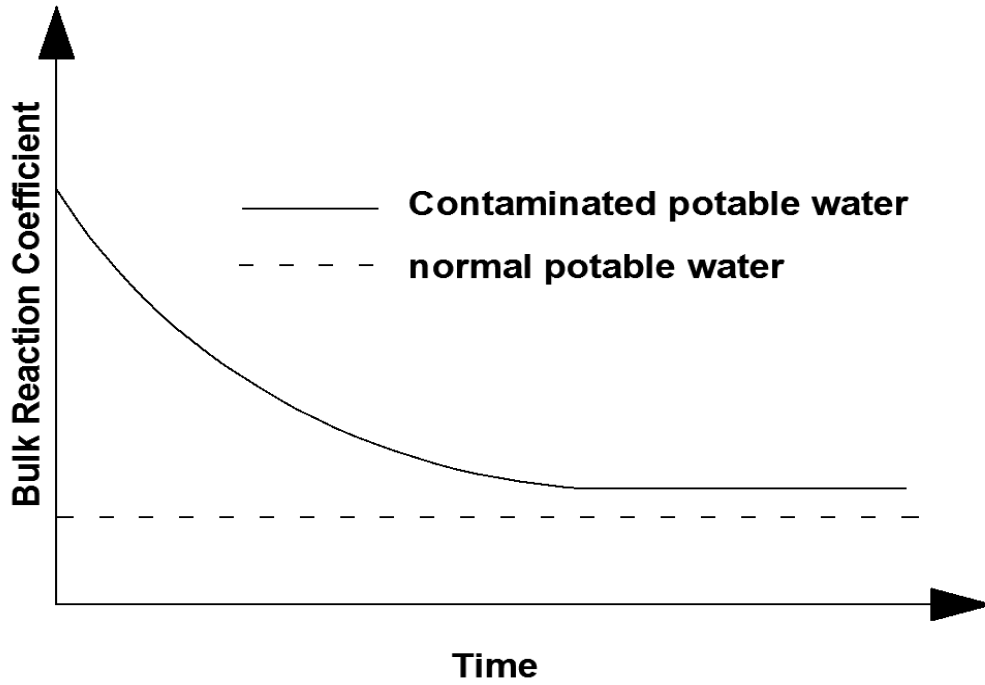


Figure 4.2 Bulk reaction coefficients

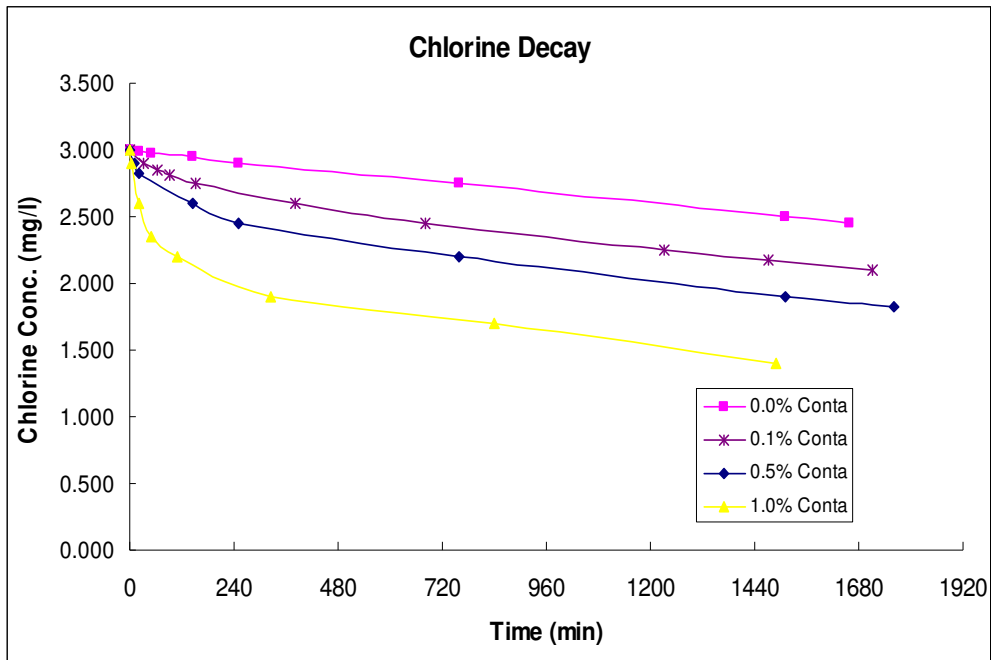


Figure 4.3 Chlorine decay at contaminant attack

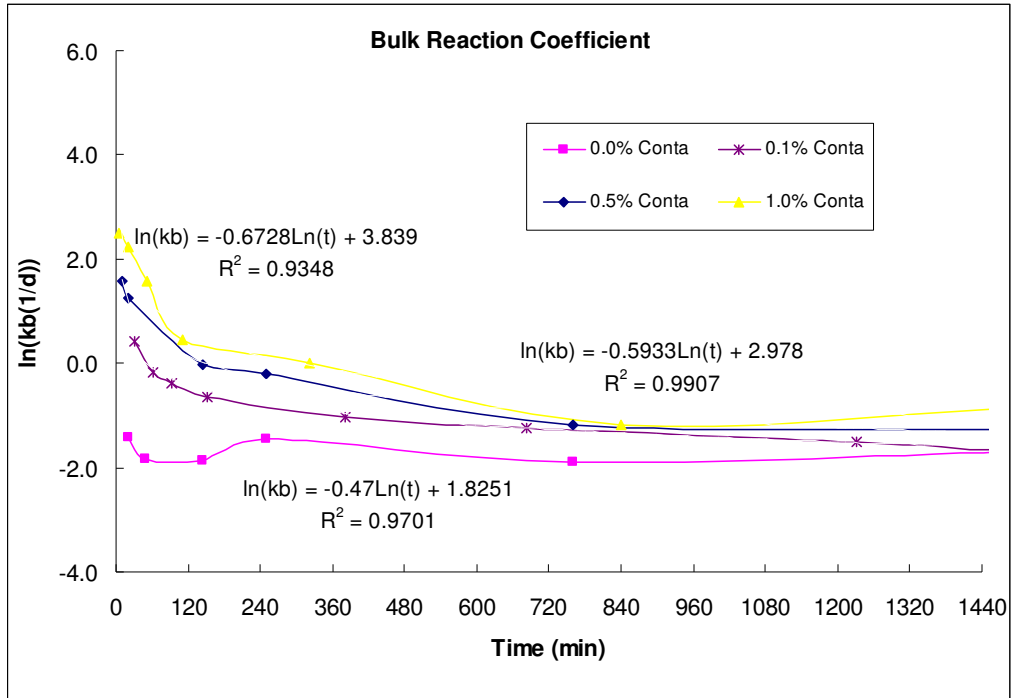


Figure 4.4 Bulk reaction coefficient curves

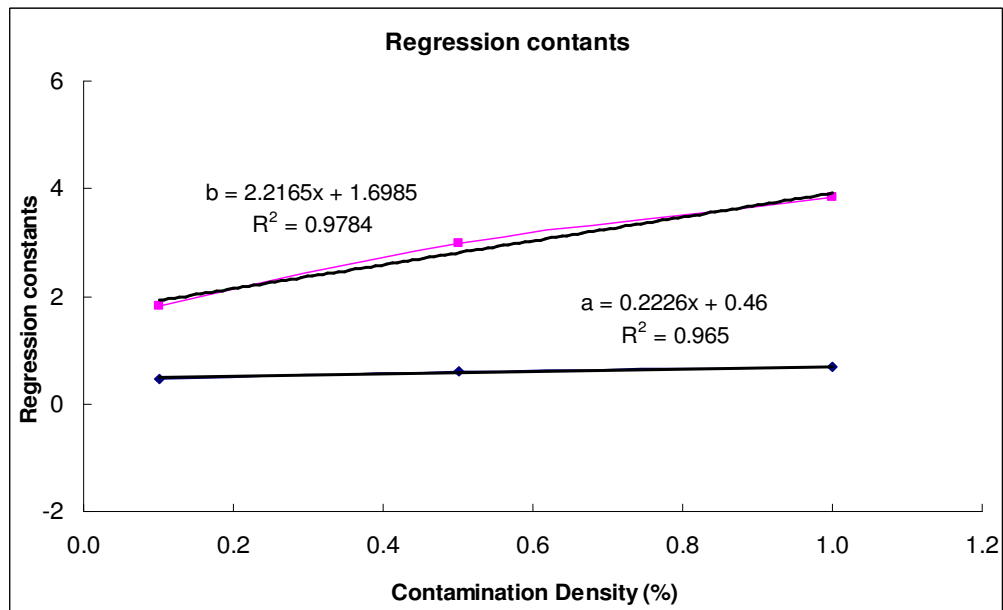


Figure 4.5 Regression constants for bulk reaction coefficients

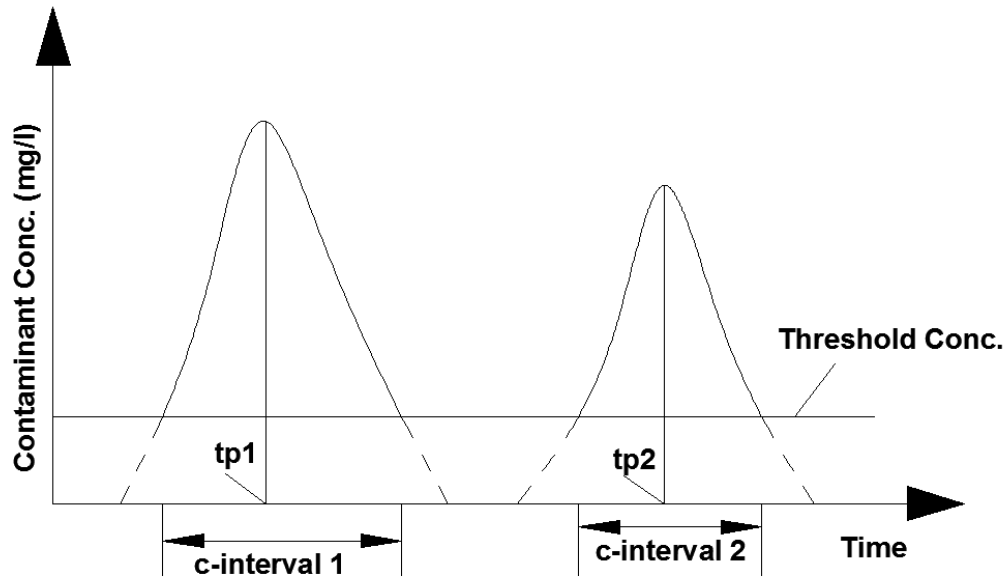


Figure 4.6 Nonreactive contaminant concentrations



Figure 4.7(a) Contaminant matrix in single pipe

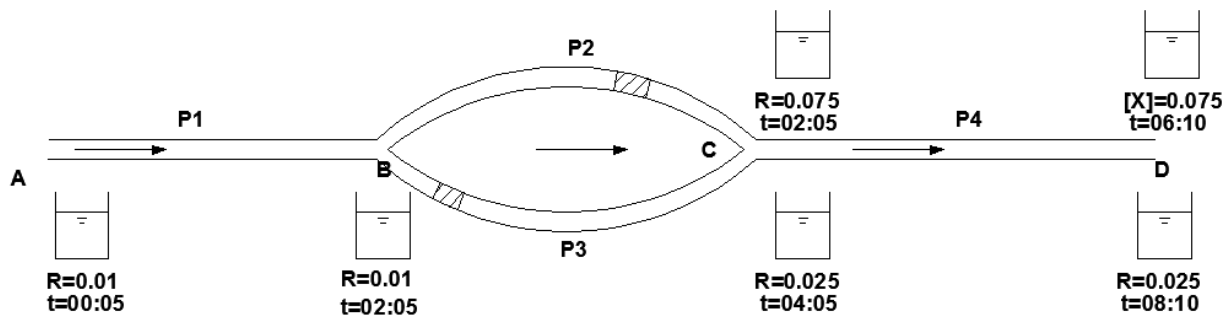


Figure 4.7(b) Contaminant matrix in branch pipe network

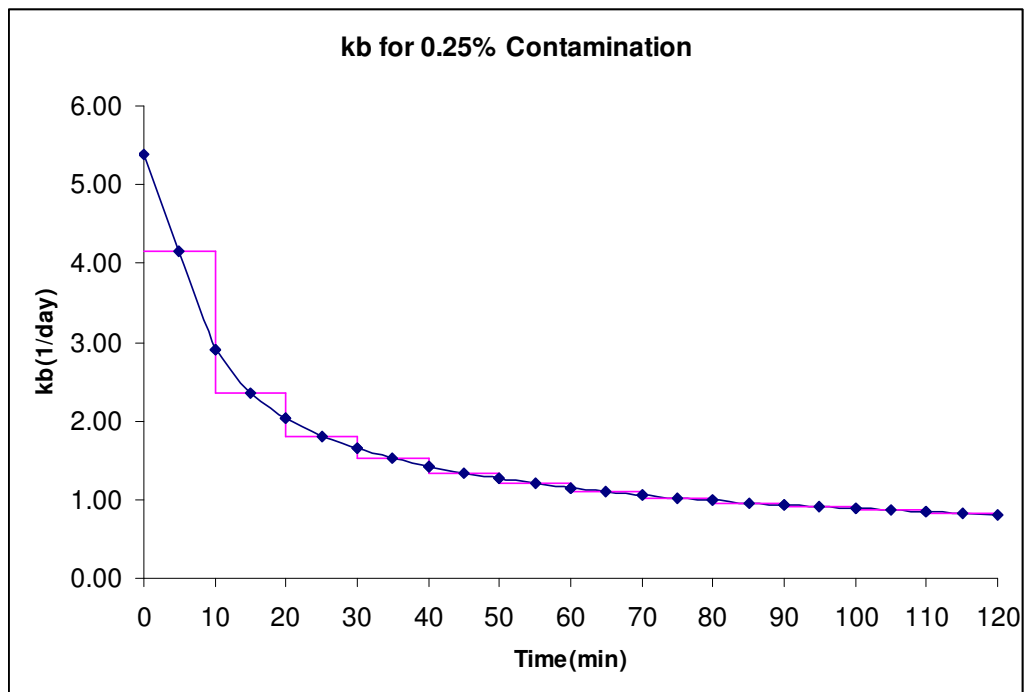


Figure 4.8 Step function of bulk reaction coefficient

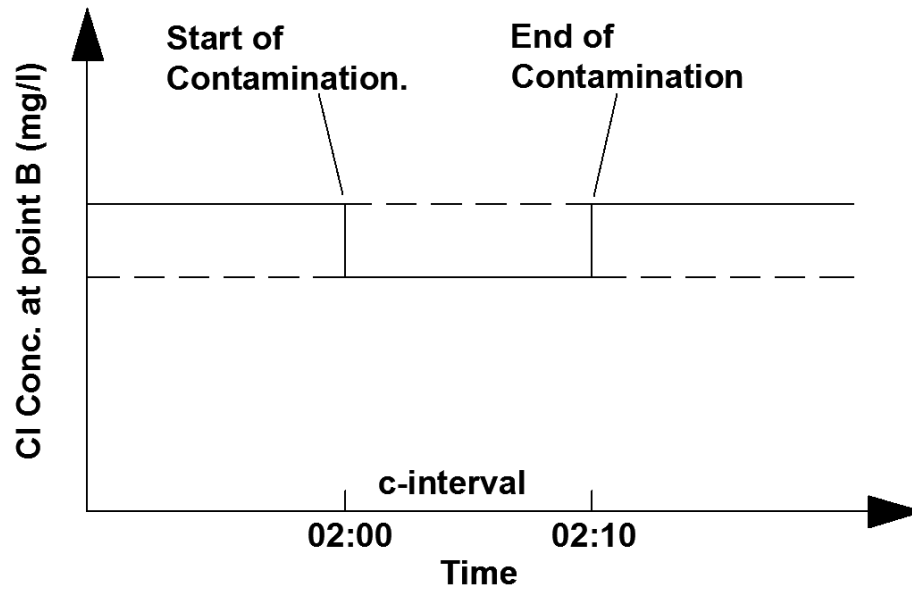


Figure 4.9 Step function of chlorine residuals

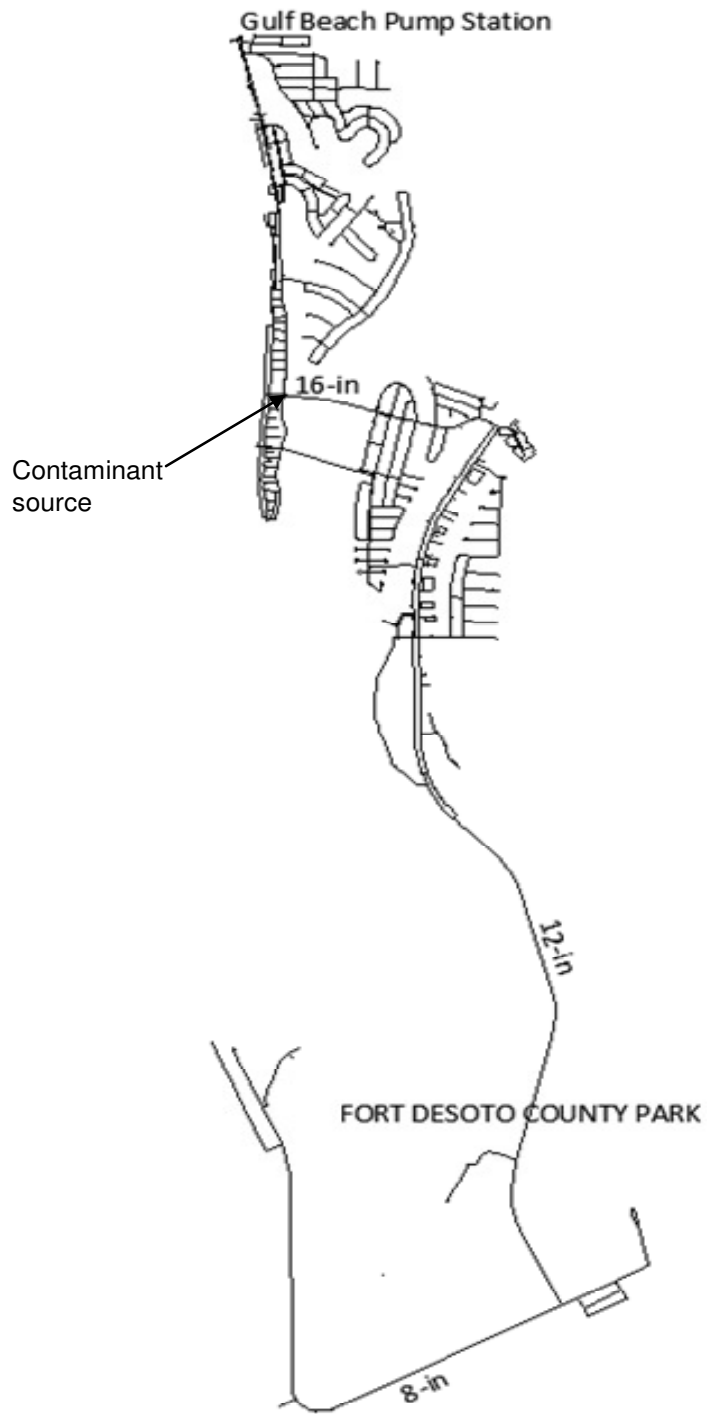


Figure 4.10 Studied water network

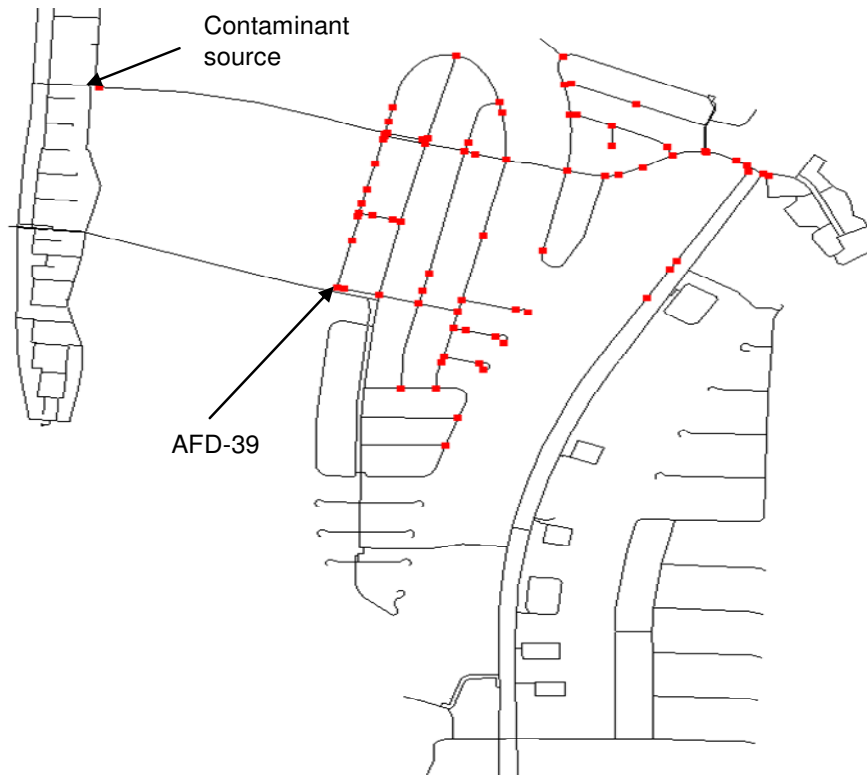


Figure 4.11(a) Contaminated junctions for the first contamination sub-event



Figure 4.11(b) Contaminated junctions for the second contamination sub-event

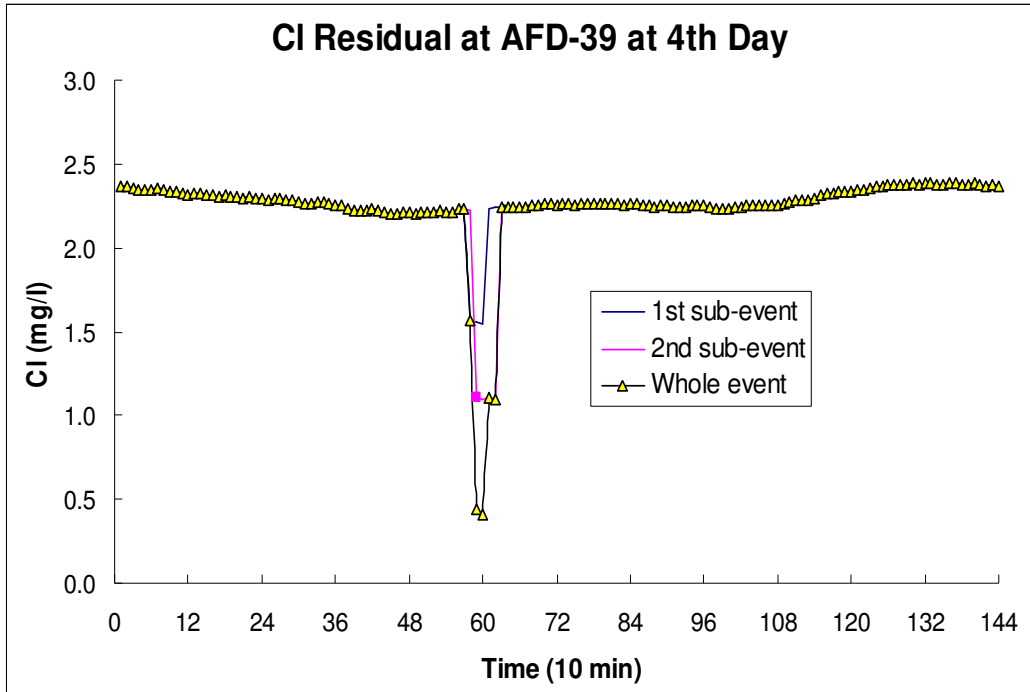


Figure 4.12 Concentrations of AFD-39

Chapter 5: Conclusions

After water distribution system is put in service, normal operations and maintenances are very import for water utilities. This research investigates three topics that are closely related to the normal operation and operation optimization of water distribution system. The first and second studies are about maintenance and operation optimizations of water distribution system. The third study is on water quality simulation, it is the basis of some optimization questions such as sensor placement for contaminant detection and contamination source characterization. Therefore, these three topics are common in the following aspects: 1) they are all about water quality in water distribution system; 2) they are all about operation and maintenance of water distribution system; and, 3) they are all about or related to operation optimizations of water distribution system.

The first study presents an innovative approach of sampling location design for calibrating chlorine decay simulation. The advantage of this method, compared to the traditional iterative sensitivity matrix method, is that a prior knowledge or estimation of wall reaction coefficients is not necessary. The study mainly investigates first-order wall reaction in a steady-state flow condition. Its application can be extended to two directions: (1) zero order wall reaction, and (2) semi-steady state, with a diurnal water demand pattern and/or chlorine injection pattern. In both cases, only sampling point matrices needs modifications. This technique was applied in a pilot water distribution system; it can be used in large-scale WDS without any

changes in the algorithm. A large distribution system can be divided into several small systems. Water utilities engineer can analyze each small system individually and find optimal sampling location design for each small system.

The second study provides an insightful approach on AFD operation optimization in a water distribution system. This problem is formulated as a single objective discrete optimization problem and is solved in three phases. This method is applied to a chloraminated water distribution system. The results suggest that water flushing volume calculated by optimal AFD operation configuration is significantly less than current field practice. Since this methodology was developed based on EPANET simulation, it is readily applicable to chlorinated or any other water distribution systems that EPANET can simulate. Optimizing the AFD operations in a large water network using EPANET 2.0 is challenging. This can be improved by implementing two methods: 1) studying the network, identifying the areas with high AFD density, isolating and studying the key areas. This is the method we used in this study; and, 2) speeding up water system simulation using techniques such as parallel computation, or domain decomposition. As long as the hydraulic and water quality simulator works at fast speed, methodology presented herein will be applicable in solving big water networks.

The third study developed an EPANET-based methodology to simulate the chlorine residuals of water distribution system in the event of contaminant intrusion. Contaminants are considered as a group of chlorine-demanding materials that react with chlorine into bulk water. Regular chlorine decay and transport model is used to describe the chlorine decay in the event of contaminant attack. Unlike simulating normally operated potable water network, where pipe bulk reaction coefficients are constants. In this study, pipe bulk reaction coefficients are temporal variables whose values depend on instantaneous contaminant concentrations.

Municipal wastewater is chosen as a contaminant matrix. This methodology is applicable for water utilities due to its two advantages: 1) simplicity in chemical analyses. The contaminant matrix is studied as a whole; no detailed chemical analyses of contaminant matrix are needed. Water utilities can use this approach to investigate other types of contaminants, such as regular groundwater, food processing wastewater, petrochemicals, and storm water runoff and establish standard databases for reference. 2) Simplicity in water quality simulation. The contaminant matrix is studied as a whole, it is not necessary to investigate the reaction principles of the contaminants with chlorine and obtain the reaction kinetics coefficients of each of the reaction. Therefore, Only EPANET is needed in this methodology. The two advantages improve the work efficiencies of lab chemists and hydraulic engineers in water utilities.

Appendices

Appendix A Copyright Permissions

The following are Copyright permissions for use of materials in Chapters 2, and 3, respectively.

RE: nurw20:Sampling design for water distribution network chlorine decay calibration Inbox x



Anderson, Lee-Ann <Lee-Ann.Anderson@tandf.co.uk>

10:46 AM (1 hour ago) ☆

to me

Our Ref: LA/NURW/P2420

30 October 2014

Dear Xiongfei Xie

Thank you for your correspondence requesting permission to reproduce the following material from our Journal in your thesis entitled 'Operation optimization and water quality simulation of potable water distribution system' and to be posted in the university's repository University of South Florida

Material Requested: Sampling design for water distribution network chlorine decay calibration, by Xiongfei Xie, Bo Zeng & Mahmood Nachabe, published in Urban Water Journal (2013)

We will be pleased to grant permission on the sole condition that you acknowledge the original source of publication and insert a reference to the article on the Journals website: <http://www.tandfonline.com/>

This is the authors accepted manuscript of an article published as the version of record in Urban Water Journal © 15 Oct 2013 <http://www.tandfonline.com/doi/full/10.1080/1573062X.2013.831911#>

Please note that this license does not allow you to post our content on any third party websites or repositories.

Thank you for your interest in our Journal.

Yours sincerely

Lee-Ann

Lee-Ann Anderson – Permissions & Licensing Administrator, Journals

Taylor & Francis Group

3 Park Square, Milton Park, Abingdon, Oxon, OX14 4RN, UK

Tel: +44 (0)20 7017 7932

Web: www.tandfonline.com

e-mail: lee-ann.anderson@tandf.co.uk

Taylor & Francis is a trading name of Informa UK Limited,
registered in England under no. 1072954



Visit <http://www.tandf.co.uk/eupdates> to receive email updates about journals, books and other news within your areas of interest.



RightsLink®

Home

Create Account

Help



Title: Optimal Scheduling of Automatic Flushing Devices in Water Distribution System

Author: Xiongfei Xie, Mahmoud Nachabe, Bo Zeng

Publication: Journal of Water Resources Planning and Management

Publisher: American Society of Civil Engineers

Date: 09/02/2014

Copyright © 2014, ASCE. All rights reserved.

User ID
Password
<input type="checkbox"/> Enable Auto Login
LOGIN
Forgot Password/User ID?
If you're a copyright.com user, you can login to RightsLink using your copyright.com credentials. Already a RightsLink user or want to learn more?

Permissions Request

As an ASCE author, you are permitted to reuse you own content for another ASCE or non-ASCE publication.

Please add the full credit line "With permission from ASCE" to your source citation. Please print this page for your records.

Type of use: Dissertation/Thesis

Portion: full article

Format: electronic

Use of this content will make up more than 25% of the new work: no

Author of this ASCE work or ASCE will publish the new work: yes

BACK

CLOSE WINDOW

Copyright © 2014 [Copyright Clearance Center, Inc.](#) All Rights Reserved. [Privacy statement.](#) Comments? We would like to hear from you. E-mail us at customercare@copyright.com

Appendix B GAMS Code for Chlorine Decay Calibration Sampling Design

```
$title Gear Train Design (GEAR,SEQ=1)
```

```
$ontext
```

```
This is a test if kf >> kw
```

```
$offtext
```

```
sets SA1 nodes / S1*S30 /
kw wall reaction coefficients /kw1*kw4/
unit /unit1*unit4/
;
```

```
alias (SA1,SA);
```

```
scalar M "scaling constant" /570/;
```

```
table UnitVector unit vector
```

	kw1	kw2	kw3	kw4
unit1	1	0	0	0
unit2	0	1	0	0
unit3	0	0	1	0
unit4	0	0	0	1

```
;
```

```
binary variables
```

```
x(SA1) '30 sampling points'
```

```
z(SA,SA1) 'the binary product of x,y';
```

```
‘*positive variables
```

```
free variables
```

```
lambda_1(SA,SA1) 'lambda for kw1',
```

```
lambda_2(SA,SA1) 'lambda for kw2',
```

```
lambda_3(SA,SA1) 'lambda for kw3',
```

```
lambda_4(SA,SA1) 'lambda for kw4',
```

```
w_1(SA,SA1) 'the linearization for kw1',
```

```
w_2(SA,SA1) 'the linearization for kw2',
```

```
w_3(SA,SA1) 'the linearization for kw3',
```

```
w_4(SA,SA1) 'the linearization for kw4',
```

```
zz 'objective function value';
```


Table matrix1(SA1,kw)

	kw1	kw2	kw3	kw4
S1	0.0000	0.0000	0.0000	0.0000
S2	0.0000	0.0000	0.0000	0.0000
S3	0.0000	0.0000	0.0000	0.0000
S4	0.0000	0.0000	0.0000	0.0000
S5	0.0000	0.0000	0.0000	0.0000
S6	0.0000	0.0000	0.0000	0.0000
S7	0.0000	0.0000	0.0000	0.0000
S8	0.0000	0.0000	0.0000	0.0000
S9	0.0000	0.0000	0.0000	0.0000
S10	0.0000	0.0000	0.0000	0.0000
S11	0.0000	0.0000	0.0000	0.0000
S12	0.0000	0.0000	0.0000	0.0000
S13	0.0000	0.0000	0.0000	0.0000
S14	0.0000	0.0000	0.0000	0.0000
S15	0.0000	0.0000	0.0000	0.0000
S16	0.0000	0.0000	0.0000	0.0000
S17	0.0000	0.0000	0.0000	0.0000
S18	0.0000	0.0000	0.0000	0.0000
S19	0.0000	0.0000	0.0000	0.0000
S20	0.0000	0.0000	0.0000	0.0000
S21	0.0000	0.0000	0.0000	0.0000
S22	0.0000	0.0000	0.0000	0.0000
S23	0.0000	0.0000	0.0000	0.0000
S24	0.0000	0.0000	0.0000	0.0000
S25	0.0000	0.0000	0.0000	0.0000
S26	0.0000	0.0000	0.0000	0.0000
S27	0.0000	0.0000	0.0000	0.0000
S28	0.0000	0.0000	0.0000	0.0000
S29	0.0000	0.0000	0.0000	0.0000
S30	0.0000	0.0000	0.0000	0.0000

;

Table matrix2(SA1,kw) 'accounting matrix for commodities'

	kw1	kw2	kw3	kw4
S1	0.0000	1.0000	0.0000	-1.0000
S2	0.0000	0.0000	0.0000	0.0000
S3	0.0000	0.0000	0.0000	0.0000
S4	0.0000	0.0000	0.0000	0.0000
S5	0.0000	0.0000	0.0000	0.0000

S6	0.0000	0.0000	0.0000	0.0000
S7	0.0000	0.0000	0.0000	0.0000
S8	0.0000	0.0000	0.0000	0.0000
S9	0.0000	0.0000	0.0000	0.0000
S10	0.0000	0.0000	0.0000	0.0000
S11	0.0000	0.0000	0.0000	0.0000
S12	0.0000	0.0000	0.0000	0.0000
S13	0.0000	0.0000	0.0000	0.0000
S14	0.0000	0.0000	0.0000	0.0000
S15	0.0000	0.0000	0.0000	0.0000
S16	0.0000	0.0000	0.0000	0.0000
S17	0.0000	0.0000	0.0000	0.0000
S18	0.0000	0.0000	0.0000	0.0000
S19	0.0000	0.0000	0.0000	0.0000
S20	0.0000	0.0000	0.0000	0.0000
S21	0.0000	0.0000	0.0000	0.0000
S22	0.0000	0.0000	0.0000	0.0000
S23	0.0000	0.0000	0.0000	0.0000
S24	0.0000	0.0000	0.0000	0.0000
S25	0.0000	0.0000	0.0000	0.0000
S26	0.0000	0.0000	0.0000	0.0000
S27	0.0000	0.0000	0.0000	0.0000
S28	0.0000	0.0000	0.0000	0.0000
S29	0.0000	0.0000	0.0000	0.0000
S30	0.0000	0.0000	0.0000	0.0000
;				

Table matrix3(SA1,kw) accounting matrix for commodities

	kw1	kw2	kw3	kw4
S1	0.0000	0.0000	0.0000	0.0000
S2	0.0000	0.0000	0.0000	0.0000
S3	0.0000	0.0000	0.0000	0.0000
S4	0.0000	0.0000	0.0000	0.0000
S5	0.0000	0.0000	0.0000	0.0000
S6	0.0000	0.0000	0.0000	0.0000
S7	0.0000	0.0000	0.0000	0.0000
S8	0.0000	0.0000	0.0000	0.0000
S9	0.0000	0.0000	0.0000	0.0000
S10	0.0000	0.0000	0.0000	0.0000
S11	0.0000	0.0000	0.0000	0.0000
S12	0.0000	0.0000	0.0000	0.0000
S13	0.0000	0.0000	0.0000	0.0000
S14	0.0000	0.0000	0.0000	0.0000

S15	0.0000	0.0000	0.0000	0.0000
S16	0.0000	0.0000	0.0000	0.0000
S17	0.0000	0.0000	0.0000	0.0000
S18	0.0000	0.0000	0.0000	0.0000
S19	0.0000	0.0000	0.0000	0.0000
S20	0.0000	0.0000	0.0000	0.0000
S21	0.0000	0.0000	0.0000	0.0000
S22	0.0000	0.0000	0.0000	0.0000
S23	0.0000	0.0000	0.0000	0.0000
S24	0.0000	0.0000	0.0000	0.0000
S25	0.0000	0.0000	0.0000	0.0000
S26	0.0000	0.0000	0.0000	0.0000
S27	0.0000	0.0000	0.0000	0.0000
S28	0.0000	0.0000	0.0000	0.0000
S29	0.0000	0.0000	0.0000	0.0000
S30	0.0000	0.0000	0.0000	0.0000
;				

Table matrix4(SA1,kw)

	kw1	kw2	kw3	kw4
S1	0.0000	0.0000	0.0000	0.0000
S2	0.0000	0.0000	0.0000	0.0000
S3	1.0000	0.0000	0.0000	1.0000
S4	0.0000	0.0000	0.0000	0.0000
S5	0.0000	0.0000	0.0000	0.0000
S6	0.0000	0.0000	0.0000	0.0000
S7	0.0000	0.0000	0.0000	0.0000
S8	0.0000	0.0000	0.0000	0.0000
S9	0.0000	0.0000	0.0000	0.0000
S10	0.0000	0.0000	0.0000	0.0000
S11	0.0000	0.0000	0.0000	0.0000
S12	0.0000	0.0000	0.0000	0.0000
S13	0.0000	0.0000	0.0000	0.0000
S14	0.0000	0.0000	0.0000	0.0000
S15	0.0000	0.0000	0.0000	0.0000
S16	0.0000	0.0000	0.0000	0.0000
S17	0.0000	0.0000	0.0000	0.0000
S18	0.0000	0.0000	0.0000	0.0000
S19	0.0000	0.0000	0.0000	0.0000
S20	0.0000	0.0000	0.0000	0.0000
S21	0.0000	0.0000	0.0000	0.0000
S22	0.0000	0.0000	0.0000	0.0000
S23	0.0000	0.0000	0.0000	0.0000

S24	0.0000	0.0000	0.0000	0.0000
S25	0.0000	0.0000	0.0000	0.0000
S26	0.0000	0.0000	0.0000	0.0000
S27	0.0000	0.0000	0.0000	0.0000
S28	0.0000	0.0000	0.0000	0.0000
S29	0.0000	0.0000	0.0000	0.0000
S30	0.0000	0.0000	0.0000	0.0000
;				

Table matrix5(SA1,kw)

	kw1	kw2	kw3	kw4
S1	0.0000	0.0000	0.0000	0.0000
S2	0.0000	0.0000	0.0000	0.0000
S3	2.0000	0.0000	0.0000	1.0000
S4	1.0000	0.0000	0.0000	0.0000
S5	0.0000	0.0000	0.0000	0.0000
S6	0.0000	0.0000	0.0000	0.0000
S7	0.0000	0.0000	0.0000	0.0000
S8	0.0000	0.0000	0.0000	0.0000
S9	0.0000	0.0000	0.0000	0.0000
S10	0.0000	0.0000	0.0000	0.0000
S11	0.0000	0.0000	0.0000	0.0000
S12	0.0000	0.0000	0.0000	0.0000
S13	0.0000	0.0000	0.0000	0.0000
S14	0.0000	0.0000	0.0000	0.0000
S15	0.0000	0.0000	0.0000	0.0000
S16	0.0000	0.0000	0.0000	0.0000
S17	0.0000	0.0000	0.0000	0.0000
S18	0.0000	0.0000	0.0000	0.0000
S19	0.0000	0.0000	0.0000	0.0000
S20	0.0000	0.0000	0.0000	0.0000
S21	0.0000	0.0000	0.0000	0.0000
S22	0.0000	0.0000	0.0000	0.0000
S23	0.0000	0.0000	0.0000	0.0000
S24	0.0000	0.0000	0.0000	0.0000
S25	0.0000	0.0000	0.0000	0.0000
S26	0.0000	0.0000	0.0000	0.0000
S27	0.0000	0.0000	0.0000	0.0000
S28	0.0000	0.0000	0.0000	0.0000
S29	0.0000	0.0000	0.0000	0.0000
S30	0.0000	0.0000	0.0000	0.0000
;				

Table matrix6(SA1,kw)

	kw1	kw2	kw3	kw4
S1	0.0000	0.0000	0.0000	0.0000
S2	0.0000	0.0000	0.0000	0.0000
S3	0.0000	0.0000	0.0000	0.0000
S4	0.0000	0.0000	0.0000	0.0000
S5	0.0000	0.0000	0.0000	0.0000
S6	0.0000	0.0000	0.0000	0.0000
S7	0.0000	0.0000	0.0000	0.0000
S8	0.0000	0.0000	0.0000	0.0000
S9	0.0000	0.0000	0.0000	0.0000
S10	0.0000	0.0000	0.0000	0.0000
S11	0.0000	0.0000	0.0000	0.0000
S12	0.0000	0.0000	0.0000	0.0000
S13	0.0000	0.0000	0.0000	0.0000
S14	0.0000	0.0000	0.0000	0.0000
S15	0.0000	0.0000	0.0000	0.0000
S16	0.0000	0.0000	0.0000	0.0000
S17	0.0000	0.0000	0.0000	0.0000
S18	0.0000	0.0000	0.0000	0.0000
S19	0.0000	0.0000	0.0000	0.0000
S20	0.0000	0.0000	0.0000	0.0000
S21	0.0000	0.0000	0.0000	0.0000
S22	0.0000	0.0000	0.0000	0.0000
S23	0.0000	0.0000	0.0000	0.0000
S24	0.0000	0.0000	0.0000	0.0000
S25	0.0000	0.0000	0.0000	0.0000
S26	0.0000	0.0000	0.0000	0.0000
S27	0.0000	0.0000	0.0000	0.0000
S28	0.0000	0.0000	0.0000	0.0000
S29	0.0000	0.0000	0.0000	0.0000
S30	0.0000	0.0000	0.0000	0.0000
;				

Table matrix7(SA1,kw)

	kw1	kw2	kw3	kw4
S1	0.0000	0.0000	0.0000	0.0000
S2	0.0000	0.0000	0.0000	0.0000
S3	0.0000	0.0000	0.0000	0.0000
S4	0.0000	0.0000	0.0000	0.0000
S5	0.0000	0.0000	0.0000	0.0000

S6	0.0000	0.0000	0.0000	0.0000
S7	0.0000	0.0000	0.0000	0.0000
S8	0.0000	0.0000	0.0000	0.0000
S9	0.0000	0.0000	0.0000	0.0000
S10	0.0000	0.0000	0.0000	0.0000
S11	0.0000	0.0000	0.0000	0.0000
S12	0.0000	0.0000	0.0000	0.0000
S13	0.0000	0.0000	0.0000	0.0000
S14	0.0000	0.0000	0.0000	0.0000
S15	0.0000	0.0000	0.0000	0.0000
S16	0.0000	0.0000	0.0000	0.0000
S17	0.0000	0.0000	0.0000	0.0000
S18	0.0000	0.0000	0.0000	0.0000
S19	0.0000	0.0000	0.0000	0.0000
S20	0.0000	0.0000	0.0000	0.0000
S21	0.0000	0.0000	0.0000	0.0000
S22	0.0000	0.0000	0.0000	0.0000
S23	0.0000	0.0000	0.0000	0.0000
S24	0.0000	0.0000	0.0000	0.0000
S25	0.0000	0.0000	0.0000	0.0000
S26	0.0000	0.0000	0.0000	0.0000
S27	0.0000	0.0000	0.0000	0.0000
S28	0.0000	0.0000	0.0000	0.0000
S29	0.0000	0.0000	0.0000	0.0000
S30	0.0000	0.0000	0.0000	0.0000
;				

Table matrix8(SA1,kw)

	kw1	kw2	kw3	kw4
S1	0.0000	0.0000	0.0000	0.0000
S2	0.0000	3.1000	0.0000	1.0000
S3	0.0000	3.1000	0.0000	-2.0000
S4	1.0000	-3.1000	0.0000	3.0000
S5	2.0000	-3.1000	0.0000	3.0000
S6	0.0000	0.0000	0.0000	0.0000
S7	0.0000	2.0000	0.0000	0.0000
S8	0.0000	0.0000	0.0000	0.0000
S9	0.0000	0.0000	0.0000	0.0000
S10	0.0000	0.0000	0.0000	0.0000
S11	0.0000	0.0000	0.0000	0.0000
S12	0.0000	0.0000	0.0000	0.0000
S13	0.0000	0.0000	0.0000	0.0000
S14	0.0000	0.0000	0.0000	0.0000

S15	0.0000	0.0000	0.0000	0.0000
S16	0.0000	0.0000	0.0000	0.0000
S17	0.0000	0.0000	0.0000	0.0000
S18	0.0000	0.0000	0.0000	0.0000
S19	0.0000	0.0000	0.0000	0.0000
S20	0.0000	0.0000	0.0000	0.0000
S21	0.0000	0.0000	0.0000	0.0000
S22	0.0000	0.0000	0.0000	0.0000
S23	0.0000	0.0000	0.0000	0.0000
S24	0.0000	0.0000	0.0000	0.0000
S25	0.0000	0.0000	0.0000	0.0000
S26	0.0000	0.0000	0.0000	0.0000
S27	0.0000	0.0000	0.0000	0.0000
S28	0.0000	0.0000	0.0000	0.0000
S29	0.0000	0.0000	0.0000	0.0000
S30	0.0000	0.0000	0.0000	0.0000
;				

Table matrix9(SA1,kw)

	kw1	kw2	kw3	kw4
S1	0.0000	0.1000	0.0000	2.0000
S2	0.0000	1.1000	0.0000	1.0000
S3	0.0000	1.1000	0.0000	-2.0000
S4	1.0000	-1.1000	0.0000	3.0000
S5	2.0000	-1.1000	0.0000	3.0000
S6	0.0000	0.0000	0.0000	0.0000
S7	0.0000	0.0000	0.0000	0.0000
S8	0.0000	2.0000	0.0000	0.0000
S9	0.0000	0.0000	0.0000	0.0000
S10	0.0000	0.0000	0.0000	0.0000
S11	0.0000	0.0000	0.0000	0.0000
S12	0.0000	0.0000	0.0000	0.0000
S13	0.0000	0.0000	0.0000	0.0000
S14	0.0000	0.0000	0.0000	0.0000
S15	0.0000	0.0000	0.0000	0.0000
S16	0.0000	0.0000	0.0000	0.0000
S17	0.0000	0.0000	0.0000	0.0000
S18	0.0000	0.0000	0.0000	0.0000
S19	0.0000	0.0000	0.0000	0.0000
S20	0.0000	0.0000	0.0000	0.0000
S21	0.0000	0.0000	0.0000	0.0000
S22	0.0000	0.0000	0.0000	0.0000
S23	0.0000	0.0000	0.0000	0.0000

S24	0.0000	0.0000	0.0000	0.0000
S25	0.0000	0.0000	0.0000	0.0000
S26	0.0000	0.0000	0.0000	0.0000
S27	0.0000	0.0000	0.0000	0.0000
S28	0.0000	0.0000	0.0000	0.0000
S29	0.0000	0.0000	0.0000	0.0000
S30	0.0000	0.0000	0.0000	0.0000

;

Table matrix10(SA1,kw)

	kw1	kw2	kw3	kw4
S1	1.1000	-1.0000	0.0000	0.0000
S2	1.1000	0.0000	0.0000	-1.0000
S3	0.0000	0.0000	0.0000	0.0000
S4	0.0000	0.0000	0.0000	0.0000
S5	0.0000	0.0000	0.0000	0.0000
S6	0.0000	0.0000	0.0000	0.0000
S7	0.0000	0.0000	0.0000	0.0000
S8	1.1000	-3.1000	0.0000	-2.0000
S9	1.1000	-1.1000	0.0000	-2.0000
S10	0.0000	0.0000	0.0000	0.0000
S11	0.0000	0.0000	0.0000	0.0000
S12	0.0000	0.0000	0.0000	0.0000
S13	0.0000	0.0000	0.0000	0.0000
S14	0.0000	0.0000	0.0000	0.0000
S15	0.0000	0.0000	0.0000	0.0000
S16	0.0000	0.0000	0.0000	0.0000
S17	0.0000	0.0000	0.0000	0.0000
S18	0.0000	0.0000	0.0000	0.0000
S19	0.0000	0.0000	0.0000	0.0000
S20	0.0000	0.0000	0.0000	0.0000
S21	0.0000	0.0000	0.0000	0.0000
S22	0.0000	0.0000	0.0000	0.0000
S23	0.0000	0.0000	0.0000	0.0000
S24	0.0000	0.0000	0.0000	0.0000
S25	0.0000	0.0000	0.0000	0.0000
S26	0.0000	0.0000	0.0000	0.0000
S27	0.0000	0.0000	0.0000	0.0000
S28	0.0000	0.0000	0.0000	0.0000
S29	0.0000	0.0000	0.0000	0.0000
S30	0.0000	0.0000	0.0000	0.0000

;

Table matrix11(SA1,kw)

	kw1	kw2	kw3	kw4
S1	2.1000	-1.0000	0.0000	0.0000
S2	2.1000	0.0000	0.0000	-1.0000
S3	0.0000	0.0000	0.0000	0.0000
S4	0.0000	0.0000	0.0000	0.0000
S5	0.0000	0.0000	0.0000	0.0000
S6	0.0000	0.0000	0.0000	0.0000
S7	0.0000	0.0000	0.0000	0.0000
S8	2.1000	-3.1000	0.0000	-2.0000
S9	2.1000	-1.1000	0.0000	-2.0000
S10	1.0000	0.0000	0.0000	0.0000
S11	0.0000	0.0000	0.0000	0.0000
S12	0.0000	0.0000	0.0000	0.0000
S13	0.0000	0.0000	0.0000	0.0000
S14	0.0000	0.0000	0.0000	0.0000
S15	0.0000	0.0000	0.0000	0.0000
S16	0.0000	0.0000	0.0000	0.0000
S17	0.0000	0.0000	0.0000	0.0000
S18	0.0000	0.0000	0.0000	0.0000
S19	0.0000	0.0000	0.0000	0.0000
S20	0.0000	0.0000	0.0000	0.0000
S21	0.0000	0.0000	0.0000	0.0000
S22	0.0000	0.0000	0.0000	0.0000
S23	0.0000	0.0000	0.0000	0.0000
S24	0.0000	0.0000	0.0000	0.0000
S25	0.0000	0.0000	0.0000	0.0000
S26	0.0000	0.0000	0.0000	0.0000
S27	0.0000	0.0000	0.0000	0.0000
S28	0.0000	0.0000	0.0000	0.0000
S29	0.0000	0.0000	0.0000	0.0000
S30	0.0000	0.0000	0.0000	0.0000

;

Table matrix12(SA1,kw)

	kw1	kw2	kw3	kw4
S1	3.1000	-1.0000	1.0000	0.0000
S2	3.1000	0.0000	1.0000	-1.0000
S3	0.0000	0.0000	0.0000	0.0000
S4	0.0000	0.0000	0.0000	0.0000
S5	0.0000	0.0000	0.0000	0.0000
S6	0.0000	0.0000	0.0000	0.0000

S7	0.0000	0.0000	0.0000	0.0000
S8	3.1000	-3.1000	1.0000	-2.0000
S9	3.1000	-1.1000	1.0000	-2.0000
S10	2.0000	0.0000	1.0000	0.0000
S11	1.0000	0.0000	1.0000	0.0000
S12	0.0000	0.0000	0.0000	0.0000
S13	0.0000	0.0000	0.0000	0.0000
S14	0.0000	0.0000	0.0000	0.0000
S15	0.0000	0.0000	0.0000	0.0000
S16	0.0000	0.0000	0.0000	0.0000
S17	0.0000	0.0000	0.0000	0.0000
S18	0.0000	0.0000	0.0000	0.0000
S19	0.0000	0.0000	0.0000	0.0000
S20	0.0000	0.0000	0.0000	0.0000
S21	0.0000	0.0000	0.0000	0.0000
S22	0.0000	0.0000	0.0000	0.0000
S23	0.0000	0.0000	0.0000	0.0000
S24	0.0000	0.0000	0.0000	0.0000
S25	0.0000	0.0000	0.0000	0.0000
S26	0.0000	0.0000	0.0000	0.0000
S27	0.0000	0.0000	0.0000	0.0000
S28	0.0000	0.0000	0.0000	0.0000
S29	0.0000	0.0000	0.0000	0.0000
S30	0.0000	0.0000	0.0000	0.0000

;

Table matrix13(SA1,kw)

	kw1	kw2	kw3	kw4
S1	0.0000	0.0000	0.0000	0.0000
S2	0.0000	0.0000	0.0000	0.0000
S3	0.0000	0.0000	0.0000	0.0000
S4	0.0000	0.0000	0.0000	0.0000
S5	0.0000	0.0000	0.0000	0.0000
S6	0.0000	0.0000	0.0000	0.0000
S7	0.0000	0.0000	0.0000	0.0000
S8	0.0000	0.0000	0.0000	0.0000
S9	0.0000	0.0000	0.0000	0.0000
S10	0.0000	0.0000	0.0000	0.0000
S11	0.0000	0.0000	0.0000	0.0000
S12	0.0000	0.0000	0.0000	0.0000
S13	0.0000	0.0000	0.0000	0.0000
S14	0.0000	0.0000	0.0000	0.0000
S15	0.0000	0.0000	0.0000	0.0000

S16	0.0000	0.0000	0.0000	0.0000
S17	0.0000	0.0000	0.0000	0.0000
S18	0.0000	0.0000	0.0000	0.0000
S19	0.0000	0.0000	0.0000	0.0000
S20	0.0000	0.0000	0.0000	0.0000
S21	0.0000	0.0000	0.0000	0.0000
S22	0.0000	0.0000	0.0000	0.0000
S23	0.0000	0.0000	0.0000	0.0000
S24	0.0000	0.0000	0.0000	0.0000
S25	0.0000	0.0000	0.0000	0.0000
S26	0.0000	0.0000	0.0000	0.0000
S27	0.0000	0.0000	0.0000	0.0000
S28	0.0000	0.0000	0.0000	0.0000
S29	0.0000	0.0000	0.0000	0.0000
S30	0.0000	0.0000	0.0000	0.0000
;				

Table matrix14(SA1,kw)

	kw1	kw2	kw3	kw4
S1	0.0000	0.0000	0.0000	0.0000
S2	0.0000	0.0000	0.0000	0.0000
S3	0.0000	0.0000	0.0000	0.0000
S4	0.0000	0.0000	0.0000	0.0000
S5	0.0000	0.0000	0.0000	0.0000
S6	0.0000	0.0000	0.0000	0.0000
S7	0.0000	0.0000	0.0000	0.0000
S8	0.0000	0.0000	0.0000	0.0000
S9	0.0000	0.0000	0.0000	0.0000
S10	0.0000	0.0000	0.0000	0.0000
S11	0.0000	0.0000	0.0000	0.0000
S12	0.0000	0.0000	0.0000	0.0000
S13	1.0000	1.0000	0.0000	0.0000
S14	0.0000	0.0000	0.0000	0.0000
S15	0.0000	0.0000	0.0000	0.0000
S16	0.0000	0.0000	0.0000	0.0000
S17	0.0000	0.0000	0.0000	0.0000
S18	0.0000	0.0000	0.0000	0.0000
S19	0.0000	0.0000	0.0000	0.0000
S20	0.0000	0.0000	0.0000	0.0000
S21	0.0000	0.0000	0.0000	0.0000
S22	0.0000	0.0000	0.0000	0.0000
S23	0.0000	0.0000	0.0000	0.0000
S24	0.0000	0.0000	0.0000	0.0000

S25	0.0000	0.0000	0.0000	0.0000
S26	0.0000	0.0000	0.0000	0.0000
S27	0.0000	0.0000	0.0000	0.0000
S28	0.0000	0.0000	0.0000	0.0000
S29	0.0000	0.0000	0.0000	0.0000
S30	0.0000	0.0000	0.0000	0.0000
;				

Table matrix15(SA1,kw)

	kw1	kw2	kw3	kw4
S1	0.0000	0.0000	0.0000	0.0000
S2	0.0000	0.0000	0.0000	0.0000
S3	0.0000	0.0000	0.0000	0.0000
S4	0.0000	0.0000	0.0000	0.0000
S5	0.0000	0.0000	0.0000	0.0000
S6	0.0000	0.0000	0.0000	0.0000
S7	0.0000	0.0000	0.0000	0.0000
S8	0.0000	0.0000	0.0000	0.0000
S9	0.0000	0.0000	0.0000	0.0000
S10	0.0000	0.0000	0.0000	0.0000
S11	0.0000	0.0000	0.0000	0.0000
S12	0.0000	0.0000	0.0000	0.0000
S13	0.0000	0.0000	0.0000	0.0000
S14	0.0000	0.0000	0.0000	0.0000
S15	0.0000	0.0000	0.0000	0.0000
S16	0.0000	0.0000	0.0000	0.0000
S17	0.0000	0.0000	0.0000	0.0000
S18	0.0000	0.0000	0.0000	0.0000
S19	0.0000	0.0000	0.0000	0.0000
S20	0.0000	0.0000	0.0000	0.0000
S21	0.0000	0.0000	0.0000	0.0000
S22	0.0000	0.0000	0.0000	0.0000
S23	0.0000	0.0000	0.0000	0.0000
S24	0.0000	0.0000	0.0000	0.0000
S25	0.0000	0.0000	0.0000	0.0000
S26	0.0000	0.0000	0.0000	0.0000
S27	0.0000	0.0000	0.0000	0.0000
S28	0.0000	0.0000	0.0000	0.0000
S29	0.0000	0.0000	0.0000	0.0000
S30	0.0000	0.0000	0.0000	0.0000
;				

Table matrix16(SA1,kw)

	kw1	kw2	kw3	kw4
S1	0.0000	0.0000	0.0000	0.0000
S2	0.0000	0.0000	0.0000	0.0000
S3	0.0000	0.0000	0.0000	2.0000
S4	-1.0000	0.0000	0.0000	1.0000
S5	-2.0000	0.0000	0.0000	1.0000
S6	0.0000	0.0000	0.0000	0.0000
S7	0.0000	0.0000	0.0000	0.0000
S8	0.0000	0.0000	0.0000	0.0000
S9	0.0000	0.0000	0.0000	0.0000
S10	0.0000	0.0000	0.0000	0.0000
S11	0.0000	0.0000	0.0000	0.0000
S12	0.0000	0.0000	0.0000	0.0000
S13	0.0000	0.0000	0.0000	0.0000
S14	0.0000	0.0000	0.0000	0.0000
S15	0.0000	0.0000	0.0000	0.0000
S16	0.0000	0.0000	0.0000	0.0000
S17	0.0000	0.0000	0.0000	0.0000
S18	0.0000	0.0000	0.0000	0.0000
S19	0.0000	0.0000	0.0000	0.0000
S20	0.0000	0.0000	0.0000	0.0000
S21	0.0000	0.0000	0.0000	0.0000
S22	0.0000	0.0000	0.0000	0.0000
S23	0.0000	0.0000	0.0000	0.0000
S24	0.0000	0.0000	0.0000	0.0000
S25	0.0000	0.0000	0.0000	0.0000
S26	0.0000	0.0000	0.0000	0.0000
S27	0.0000	0.0000	0.0000	0.0000
S28	0.0000	0.0000	0.0000	0.0000
S29	0.0000	0.0000	0.0000	0.0000
S30	0.0000	0.0000	0.0000	0.0000

;

Table matrix17(SA1,kw)

	kw1	kw2	kw3	kw4
S1	3.1000	-1.0000	2.0000	1.1000
S2	3.1000	0.0000	2.0000	0.1000
S3	0.0000	0.0000	0.0000	0.0000
S4	0.0000	0.0000	0.0000	0.0000
S5	0.0000	0.0000	0.0000	0.0000
S6	0.0000	0.0000	0.0000	0.0000

S7	0.0000	0.0000	0.0000	0.0000
S8	3.1000	-3.1000	2.0000	-0.9000
S9	3.1000	-1.1000	2.0000	-0.9000
S10	2.0000	0.0000	2.0000	1.1000
S11	1.0000	0.0000	2.0000	1.1000
S12	0.0000	0.0000	1.0000	1.1000
S13	0.0000	0.0000	0.0000	0.0000
S14	0.0000	0.0000	0.0000	0.0000
S15	0.0000	0.0000	0.0000	0.0000
S16	0.0000	0.0000	0.0000	0.0000
S17	0.0000	0.0000	0.0000	0.0000
S18	0.0000	0.0000	0.0000	0.0000
S19	0.0000	0.0000	0.0000	0.0000
S20	0.0000	0.0000	0.0000	0.0000
S21	0.0000	0.0000	0.0000	0.0000
S22	0.0000	0.0000	0.0000	0.0000
S23	0.0000	0.0000	0.0000	0.0000
S24	0.0000	0.0000	0.0000	0.0000
S25	0.0000	0.0000	0.0000	0.0000
S26	0.0000	0.0000	0.0000	0.0000
S27	0.0000	0.0000	0.0000	0.0000
S28	0.0000	0.0000	0.0000	0.0000
S29	0.0000	0.0000	0.0000	0.0000
S30	0.0000	0.0000	0.0000	0.0000
;				

Table matrix18(SA1,kw)

	kw1	kw2	kw3	kw4
S1	0.0000	0.0000	0.0000	0.0000
S2	0.0000	0.0000	0.0000	0.0000
S3	0.0000	0.0000	0.0000	0.0000
S4	0.0000	0.0000	0.0000	0.0000
S5	0.0000	0.0000	0.0000	0.0000
S6	0.0000	0.0000	0.0000	0.0000
S7	0.0000	0.0000	0.0000	0.0000
S8	0.0000	0.0000	0.0000	0.0000
S9	0.0000	0.0000	0.0000	0.0000
S10	0.0000	0.0000	0.0000	0.0000
S11	0.0000	0.0000	0.0000	0.0000
S12	0.0000	0.0000	0.0000	0.0000
S13	0.0000	0.0000	0.0000	0.0000
S14	0.0000	0.0000	0.0000	0.0000
S15	1.0000	0.0000	1.0000	0.0000

S16	0.0000	0.0000	0.0000	0.0000
S17	0.0000	0.0000	0.0000	0.0000
S18	0.0000	0.0000	0.0000	0.0000
S19	0.0000	0.0000	0.0000	0.0000
S20	0.0000	0.0000	0.0000	0.0000
S21	0.0000	0.0000	0.0000	0.0000
S22	0.0000	0.0000	0.0000	0.0000
S23	0.0000	0.0000	0.0000	0.0000
S24	0.0000	0.0000	0.0000	0.0000
S25	0.0000	0.0000	0.0000	0.0000
S26	0.0000	0.0000	0.0000	0.0000
S27	0.0000	0.0000	0.0000	0.0000
S28	0.0000	0.0000	0.0000	0.0000
S29	0.0000	0.0000	0.0000	0.0000
S30	0.0000	0.0000	0.0000	0.0000
;				

Table matrix19(SA1,kw)

	kw1	kw2	kw3	kw4
S1	0.0000	0.0000	0.0000	0.0000
S2	0.0000	0.0000	0.0000	0.0000
S3	0.0000	0.0000	0.0000	0.0000
S4	0.0000	0.0000	0.0000	0.0000
S5	0.0000	0.0000	0.0000	0.0000
S6	0.0000	0.0000	0.0000	0.0000
S7	0.0000	0.0000	0.0000	0.0000
S8	0.0000	0.0000	0.0000	0.0000
S9	0.0000	0.0000	0.0000	0.0000
S10	0.0000	0.0000	0.0000	0.0000
S11	0.0000	0.0000	0.0000	0.0000
S12	0.0000	0.0000	0.0000	0.0000
S13	0.0000	0.0000	0.0000	0.0000
S14	0.0000	0.0000	0.0000	0.0000
S15	2.0000	0.0000	1.0000	0.0000
S16	0.0000	0.0000	0.0000	0.0000
S17	0.0000	0.0000	0.0000	0.0000
S18	1.0000	0.0000	0.0000	0.0000
S19	0.0000	0.0000	0.0000	0.0000
S20	0.0000	0.0000	0.0000	0.0000
S21	0.0000	0.0000	0.0000	0.0000
S22	0.0000	0.0000	0.0000	0.0000
S23	0.0000	0.0000	0.0000	0.0000
S24	0.0000	0.0000	0.0000	0.0000

S25	0.0000	0.0000	0.0000	0.0000
S26	0.0000	0.0000	0.0000	0.0000
S27	0.0000	0.0000	0.0000	0.0000
S28	0.0000	0.0000	0.0000	0.0000
S29	0.0000	0.0000	0.0000	0.0000
S30	0.0000	0.0000	0.0000	0.0000

;

Table matrix20(SA1,kw)

	kw1	kw2	kw3	kw4
S1	0.0000	0.0000	0.0000	0.0000
S2	0.0000	0.0000	0.0000	0.0000
S3	0.0000	0.0000	0.0000	0.0000
S4	0.0000	0.0000	0.0000	0.0000
S5	0.0000	0.0000	0.0000	0.0000
S6	0.0000	0.0000	0.0000	0.0000
S7	0.0000	0.0000	0.0000	0.0000
S8	0.0000	0.0000	0.0000	0.0000
S9	0.0000	0.0000	0.0000	0.0000
S10	0.0000	0.0000	0.0000	0.0000
S11	0.0000	0.0000	0.0000	0.0000
S12	0.0000	0.0000	0.0000	0.0000
S13	0.0000	0.0000	0.0000	0.0000
S14	0.0000	0.0000	0.0000	0.0000
S15	0.0000	0.0000	0.0000	0.0000
S16	0.0000	0.0000	0.0000	0.0000
S17	0.0000	0.0000	0.0000	0.0000
S18	0.0000	0.0000	0.0000	0.0000
S19	0.0000	0.0000	0.0000	0.0000
S20	0.0000	0.0000	0.0000	0.0000
S21	0.0000	0.0000	0.0000	0.0000
S22	0.0000	0.0000	0.0000	0.0000
S23	0.0000	0.0000	0.0000	0.0000
S24	0.0000	0.0000	0.0000	0.0000
S25	0.0000	0.0000	0.0000	0.0000
S26	0.0000	0.0000	0.0000	0.0000
S27	0.0000	0.0000	0.0000	0.0000
S28	0.0000	0.0000	0.0000	0.0000
S29	0.0000	0.0000	0.0000	0.0000
S30	0.0000	0.0000	0.0000	0.0000

;

Table matrix21(SA1,kw)

	kw1	kw2	kw3	kw4
S1	0.0000	0.0000	0.0000	0.0000
S2	0.0000	0.0000	0.0000	0.0000
S3	0.0000	0.0000	0.0000	0.0000
S4	0.0000	0.0000	0.0000	0.0000
S5	0.0000	0.0000	0.0000	0.0000
S6	0.0000	0.0000	0.0000	0.0000
S7	0.0000	0.0000	0.0000	0.0000
S8	0.0000	0.0000	0.0000	0.0000
S9	0.0000	0.0000	0.0000	0.0000
S10	0.0000	0.0000	0.0000	0.0000
S11	0.0000	0.0000	0.0000	0.0000
S12	0.0000	0.0000	0.0000	0.0000
S13	0.0000	0.0000	0.0000	0.0000
S14	0.0000	0.0000	0.0000	0.0000
S15	0.0000	0.0000	0.0000	0.0000
S16	0.0000	0.0000	0.0000	0.0000
S17	0.0000	0.0000	0.0000	0.0000
S18	0.0000	0.0000	0.0000	0.0000
S19	0.0000	0.0000	0.0000	0.0000
S20	0.0000	0.0000	0.0000	2.0000
S21	0.0000	0.0000	0.0000	0.0000
S22	0.0000	0.0000	0.0000	0.0000
S23	0.0000	0.0000	0.0000	0.0000
S24	0.0000	0.0000	0.0000	0.0000
S25	0.0000	0.0000	0.0000	0.0000
S26	0.0000	0.0000	0.0000	0.0000
S27	0.0000	0.0000	0.0000	0.0000
S28	0.0000	0.0000	0.0000	0.0000
S29	0.0000	0.0000	0.0000	0.0000
S30	0.0000	0.0000	0.0000	0.0000
;				

Table matrix22(SA1,kw)

	kw1	kw2	kw3	kw4
S1	0.0000	0.0000	0.0000	0.0000
S2	0.0000	0.0000	0.0000	0.0000
S3	0.0000	0.0000	0.0000	0.0000
S4	0.0000	0.0000	0.0000	0.0000
S5	0.0000	0.0000	0.0000	0.0000
S6	0.0000	0.0000	0.0000	0.0000
S7	0.0000	0.0000	0.0000	0.0000

S8	0.0000	0.0000	0.0000	0.0000
S9	0.0000	0.0000	0.0000	0.0000
S10	0.0000	0.0000	0.0000	0.0000
S11	0.0000	0.0000	0.0000	0.0000
S12	0.0000	0.0000	0.0000	0.0000
S13	0.0000	0.0000	0.0000	0.0000
S14	0.0000	0.0000	0.0000	0.0000
S15	0.0000	0.0000	0.0000	0.0000
S16	0.0000	0.0000	0.0000	0.0000
S17	0.0000	0.0000	0.0000	0.0000
S18	0.0000	0.0000	0.0000	0.0000
S19	0.0000	0.0000	0.0000	0.0000
S20	0.0000	0.0000	0.0000	0.0000
S21	1.0000	0.0000	0.0000	2.0000
S22	0.0000	0.0000	0.0000	0.0000
S23	0.0000	0.0000	0.0000	0.0000
S24	0.0000	0.0000	0.0000	0.0000
S25	0.0000	0.0000	0.0000	0.0000
S26	0.0000	0.0000	0.0000	0.0000
S27	0.0000	0.0000	0.0000	0.0000
S28	0.0000	0.0000	0.0000	0.0000
S29	0.0000	0.0000	0.0000	0.0000
S30	0.0000	0.0000	0.0000	0.0000
;				

Table matrix23(SA1,kw)

	kw1	kw2	kw3	kw4
S1	0.0000	0.0000	0.0000	0.0000
S2	0.0000	0.0000	0.0000	0.0000
S3	0.0000	0.0000	0.0000	0.0000
S4	0.0000	0.0000	0.0000	0.0000
S5	0.0000	0.0000	0.0000	0.0000
S6	0.0000	0.0000	0.0000	0.0000
S7	0.0000	0.0000	0.0000	0.0000
S8	0.0000	0.0000	0.0000	0.0000
S9	0.0000	0.0000	0.0000	0.0000
S10	0.0000	0.0000	0.0000	0.0000
S11	0.0000	0.0000	0.0000	0.0000
S12	0.0000	0.0000	0.0000	0.0000
S13	0.0000	0.0000	0.0000	0.0000
S14	0.0000	0.0000	0.0000	0.0000
S15	0.0000	0.0000	0.0000	0.0000
S16	0.0000	0.0000	0.0000	0.0000

S17	0.0000	0.0000	0.0000	0.0000
S18	0.0000	0.0000	0.0000	0.0000
S19	0.0000	0.0000	0.0000	0.0000
S20	0.0000	0.0000	0.0000	0.0000
S21	2.0000	0.0000	0.0000	2.0000
S22	1.0000	0.0000	0.0000	0.0000
S23	0.0000	0.0000	0.0000	0.0000
S24	0.0000	0.0000	0.0000	0.0000
S25	0.0000	0.0000	0.0000	0.0000
S26	0.0000	0.0000	0.0000	0.0000
S27	0.0000	0.0000	0.0000	0.0000
S28	0.0000	0.0000	0.0000	0.0000
S29	0.0000	0.0000	0.0000	0.0000
S30	0.0000	0.0000	0.0000	0.0000
;				

Table matrix24(SA1,kw)

	kw1	kw2	kw3	kw4
S1	0.0000	0.0000	0.0000	0.0000
S2	0.0000	0.0000	0.0000	0.0000
S3	0.0000	0.0000	0.0000	0.0000
S4	0.0000	0.0000	0.0000	0.0000
S5	0.0000	0.0000	0.0000	0.0000
S6	0.0000	0.0000	0.0000	0.0000
S7	0.0000	0.0000	0.0000	0.0000
S8	0.0000	0.0000	0.0000	0.0000
S9	0.0000	0.0000	0.0000	0.0000
S10	0.0000	0.0000	0.0000	0.0000
S11	0.0000	0.0000	0.0000	0.0000
S12	0.0000	0.0000	0.0000	0.0000
S13	0.0000	0.0000	0.0000	0.0000
S14	0.0000	0.0000	0.0000	0.0000
S15	0.0000	0.0000	0.0000	0.0000
S16	0.0000	0.0000	0.0000	0.0000
S17	0.0000	0.0000	0.0000	0.0000
S18	0.0000	0.0000	0.0000	0.0000
S19	0.0000	0.0000	0.0000	0.0000
S20	0.0000	0.0000	0.0000	0.0000
S21	4.0000	0.0000	0.0000	2.0000
S22	3.0000	0.0000	0.0000	0.0000
S23	2.0000	0.0000	0.0000	0.0000
S24	0.0000	0.0000	0.0000	0.0000
S25	0.0000	0.0000	0.0000	0.0000

S26	0.0000	0.0000	0.0000	0.0000
S27	0.0000	0.0000	0.0000	0.0000
S28	0.0000	0.0000	0.0000	0.0000
S29	0.0000	0.0000	0.0000	0.0000
S30	0.0000	0.0000	0.0000	0.0000
;				

Table matrix25(SA1,kw)

	kw1	kw2	kw3	kw4
S1	0.0000	0.0000	0.0000	0.0000
S2	0.0000	0.0000	0.0000	0.0000
S3	0.0000	0.0000	0.0000	0.0000
S4	0.0000	0.0000	0.0000	0.0000
S5	0.0000	0.0000	0.0000	0.0000
S6	0.0000	0.0000	0.0000	0.0000
S7	0.0000	0.0000	0.0000	0.0000
S8	0.0000	0.0000	0.0000	0.0000
S9	0.0000	0.0000	0.0000	0.0000
S10	0.0000	0.0000	0.0000	0.0000
S11	0.0000	0.0000	0.0000	0.0000
S12	0.0000	0.0000	0.0000	0.0000
S13	0.0000	0.0000	0.0000	0.0000
S14	0.0000	0.0000	0.0000	0.0000
S15	0.0000	0.0000	0.0000	0.0000
S16	0.0000	0.0000	0.0000	0.0000
S17	0.0000	0.0000	0.0000	0.0000
S18	0.0000	0.0000	0.0000	0.0000
S19	0.0000	0.0000	0.0000	0.0000
S20	0.0000	0.0000	0.0000	0.0000
S21	5.0000	0.0000	0.0000	2.0000
S22	4.0000	0.0000	0.0000	0.0000
S23	3.0000	0.0000	0.0000	0.0000
S24	1.0000	0.0000	0.0000	0.0000
S25	0.0000	0.0000	0.0000	0.0000
S26	0.0000	0.0000	0.0000	0.0000
S27	0.0000	0.0000	0.0000	0.0000
S28	0.0000	0.0000	0.0000	0.0000
S29	0.0000	0.0000	0.0000	0.0000
S30	0.0000	0.0000	0.0000	0.0000
;				

Table matrix26(SA1,kw)

	kw1	kw2	kw3	kw4
S1	0.0000	0.0000	0.0000	0.0000
S2	0.0000	0.0000	0.0000	0.0000
S3	0.0000	0.0000	0.0000	0.0000
S4	0.0000	0.0000	0.0000	0.0000
S5	0.0000	0.0000	0.0000	0.0000
S6	0.0000	0.0000	0.0000	0.0000
S7	0.0000	0.0000	0.0000	0.0000
S8	0.0000	0.0000	0.0000	0.0000
S9	0.0000	0.0000	0.0000	0.0000
S10	0.0000	0.0000	0.0000	0.0000
S11	0.0000	0.0000	0.0000	0.0000
S12	0.0000	0.0000	0.0000	0.0000
S13	0.0000	0.0000	0.0000	0.0000
S14	0.0000	0.0000	0.0000	0.0000
S15	0.0000	0.0000	0.0000	0.0000
S16	0.0000	0.0000	0.0000	0.0000
S17	0.0000	0.0000	0.0000	0.0000
S18	0.0000	0.0000	0.0000	0.0000
S19	0.0000	0.0000	0.0000	0.0000
S20	0.0000	0.0000	0.0000	0.0000
S21	6.0000	1.0000	0.0000	2.0000
S22	5.0000	1.0000	0.0000	0.0000
S23	4.0000	1.0000	0.0000	0.0000
S24	2.0000	1.0000	0.0000	0.0000
S25	1.0000	1.0000	0.0000	0.0000
S26	0.0000	0.0000	0.0000	0.0000
S27	0.0000	0.0000	0.0000	0.0000
S28	0.0000	0.0000	0.0000	0.0000
S29	0.0000	0.0000	0.0000	0.0000
S30	0.0000	0.0000	0.0000	0.0000

;

Table matrix27(SA1,kw)

	kw1	kw2	kw3	kw4
S1	0.0000	0.0000	0.0000	0.0000
S2	0.0000	0.0000	0.0000	0.0000
S3	0.0000	0.0000	0.0000	0.0000
S4	0.0000	0.0000	0.0000	0.0000
S5	0.0000	0.0000	0.0000	0.0000
S6	0.0000	0.0000	0.0000	0.0000

S7	0.0000	0.0000	0.0000	0.0000
S8	0.0000	0.0000	0.0000	0.0000
S9	0.0000	0.0000	0.0000	0.0000
S10	0.0000	0.0000	0.0000	0.0000
S11	0.0000	0.0000	0.0000	0.0000
S12	0.0000	0.0000	0.0000	0.0000
S13	0.0000	0.0000	0.0000	0.0000
S14	0.0000	0.0000	0.0000	0.0000
S15	0.0000	0.0000	0.0000	0.0000
S16	0.0000	0.0000	0.0000	0.0000
S17	0.0000	0.0000	0.0000	0.0000
S18	0.0000	0.0000	0.0000	0.0000
S19	0.0000	0.0000	0.0000	0.0000
S20	0.0000	0.0000	0.0000	0.0000
S21	0.0000	0.0000	1.0000	2.0000
S22	-1.0000	0.0000	1.0000	0.0000
S23	-2.0000	0.0000	1.0000	0.0000
S24	-4.0000	0.0000	1.0000	0.0000
S25	-5.0000	0.0000	1.0000	0.0000
S26	-6.0000	-1.0000	1.0000	0.0000
S27	0.0000	0.0000	0.0000	0.0000
S28	0.0000	0.0000	0.0000	0.0000
S29	0.0000	0.0000	0.0000	0.0000
S30	0.0000	0.0000	0.0000	0.0000

;

Table matrix28(SA1,kw)

	kw1	kw2	kw3	kw4
S1	0.0000	0.0000	0.0000	0.0000
S2	0.0000	0.0000	0.0000	0.0000
S3	0.0000	0.0000	0.0000	0.0000
S4	0.0000	0.0000	0.0000	0.0000
S5	0.0000	0.0000	0.0000	0.0000
S6	0.0000	0.0000	0.0000	0.0000
S7	0.0000	0.0000	0.0000	0.0000
S8	0.0000	0.0000	0.0000	0.0000
S9	0.0000	0.0000	0.0000	0.0000
S10	0.0000	0.0000	0.0000	0.0000
S11	0.0000	0.0000	0.0000	0.0000
S12	0.0000	0.0000	0.0000	0.0000
S13	0.0000	0.0000	0.0000	0.0000
S14	0.0000	0.0000	0.0000	0.0000
S15	0.0000	0.0000	0.0000	0.0000

S16	0.0000	0.0000	0.0000	0.0000
S17	0.0000	0.0000	0.0000	0.0000
S18	0.0000	0.0000	0.0000	0.0000
S19	0.0000	0.0000	0.0000	0.0000
S20	0.0000	0.0000	0.0000	0.0000
S21	0.0000	0.0000	0.0000	0.0000
S22	0.0000	0.0000	0.0000	0.0000
S23	0.0000	0.0000	0.0000	0.0000
S24	0.0000	0.0000	0.0000	0.0000
S25	0.0000	0.0000	0.0000	0.0000
S26	0.0000	0.0000	0.0000	0.0000
S27	0.0000	0.0000	2.0000	0.0000
S28	0.0000	0.0000	0.0000	0.0000
S29	0.0000	0.0000	0.0000	0.0000
S30	0.0000	0.0000	0.0000	0.0000
;				

Table matrix29(SA1,kw)

	kw1	kw2	kw3	kw4
S1	0.0000	0.0000	0.0000	0.0000
S2	0.0000	0.0000	0.0000	0.0000
S3	0.0000	0.0000	0.0000	0.0000
S4	0.0000	0.0000	0.0000	0.0000
S5	0.0000	0.0000	0.0000	0.0000
S6	0.0000	0.0000	0.0000	0.0000
S7	0.0000	0.0000	0.0000	0.0000
S8	0.0000	0.0000	0.0000	0.0000
S9	0.0000	0.0000	0.0000	0.0000
S10	0.0000	0.0000	0.0000	0.0000
S11	0.0000	0.0000	0.0000	0.0000
S12	0.0000	0.0000	0.0000	0.0000
S13	0.0000	0.0000	0.0000	0.0000
S14	0.0000	0.0000	0.0000	0.0000
S15	0.0000	0.0000	0.0000	0.0000
S16	0.0000	0.0000	0.0000	0.0000
S17	0.0000	0.0000	0.0000	0.0000
S18	0.0000	0.0000	0.0000	0.0000
S19	0.0000	0.0000	0.0000	0.0000
S20	0.0000	0.0000	0.0000	0.0000
S21	0.0000	0.0000	0.0000	0.0000
S22	0.0000	0.0000	0.0000	0.0000
S23	0.0000	0.0000	0.0000	0.0000
S24	0.0000	0.0000	0.0000	0.0000

S25	0.0000	0.0000	0.0000	0.0000
S26	0.0000	0.0000	0.0000	0.0000
S27	1.1000	0.0000	2.0000	0.0000
S28	1.1000	0.0000	0.0000	0.0000
S29	0.0000	0.0000	0.0000	0.0000
S30	0.0000	0.0000	0.0000	0.0000
;				

Table matrix30(SA1,kw)

	kw1	kw2	kw3	kw4
S1	0.0000	1.0000	1.0000	0.0000
S2	0.0000	0.0000	1.0000	1.0000
S3	0.0000	0.0000	0.0000	0.0000
S4	0.0000	0.0000	0.0000	0.0000
S5	0.0000	0.0000	0.0000	0.0000
S6	0.0000	0.0000	0.0000	0.0000
S7	0.0000	0.0000	0.0000	0.0000
S8	0.0000	3.1000	1.0000	2.0000
S9	0.0000	1.1000	1.0000	2.0000
S10	1.1000	0.0000	1.0000	0.0000
S11	2.1000	0.0000	1.0000	0.0000
S12	3.1000	0.0000	2.0000	0.0000
S13	0.0000	0.0000	0.0000	0.0000
S14	0.0000	0.0000	0.0000	0.0000
S15	0.0000	0.0000	0.0000	0.0000
S16	0.0000	0.0000	0.0000	0.0000
S17	0.0000	0.0000	0.0000	0.0000
S18	0.0000	0.0000	0.0000	0.0000
S19	0.0000	0.0000	0.0000	0.0000
S20	0.0000	0.0000	0.0000	0.0000
S21	0.0000	0.0000	0.0000	0.0000
S22	0.0000	0.0000	0.0000	0.0000
S23	0.0000	0.0000	0.0000	0.0000
S24	0.0000	0.0000	0.0000	0.0000
S25	0.0000	0.0000	0.0000	0.0000
S26	0.0000	0.0000	0.0000	0.0000
S27	0.0000	0.0000	0.0000	0.0000
S28	0.0000	0.0000	0.0000	0.0000
S29	0.0000	0.0000	0.0000	0.0000
S30	0.0000	0.0000	0.0000	0.0000
;				

Equations

obj 'objective function',
ocd1(kw),
ocd2(kw),
ocd3(kw),
ocd4(kw),

linearI(SA,SA1),
linearI2(SA,SA1),
linearI3(SA,SA1),

K1_linearII(SA,SA1),
K1_linearII2(SA,SA1),
K1_linearII3(SA,SA1),
K1_linearII4(SA,SA1),

K2_linearII(SA,SA1),
K2_linearII2(SA,SA1),
K2_linearII3(SA,SA1),
K2_linearII4(SA,SA1),

K3_linearII(SA,SA1),
K3_linearII2(SA,SA1),
K3_linearII3(SA,SA1),
K3_linearII4(SA,SA1),

K4_linearII(SA,SA1),
K4_linearII2(SA,SA1),
K4_linearII3(SA,SA1),
K4_linearII4(SA,SA1),

point30;

ocd1(kw)..

sum(SA1, w_1('S1',SA1)*matrix1(SA1,kw)+w_1('S2',SA1)*matrix2(SA1,kw)
+w_1('S3',SA1)*matrix3(SA1,kw)+w_1('S4',SA1)*matrix4(SA1,kw)
+w_1('S5',SA1)*matrix5(SA1,kw)+ w_1('S6',SA1)*matrix6(SA1,kw)
+w_1('S7',SA1)*matrix7(SA1,kw)+w_1('S8',SA1)*matrix8(SA1,kw)
+w_1('S9',SA1)*matrix9(SA1,kw)+w_1('S10',SA1)*matrix10(SA1,kw)
+w_1('S11',SA1)*matrix11(SA1,kw)+w_1('S12',SA1)*matrix12(SA1,kw)
+w_1('S13',SA1)*matrix13(SA1,kw)+w_1('S14',SA1)*matrix14(SA1,kw)

```

+w_1('S15',SA1)*matrix15(SA1,kw)+w_1('S16',SA1)*matrix16(SA1,kw)
+w_1('S17',SA1)*matrix17(SA1,kw)+w_1('S18',SA1)*matrix18(SA1,kw)
+w_1('S19',SA1)*matrix19(SA1,kw)+w_1('S20',SA1)*matrix20(SA1,kw)
+w_1('S21',SA1)*matrix21(SA1,kw)+w_1('S22',SA1)*matrix22(SA1,kw)
+w_1('S23',SA1)*matrix23(SA1,kw)+w_1('S24',SA1)*matrix24(SA1,kw)
+w_1('S25',SA1)*matrix25(SA1,kw)+w_1('S26',SA1)*matrix26(SA1,kw)
+w_1('S27',SA1)*matrix27(SA1,kw)+w_1('S28',SA1)*matrix28(SA1,kw)
+w_1('S29',SA1)*matrix29(SA1,kw)+w_1('S30',SA1)*matrix30(SA1,kw))=e=
UnitVector('unit1',kw);

```

ocd2(kw)..

```

sum(SA1, w_2('S1',SA1)*matrix1(SA1,kw)+w_2('S2',SA1)*matrix2(SA1,kw)
+w_2('S3',SA1)*matrix3(SA1,kw)+w_2('S4',SA1)*matrix4(SA1,kw)
+w_2('S5',SA1)*matrix5(SA1,kw)+w_2('S6',SA1)*matrix6(SA1,kw)
+w_2('S7',SA1)*matrix7(SA1,kw)+w_2('S8',SA1)*matrix8(SA1,kw)
+w_2('S9',SA1)*matrix9(SA1,kw)+w_2('S10',SA1)*matrix10(SA1,kw)
+w_2('S11',SA1)*matrix11(SA1,kw)+w_2('S12',SA1)*matrix12(SA1,kw)
+w_2('S13',SA1)*matrix13(SA1,kw)+w_2('S14',SA1)*matrix14(SA1,kw)
+w_2('S15',SA1)*matrix15(SA1,kw)+w_2('S16',SA1)*matrix16(SA1,kw)
+w_2('S17',SA1)*matrix17(SA1,kw)+w_2('S18',SA1)*matrix18(SA1,kw)
+w_2('S19',SA1)*matrix19(SA1,kw)+w_2('S20',SA1)*matrix20(SA1,kw)
+w_2('S21',SA1)*matrix21(SA1,kw)+w_2('S22',SA1)*matrix22(SA1,kw)
+w_2('S23',SA1)*matrix23(SA1,kw)+w_2('S24',SA1)*matrix24(SA1,kw)
+w_2('S25',SA1)*matrix25(SA1,kw)+w_2('S26',SA1)*matrix26(SA1,kw)
+w_2('S27',SA1)*matrix27(SA1,kw)+w_2('S28',SA1)*matrix28(SA1,kw)
+w_2('S29',SA1)*matrix29(SA1,kw)+w_2('S30',SA1)*matrix30(SA1,kw))=e=
UnitVector('unit2',kw);

```

ocd3(kw)..

```

sum(SA1, w_3('S1',SA1)*matrix1(SA1,kw)+w_3('S2',SA1)*matrix2(SA1,kw)
+w_3('S3',SA1)*matrix3(SA1,kw)+w_3('S4',SA1)*matrix4(SA1,kw)
+w_3('S5',SA1)*matrix5(SA1,kw)+w_3('S6',SA1)*matrix6(SA1,kw)
+w_3('S7',SA1)*matrix7(SA1,kw)+w_3('S8',SA1)*matrix8(SA1,kw)
+w_3('S9',SA1)*matrix9(SA1,kw)+w_3('S10',SA1)*matrix10(SA1,kw)
+w_3('S11',SA1)*matrix11(SA1,kw)+w_3('S12',SA1)*matrix12(SA1,kw)
+w_3('S13',SA1)*matrix13(SA1,kw)+w_3('S14',SA1)*matrix14(SA1,kw)
+w_3('S15',SA1)*matrix15(SA1,kw)+w_3('S16',SA1)*matrix16(SA1,kw)
+w_3('S17',SA1)*matrix17(SA1,kw)+w_3('S18',SA1)*matrix18(SA1,kw)
+w_3('S19',SA1)*matrix19(SA1,kw)+w_3('S20',SA1)*matrix20(SA1,kw)
+w_3('S21',SA1)*matrix21(SA1,kw)+w_3('S22',SA1)*matrix22(SA1,kw)
+w_3('S23',SA1)*matrix23(SA1,kw)+w_3('S24',SA1)*matrix24(SA1,kw)
+w_3('S25',SA1)*matrix25(SA1,kw)+w_3('S26',SA1)*matrix26(SA1,kw)
+w_3('S27',SA1)*matrix27(SA1,kw)+w_3('S28',SA1)*matrix28(SA1,kw)

```

+w_3('S29',SA1)*matrix29(SA1,kw)+w_3('S30',SA1)*matrix30(SA1,kw))=e=
UnitVector('unit3',kw);

ocd4(kw)..

sum(SA1, w_4('S1',SA1)*matrix1(SA1,kw)+w_4('S2',SA1)*matrix2(SA1,kw)
+w_4('S3',SA1)*matrix3(SA1,kw)+w_4('S4',SA1)*matrix4(SA1,kw)
+w_4('S5',SA1)*matrix5(SA1,kw)+w_4('S6',SA1)*matrix6(SA1,kw)
+w_4('S7',SA1)*matrix7(SA1,kw)+w_4('S8',SA1)*matrix8(SA1,kw)
+w_4('S9',SA1)*matrix9(SA1,kw)+w_4('S10',SA1)*matrix10(SA1,kw)
+w_4('S11',SA1)*matrix11(SA1,kw)+w_4('S12',SA1)*matrix12(SA1,kw)
+w_4('S13',SA1)*matrix13(SA1,kw)+w_4('S14',SA1)*matrix14(SA1,kw)
+w_4('S15',SA1)*matrix15(SA1,kw)+w_4('S16',SA1)*matrix16(SA1,kw)
+w_4('S17',SA1)*matrix17(SA1,kw)+w_4('S18',SA1)*matrix18(SA1,kw)
+w_4('S19',SA1)*matrix19(SA1,kw)+ w_4('S20',SA1)*matrix20(SA1,kw)
+w_4('S21',SA1)*matrix21(SA1,kw)+w_4('S22',SA1)*matrix22(SA1,kw)
+w_4('S23',SA1)*matrix23(SA1,kw)+ w_4('S24',SA1)*matrix24(SA1,kw)
+w_4('S25',SA1)*matrix25(SA1,kw)+w_4('S26',SA1)*matrix26(SA1,kw)
+w_4('S27',SA1)*matrix27(SA1,kw)+w_4('S28',SA1)*matrix28(SA1,kw)
+w_4('S29',SA1)*matrix29(SA1,kw)+w_4('S30',SA1)*matrix30(SA1,kw))=e=
UnitVector('unit4',kw);

linearI(SA,SA1)..

z(SA,SA1)=l=x(SA);

linearI2(SA,SA1)..

z(SA,SA1)=l=x(SA1);

linearI3(SA,SA1)..

z(SA,SA1)=g=x(SA1)+x(SA)-1;

K1_linearII(SA,SA1)..

w_1(SA,SA1)=l=M*z(SA,SA1);

K1_linearII2(SA,SA1)..

w_1(SA,SA1)=l=lambda_1(SA,SA1);

K1_linearII3(SA,SA1)..

w_1(SA,SA1)=g=M*(z(SA,SA1)-1)+lambda_1(SA,SA1);

K1_linearII4(SA,SA1)..

w_1(SA,SA1)=g=-M*z(SA,SA1);

K2_linearII(SA,SA1)..

w_2(SA,SA1)=l=M*z(SA,SA1);

```

K2_linearII2(SA,SA1)..
  w_2(SA,SA1)=l=lambda_2(SA,SA1);

K2_linearII3(SA,SA1)..
  w_2(SA,SA1)=g=M*(z(SA,SA1)-1)+lambda_2(SA,SA1);

K2_linearII4(SA,SA1)..
  w_2(SA,SA1)=g=-M*z(SA,SA1);

K3_linearII(SA,SA1)..
  w_3(SA,SA1)=l=M*z(SA,SA1);

K3_linearII2(SA,SA1)..
  w_3(SA,SA1)=l=lambda_3(SA,SA1);

K3_linearII3(SA,SA1)..
  w_3(SA,SA1)=g=M*(z(SA,SA1)-1)+lambda_3(SA,SA1);

K3_linearII4(SA,SA1)..
  w_3(SA,SA1)=g=-M*z(SA,SA1);

K4_linearII(SA,SA1)..
  w_4(SA,SA1)=l=M*z(SA,SA1);

K4_linearII2(SA,SA1)..
  w_4(SA,SA1)=l=lambda_4(SA,SA1);

K4_linearII3(SA,SA1)..
  w_4(SA,SA1)=g=M*(z(SA,SA1)-1)+lambda_4(SA,SA1);

K4_linearII4(SA,SA1)..
  w_4(SA,SA1)=g=-M*z(SA,SA1);

point30..
  x('S30')=e=1;

obj..  zz =e= sum(SA1, x(SA1));

model m1 /all/;

solve m1 using mip minimizing zz;

```